AD-A069 517 PITTSBURGH UNIV PA DEPT OF MECHANICAL ENGINEERING F/G 11/9
MOLECULAR STRUCTURE AND COHESIVE PROPERTIES OF POLYMERIC ADHESI--ETC(U)
NOV 78 M J DOYLE F33615-76-C-5108

UNCLASSIFIED AFML-TR-78-117 NL

1 OF 2
AD
A069517

AD A069517

DDC FILE COPY

(12)
B.S.
LEVEL II

AFML-TR-78-117

MOLECULAR STRUCTURE AND COHESIVE PROPERTIES OF POLYMERIC ADHESIVES

Michael J. Doyle

University of Pittsburgh
Department of Mechanical Engineering
Pittsburgh, Pennsylvania 15261

NOVEMBER 1978

Final Report April 1976 - April 1978

Approved for public release; distribution unlimited.

AIR FORCE MATERIALS LABORATORY
AIR FORCE WRIGHT AERONAUTICAL LABORATORIES
AIR FORCE SYSTEMS COMMAND
WRIGHT-PATTERSON AIR FORCE BASE, OHIO 45433

DDC
RECEIVED
JUN 6 1979
E

79 05 30 215

NOTICE

When Government drawings, specifications, or other data are used for any purpose other than in connection with a definitely related Government procurement operation, the United States Government thereby incurs no responsibility nor any obligation whatsoever; and the fact that the government may have formulated, furnished, or in any way supplied the said drawings, specifications, or other data, is not to be regarded by implication or otherwise as in any manner licensing the holder or any other person or corporation, or conveying any rights or permission to manufacture, use, or sell any patented invention that may in any way be related thereto.

This technical report has been reviewed and is approved for publication.

T E Helminiak

Project Monitor

FOR THE COMMANDER

T J Reinhart Jr

T.J. REINHART, JR., Chief
Composites, Adhesives & Fibrous
Materials Branch
Nonmetallic Materials Division

J. M. KELBLE, Chief
Nonmetallic Materials Division

Copies of this report should not be returned unless return is required by security considerations, contractual obligations, or notice on a specific document.

AIR FORCE/56[illegible]/41 May 1979 — 360

UNCLASSIFIED

SECURITY CLASSIFICATION OF THIS PAGE *(When Data Entered)*

REPORT DOCUMENTATION PAGE

READ INSTRUCTIONS BEFORE COMPLETING FORM

1. REPORT NUMBER: AFML-TR-78-117	2. GOVT ACCESSION NO.
3. RECIPIENT'S CATALOG NUMBER	
4. TITLE *(and Subtitle)*: Molecular Structure and Cohesive Properties of Polymeric Adhesives.	5. TYPE OF REPORT & PERIOD COVERED: Final Report, 15 April 1976 - 15 April 1978
6. PERFORMING ORG. REPORT NUMBER	
7. AUTHOR(s): Michael J. Doyle	8. CONTRACT OR GRANT NUMBER(s): F33615-76-C-5108
9. PERFORMING ORGANIZATION NAME AND ADDRESS: University of Pittsburgh, Dept. of Mechanical Engineering, Pittsburgh, PA 15261	10. PROGRAM ELEMENT, PROJECT, TASK AREA & WORK UNIT NUMBERS: 2303 0404
11. CONTROLLING OFFICE NAME AND ADDRESS: Air Force Materials Laboratory (AFML/MBC), Air Force Wright Aeronautical Laboratories, Wright-Patterson AFB, Ohio 45433	12. REPORT DATE: November 1978
	13. NUMBER OF PAGES: 154
14. MONITORING AGENCY NAME & ADDRESS *(if different from Controlling Office)*	15. SECURITY CLASS. *(of this report)*: UNCLASSIFIED
	15a. DECLASSIFICATION/DOWNGRADING SCHEDULE

16. DISTRIBUTION STATEMENT *(of this Report)*

Approved for public release; distribution unlimited.

17. DISTRIBUTION STATEMENT *(of the abstract entered in Block 20, if different from Report)*

18. SUPPLEMENTARY NOTES

19. KEY WORDS *(Continue on reverse side if necessary and identify by block number)*

20. ABSTRACT *(Continue on reverse side if necessary and identify by block number)*

The objective of the program was to develop quantitative relationships between molecular structure and cohesive strength properties of modified epoxy adhesives. Two commercial adhesives, a nylon-epoxy resin and a rubber-epoxy resin, were characterized and quantitatively analyzed. Model compositions were prepared in the laboratory equivalent to these two commercial materials. The rheological behavior as a function of curing conditions was characterized by torsional braid analysis. Results showed that at fixed composition the glass transition of the epoxy varied from 110°C to 140°C depending on cure history. (Continued)

DD FORM 1 JAN 73 1473 EDITION OF 1 NOV 65 IS OBSOLETE

UNCLASSIFIED

SECURITY CLASSIFICATION OF THIS PAGE *(When Data Entered)*

411206 LB

The compatibility of the main components of the rubber modified the model adhesive versus composition and temperature was determined by cloud point measurements. The observed morphology of cured CTBN modified epoxy resins was consistent with the miscibility diagram.

Accession For
NTIS GRA&I [X]
DDC TAB [ ]
Unannounced [ ]
Justification
By
Distribution/
Availability Codes
Dist | Avail and/or special
A

FOREWORD

This report covers work performed on Contract F33615-76-C-5108 from April 15, 1976 to April 15, 1978 in the School of Engineering of the University of Pittsburgh. The program was sponsored by the Air Force Materials Laboratory; Dr. T. Helminiak was the Project Engineer. Personnel contributing to the Program were Dr. Michael J. Doyle and Dr. Robert L. Patrick, Principal Investigators; Dr. A. F. Lewis, Senior Materials Scientist, Lord Corp. Dr. P. Agarwal, Dr. H. M. Li, research associates in the Department of Materials Engineering; R. Goldthwaite of the Department of Mechanical Engineering and D. Biber and M. Naccarato, undergraduate research assistants.

TABLE OF CONTENTS

	Page
SECTION I -- SUMMARY	1
1.1 NE-A Nylon-Epoxy Adhesives	1
1.2 RE-A Elastomer-Epoxy Adhesives	1
SECTION II -- INTRODUCTION	3
2.1 Program Objectives	3
2.2 Discussion	3
SECTION III -- NYLON-EPOXY ADHESIVE - NE-A	7
3.1 Materials	7
3.2 Acceptance Tests	7
3.3 Chemical Analysis	7
A. Infra Red Analysis	7
B. Chemical Composition	7
C. Preparation of Model Epoxy-Nylon Adhesive	8
3.4 Time/Temperature Cure Study of NE-A (Nylon-Epoxy) Adhesive	9
3.5 Characterization of Cured NE-A	11
A. Differential Scanning Calorimetry (DSC)	11
B. Dynamic Mechanical Analysis	12
1. Rheovibron: Dynamic Tensile Modulus	12
2. Shear Creep Compliance	12
3.6 Conclusions	13

Page

SECTION IV -- ELASTOMER MODIFIED EPOXY RESIN - RE-A..... 14

4.0 Introduction..... 14

4.1 Materials..... 17

4.2 Acceptance Tests of RE-A..... 18

4.3 Analysis of RE-A..... 18

A. Infra Red Spectrum Analysis..... 18

B. Gel Permeation Chromatography..... 20

4.4 Time/Temperature Cure Study of RE-A Adhesive..... 24

4.5 Characterization of Cured Re-A..... 25

A. Differential Scanning Calorimetry..... 25

B. Dynamic Mechanical Analysis - RE-A..... 25

1. Rheovibron..... 25

4.6 Morphology of RE-A Resin..... 26

A. Optical Microscopy..... 26

B. Transmission Electron Microscopy..... 27

C. Scanning Electron Microscopy..... 28

D. Correlation of the Adhesive Joint Strength and the Morphology of Variously Cured Systems..... 29

SECTION V - MODEL EPOXY-CTBN RESIN SYSTEM..... 31

5.0 Introduction..... 31

5.1 Materials..... 31

5.2 Epoxy-Elastomer Compatibility..... 33

5.3 Gel-Cure Characterization..... 38

A. Experimental..... 38

B. Results and Discussion..... 39

1. Gel-cure phase diagram..... 39

2. Cure history and crosslink density..... 41

3. Modulus and crosslink density..... 42

Page

4. Effect of elastomer adduct..... 43

5.4 Fracture Toughness of Model Rubber Modified Epoxy..... 43

TABLES..... 45

FIGURES..... 55

APPENDIX A -- THE EFFECT OF MOISTURE ON THE MECHANICAL BEHAVIOR OF A NYLON EPOXY ADHESIVE..... 103

SYNOPSIS..... 104

A.1 Introduction..... 105

A.2 Materials and Experiments..... 105

A.3 Results and Discussion..... 108

A.4 Conclusions..... 115

Tables (Appendix A)..... 116

Figures (Appendix A)..... 117

APPENDIX B -- ANALYSIS OF SOME COMMERCIAL EPOXY RESINS USING GEL PERMEATION CHROMATOGRAPHY..... 128

Tables (Appendix B)..... 131

Figures (Appendix B)..... 135

REFERENCES..... 150

LIST OF TABLES

Table		Page
1	Acceptance Test Results of Commercial NE-A Adhesive and Model Resin	45
2	Acceptance Test Results of Commercial RE-A Adhesive	46
3	Characteristic Infra-Red Absorbance Ratios Epoxy-CTBN Adducts Isolated by GPC	47
4	Inclusion Volume Fracitons in RE-A Cured Resin	48
5	Lap Shear Adhesive Strength Tests for RE-A	49
6	Glass Transition Temperature of Model Epoxy Resin versus Isothermal Cure Temperature	50
7	Glass Transition Temperature of Model Epoxy-Rubber Resin versus Isothermal Cure Temperature	51
8	Glass Transition Temperature of Model Epoxy Resin versus Linear Temperature Programmed Cure	52
9	Glass Transition Temperatures (Epoxy Matrix and Rubber Inclusions) of Model Epoxy-Rubber Resin versus Linear Temperature Programmed Cure	53
10	Fracture Toughness of Model Resins (Double Torsion Test)	54
A.1	Temperature Dependence of Shift Factors	116
B.1	Effective Chain Length of Atomic and Functional Groups	131
B.2	Effective Chain Lengths of Various Epoxy Oligomers	132
B.3	Specifications (B.F. Goodrich Co.) of Various Carboxy Terminated Butadiene-Acrylonitrile Copolymers	133
B.4	Specifications of VArious Bisphenol Epoxy Resins	134

LIST OF ILLUSTRATIONS

Figure		Page
1	Molecular Structure of Bisphenol A Diglycidyl Ether (DGEBA) Epoxy Resins.	55
2	Gel Permeation Chromatograms of Selected Commercial DGEBA Epoxy Resins	56
3	Program Schematic	57
4	Infra-red Spectra of Uncured NE-A and Model Adhesives	58
5	DSC Scans of Uncured NE-A and Model Adhesives	59
6	Schematic Rheological "Phase Diagram" for Cure of a Thermoset Resin	60
7	Cure Time-Temperature-Damping Profile for NE-A	61
8	Cure Time-Temperature-Modulus Profile for NE-A	62
9	DSC Scans of Cured NE-A, A; and Model Adhesive; B; Partially Cured NE-A; C; and Elvamide 8061 (nylon), D.	63
10	Dynamic Tensile Modulus, E', versus Temperature for Cured NE-A at 3.5 Hz.	64
11	Dynamic Tensile Modulus, E', versus Temperature for Cured NE-A at 110 Hz.	65
12	Infra-red Spectrum of RE-A, Extracted Resin	66
13	Infra-red Spectrum of Epon 836, Diglycidyl Ether of Bisphenol A Resin, Epoxy Equivalent Weight 290-335	67
14	Infra-red Spectra: (a) Carboxy Terminated Polybutadiene (B.F. Goodrich, CTB 2000 x 162), (b) Carboxy Terminated Polybutadiene-Acrylonitrile Copolymer (B.F. Goodrich, CTBN 1300 x 15)	68
15	Infra-red Spectrum of 2,4 Toluene 1,1' bis (3,3 Dimethyl Urea). Laboratory Preparation, Melting Point 184°C.	69
16,17	Gel Permeation Chromatograms of Epoxy Resins. (Reproduced from Reference 3, F. N. Larsen, Figures 4 and 6)	70
18	Gel Permeation Chromatograms (a) RE-A, (b) Epon 836, (c) Epon 1001 Waters Model 200, Instrument A, Solvent: Toluene	71

Figure		Page
19	Gel Permeation Chromatograms (a) RE-A, (b) Epon 836 Waters Model 200 Instrument B, Solvent: THF	72
20	Gel Permeation Chromatogram of RE-A, Waters Model 200, Instrument B, Solvent: THF	73
21	Infra-red Spectrum of the High Molecular Weight Fraction Separated by GPC (see Figure 20)	74
22	Molecular Structures of Epoxy-Elastomer (CTBN) Adducts	75
23	Gel Permeation Chromatograms of CTBN Adducts	76
24	Infra-red Spectra of CTBN Adducts	77
25	Log Decrement (Damping) versus Time at Different Cure Temperatures for RE-A Adhesive Resin	78
26	Dynamic Modulus versus Time at Different Isothermal Cure Temperatures for RE-A Resin	79
27	Dynamic Mechanical Properties, E' and Tan δ, versus Temperature for RE-A Cured at Different Temperatures: (a) 75°C for 30 Hours (A) and then Post Cured for 2 Hours at 150°C (B); (b) 120°C for 2 Hours; (c) 165°C for 2 Hours	80
28	DSC Scan of RE-A Adhesive Resin. Heating (and Curing) at 10°C/min Followed by Cooling at 5°C/min then Heating at 10°C/min	81
29	Optical Micrographs (with Nomarski Interference Contrast) of RE-A Neat Resin Cured at (a) 75°C/30 Hours, (b) 75°C/ 30 Hrs + 150°C/2 Hrs, (c) 100°C/1.5 Hrs, (d) 100°C/20 Hrs, 500X.	82
30	Optical Micrographs (with Nomarski Interference Contrast) of RE-A Resin Cured at (a) 150°C/1 Hour, (b) 150°C/2 Hrs, (c) 120°C/2 Hrs, (d) 165°C/2 Hrs, 500X.	83
31	Transmission Electron Micrographs of RE-A Resin Cured at (a) 75°C/30 Hours, (b) 100°C/1.5 Hrs, (c) 100°C/20 Hrs, (d) 120°C/2 Hrs, (e) 150°C/2 Hrs, (f) 165°C/2 Hrs. Magnification 3,200X	84
32	Transmission Electron Micrographs of RE-A Resin Cured at (a) 75°C/30 Hrs, (b) 165°C/2 Hrs, (c) 100°C/20 Hrs, (d) 100°C/20 Hrs. Magnification 20,000X	85
33	Scanning Electron Micrographs of Fracture Surfaces of RE-A Neat Resin Cured at (a) 75°C for 30 Hours (b) 120°C for 2 Hours (c) 150°C for 2 Hours (d) 165°C for 2 Hours. Cured Specimens Fractured After Cooling in Liquid Nitrogen	86

Figure		Page
34	Scanning Electron Micrographs of Fracture Surfaces of RE-A Lap Shear Adhesive Joints Cured at (a) 100°C for 90 mins. (b) 100°C for 20 Hours (c) 150°C for Hour. Fractured at R.T.	87
35	Cloud Point Temperature versus Reaction Time for Epoxy-CTBN Resin	88
36	Gibbs Free Energy of Mixing (ΔG) as a Function of Concentration in a Binary Liquid System Showing Partial Miscibility	89
37	Computed Stability Limits for a Two Polymer Mixture with Different Ratios of Weight Averaged Molecular Weights (from Koningsveld ref. 44)	90
38	Miscibility Diagram for CTBN 1300 x 8 Elastomer Adduct with (a) Epon 828, (b) DER 337, (c) Epon 836	91
39	Computed Dependence of Miscibility Gap in Two-Polymer Mixtures on Equation of State Parameters (a) α = Thermal Expansion Coefficient, (b) γ = Thermal Pressure Coefficient, (c) Interaction Energy Parameter, X_{12}. (From McMaster ref. 50)	92
40	Activation Energy Plot for (a) Epon 836, (b) Epon 836/CTBN Cured with 'Bis Urea' Curing Agent	93
41	Rigidity and Damping versus Time (TBA plot) for Isothermal Cure of Epon 836/5% Curing Agent at 80°C.	94
42	Rigidity and Damping versus Time (TBA plot) for Isothermal Cure of Epon 836/5% Curing Agent at 152°C.	95
43	Time-Temperature Gel/Cure Diagram from Isothermal Cure: (TBA Data)	96
44	Rigidity and Damping versus Time (TBA plot) for Linear Heating Rate Cure of Epon 836/5% Curing Agent at 0.047°C/min.	97
45	Time-Temperature Gel/Cure Diagram for Linear Heating Rate Cure, (TBA Data)	98
46	Rigidity and Damping versus Temperature (TBA plot) of Epon 836/5% Curing Agent Cured for 200 Hours at 80°C.	99
	(a) Decreasing Temperature from 80°C → -190°C	100
	(b) Increasing Temperature from -190°C → 200°C	
	(c) Decreasing Temperature from 200°C → -190°C	

Figure		Page
47	Rigidity and Damping versus Temperature (TBA plot) of Epon 836/5% Curing Agent Cured at (a) 125°C for 124 Hours, (Isothermal) (b) 0.047°C/min to 200°C, (Linear Heating Rate) (c) 5.0°C/min to 200°C, (Linear Heating Rate)	101
48	Schematic Load versus Displacement Plot for Double Torsion Test Illustrating "Stick-Slip" Crack Propagation	102
A.1	Setup for the Sample Molding	117
A.2	Logarithmic Plot of the Measured Compliance $(J(t)\ \frac{T\cdot\rho}{T_o\rho_o})\ cm^2/dyne$ versus Time, t, sec, for Sample I-D at the Indicated Temperatures.	118
A.3	Semilogarithmic Plot of the Inverse Compliance versus Temperature °C at Three Frequencies viz, 6.28, 6.28×10^{-2}, 1.99×10^{-3} radians/sec.	119
A.4	Logarithmic Plot of the Measured Compliance versus Time for Sample II-W at the Indicated Temperatures	120
A.5	Logarithmic Reduced Creep Curve for the Sample II-W, a_T is the Shift Factor for the Creep Compliance. Reference Temperature T_o = 43.7°C	121
A.6	Logarithmic Plot of the Measured Compliance versus Time for Sample II-D at the Indicated Temperatures	122
A.7	Logarithmic Reduced Creep Curve for the Sample II-D, a_T is the Shift Factor for the Creep Compliance. Reference Temperature T_o = 43.7°C	123
A.8	Semilogarithmic Plot of Shift Factors versus Temperature °C and versus Inverse of Absolute Temperature $°K^{-1}$	124
A.9	Logarithmic Plot of the Reduced Curves of Samples II-W and II-D. Reference Temperature T_o = 43.7°C.	125
A.10	Plot of Creep Compliance versus Time According to Equation A.4 on a Normal Probability Graph Paper.	126
A.11	Logarithmic Plot of the Retardation Function, L, versus Retardation Time, t, for Samples II-W and II-D. Reference Temperature T_o = 43.7°C.	127
B.1	Infra-red Spectra of DGEBA Epoxy Resins; Dow Chem: DER 332,337,661	135

Figure		Page
B.2	IR Spectra of DGEBA Epoxy Resins; Dow Chem. DER 667, Shell Chem. Epon 1001, Shell Chem. Epon 1031, tetra glycidyl ether of 1,1',2,2' tetrakis p-hydryxy phenyl ethane	136
B.3	IR Spectra of Carboxy Terminated Butadiene-Acrylonitrile Elastomers: CTBN 1300 x 15, CTBN 1300 x 8, CTBN 1300 x 13 (B.F. Goodrich Co.)	137
B.4	IR Spectra of CTBN Elastomers: CTBN 1300 x 9 and CTBN x 1300 x 18	138
B.5	IR Spectra of Carboxy Terminated Butadiene Elastomer CTB 1200 x 162, and Butadiene-Acrylonitrile Elastomer Hycar 1072	139
B.6	Gel Permeation Chromatograms (GPC); THF Solvent, Instrument B: (a) DER 661, (b) DER 337, (c) Epon 1001, (d) DER 667	140
B.7	GPC Chromatograms; THF Solvent, Instrument B: (a) CIBA 6060, (b) Epon 1031, (c) Epi-Rez 520-C, (d) Epi-Rez 540-C	141
B.8	GPC Chromatograms of Epoxy Resins Prepared by the "Taffy" Process and by the "Advancement" Process. (Reproduced from Batzer and Zahir, Ref. 6, Figures 4 and 5)	142
B.9	GPC Chromatograms of Intermediates in Epoxy Resin Syntehsis. (Reproduced from Batzer and Zahir, Ref. 12, Figure 4)	143
B.10	Elution Volume versus Effective Chain Length (Data from Figure B.8)	144
B.11	GPC Chromatograms of Commercial DGEBA Epoxy Resins: Epon 1004, DER 664, UCC 2013 (Union Carbide), CIBA 6084, (Reproduced from Beisenberger, et al., Ref. 9)	145
B.12	Elution Volume versus Effective Chain Length (Data from Figure B.11)	146
B.13	Elution Volume versus Effective Chain Length for Epon 836. (Data from Larsen, Ref. 3, see Figure 17 above)	147
B.14	Elution Volume versus Effective Chain Length for Epon 1001. (Data from Larsen, Ref. 3, see Figure 17 above)	148
B.15	Elution Volume versus Effective Chain Length for RE-A. Data from Figure 19a.	149

SECTION I

SUMMARY

1.1 NE-A Nylon-Epoxy Adhesives

Chemical composition analysis, dynamic mechanical analysis and adhesive joint strength tests have been carried out on a commercial nylon-epoxy adhesive, hereafter referred to as NE-A. Torsional creep compliance, J(t), was measured from 43°C to 160°C, and provided a complete viscoelastic characterization of the cured adhesive in the linear range. The time-temperature cure behavior was determined by the torsional braid analysis (TBA) technique from which a rheological 'phase state' cure diagram was constructed. DSC experiments on the uncured film indicated the presence of crystallinity in the nylon component. Some evidence was also found for an enthalpy relaxation; for cured material the apparent Tg, which is close to room temperature, increased on storage under dry conditions. The Tg decreased on absorption of moisture as might be expected for a composition containing 65% nylon.

A model epoxy-nylon material was formulated containing:

resorcinol diglycidyl ether	25 parts
Epon 1031	10 parts
Elvamide 8061 (Nylon)	65 parts
Diallyl melamine	4 parts

which was equivalent to the commercial resin on the basis of infra-red spectra, DSC analysis and adhesive joint strength tests.

The investigation of the nylon-epoxy materials was discontinued after six months into the program.

1.2 RE-A Elastomer-Epoxy Adhesives

Adhesive joint acceptance tests were carried out on a commercial elastomer modified epoxy adhesive; the test data ran generally lower than manufacturer's specifications but higher than the Mil. Specs. Characterization of the commercial

material, hereafter referred to as RE-A, included a complete gel-cure study using TBA, dynamic mechanical spectroscopy with the Rheovibron from -100°C to 200°C and DSC thermograms of uncured and cured film. Analysis of RE-A by gel permeation chromatography (GPC) and infra red (IR) spectrum analysis showed a bisphenol A diglycidyl ether epoxy resin identical to Epon 836 (Shell Chemical Co.), a carboxy terminated acrylonitrile-butadiene copolymer ("elastomer") identical to CTBN 1300 x 8 (18% AN) (B. F. Goodrich) and a curing agent, 2,4 toluene-1,1' bis (3,3 dimethyl urea) which is not commercially available.

A model elastomer-epoxy was formulated containing:

Epon 836	90 parts
CTBN 1300x8	10 parts
Curing agents	5 parts

which was equivalent to RE-A on the basis of GPC, IR spectrum and dynamic mechanical spectroscopy. The phase separation properties of the model CTBN elastomer-epoxy resin mixture (uncured) were characterized using the cloud point technique. From the TBA analysis of the cure behavior it was found that the Tg of the cured resin varied from 100°C to 130°C depending on the cure cycle even when postcured at high temperature until all reaction was exhausted. The highest glass transition temperature was observed for the slowest cure cycle investigated: 30°C → 200°C at 0.05°C/min.

SECTION II

INTRODUCTION

2.1 Program Objectives

The objective of this program was to develop quantitative methodology for correlating the molecular structure and morphology of polymeric adhesive systems and their mechanical strength properties. In the first phase of the program two representative commercial adhesives were to be characterized and analyzed followed by the preparation and characterization of matching formulations from known, well characterized constituent materials. From these reference materials others would be prepared using controlled variation of chemical composition and morphology. In the second phase of the program the above families of materials were to be characterized by parameters related directly to molecular structure and by those engineering properties relating to strength and toughness. The goals of the first phase were acheived although with considerably more time and effort than had been planned; the goals of the second phase were not achieved although some new results of some interest and importance were found.

2.2 Discussion

High performance structural adhesives for applications in aircraft are commercially available. The more important properties required of these materials are high toughness and low creep over the temperature range from -65°F to 250°F and durability under high humidity. Roughly equivalent mechanical performance may be obtained from formulations based on epoxide thermosetting resins containing either a nylon resin or an elastomer as a modifying agent. The nylon modified resins suffer from high sensitivity to moisture with a deterioration of mechanical properties and are no longer satisfactory for the above mentioned application. The "new technology" adhesives depend on the use of elastomeric (usually nitrile rubber) materials

as a toughening agent. Since these two classes of adhesives appear to represent two different mechanisms for achieving toughness two commercial resins were chosen for study as prototypes for the model materials.

For engineering purposes it is necessary to characterize the stress-strain, strength and fracture properties of the adhesive system as a function of stress state, time, temperature and chemical environment (e.g., moisture, jet fuel and hydraulic fluid); in what follows the term "mechanical properties" is understood to include all of these variables. The material parameters which appear in the constitutive equations relating stress and strain are, for example, the elastic moduli, Poisson's ratio and the yield stress. The small strain elastic modulus is determined by the interatomic forces, or more exactly by the repulsive interaction forces, and would be expected, in the case of an amorphous isotropic polymer, to correlate with the chemical composition and the nature of the chemical bonding. The plastic flow and strength properties however usually depend more strongly on microstructural heterogeneities at some supramolecular level than directly on the molecular structure. Among polymeric materials a well developed connection between molecular structure and constitutive behavior is found in rubber elasticity; more recent statistical mechanical approaches can, in principle, take into account the detailed conformational properties of the polymer chains (1,2). For elastomer networks with relatively simple structures agreement between theory and experiment is good. In the highly crosslinked glassy epoxy resins studied in the present program, the network structures are far more complex. There are several difficulties to the development of a full molecular theory of mechanical behavior. Firstly, since the network arises from the chemistry of the crosslinking (curing) reaction different topologies for the final state may arise from different cure histories, particularly where more than one chemical

crosslinking reaction is possible. Secondly, for the class of materials to be studied, e.g. the bisphenol A diglycidyl ether (DGEBA) epoxy resins (Figure 1), the molecular species include different molecular weights in a way which may not be usefully characterized by the usual average molecular weight parameters. Examined by gel permeation chromatography (GPC) the Shell Epon 1001 DGEBA type epoxy resin, for instance, shows (3) an apparently smooth distribution (Figure 2) of higher molecular weight oligomers but significant fractions of the lower molecular weight oligomers n=0, and n=2 are also present. A third and controversial (4) aspect is the existence of "nodules", heterogeneities on the scale of tens of Ångströms, in cured epoxy resins. The nodules are observed directly by transmission electron microscopy and predicted theoretically, in the case of crosslinked systems, as crosslink density fluctuations arising from developing configurational constraints during the cure reaction (5).

For both types of modified epoxy systems, NE-A and RE-A, there are also larger heterogeneities on the scale of 10 to 10^3 nm which would be expected to have a large effect on the strength properties of the cured resins. It was found that the nylon in the uncured NE-A may exist as spherulites which suggests the possibility that the nylon may persist as a separate phase after cure. In the RE-A, elastomer modified epoxy system, it is clear that the rubber component exists mostly as a distinct, separate phase whose presence is of critical importance to the mechanical behavior of the adhesive. The rubber modified epoxies, as a generic type, are composites containing inclusions embedded in a rigid, continuous matrix. It is expected, then, that the mechanical properties of the composite can be understood in continuum mechanics terms on the basis of the morphology of the composite and the mechanical properties of the individual phases. The dependence of the mechanical properties of the latter on molecular structure could, once their composition is established, then be attempted as separate

tasks. This general approach is illustrated in Figure 3. The properties and structure of the interface (or interphase) may or may not be critical depending the limiting modes of failure. Some interfacial strength is necessary, of course, to transmit force between the inclusion and the matrix.

SECTION III

NYLON-EPOXY ADHESIVE - NE-A

3.1 Materials

Thirty square feet of unsupported 10 mil film of NE-A was obtained from the manufacturer, wrapped and stored in a freezer at $0^{\circ}F$.

3.2 Acceptance Tests

Adhesive joint specimens for lap shear and $180^{\circ}T$ peel tests were fabricated using NE-A and aluminum sheet according to MMM-A-132 specifications. The test conditions used were also taken from the same specification. The adhesive joints were formed in a jig to give the required bond line thickness and cured at $350^{\circ}F$ for 1 hour as recommended by the manufacturer. The test results are shown in Table 1. The data exceed the specifications claimed by the manufacturer and of the MMM-A-132 specification except for the R.T. lap shear which is 3% lower.

3.3 Chemical Analysis

A. Infra Red Analysis

From review of the technical and patent literature a number of typical epoxy and nylon components were selected. Infra-red spectra of these materials were compared with that of the uncured NE-A both as solid films and dissolved in methylene chloride/methanol (60/40) solvent mixture run against pure solvent as reference.

B. Chemical Composition

On the basis of these experiments the following composition was derived:

Resorcinol diglycidyl ether, (Heloxy 69)	25 pts
1, 1', 2, 2' tetra p-hydroxy phenyl ethane tetra glycidyl ether (Epon 1031)	10

Elvamide 8061	65
Diallyl melamine	4

C. Preparation of Model Epoxy-Nylon Adhesive

Solutions of the above formulation in methanol/chloroform mixture (80/20) were treated as follows:

1. K milled
2. High speed stir mixed with 0.5% Cab-O-Sil added
3. K milled with 0.5% Cab-O-Sil

Films were drawn down on glass plates using a 50μ gauge. Best results were obtained by method 3; use of Cab-O-Sil with good dispersion was found necessary to prevent segregation of the components during drying.

Films of this basic formula were prepared with and without 4% dicyandiamide (dicy). Their infra-red (IR) spectra are shown in Figure 4 and compared to the IR spectrum of the commercial NE-A material. Each absorption band present in the NE-A spectrum is duplicated in the model material and the ratios of absorbance of primary amide (3.4 microns) to epoxide (10.9 microns) are also in agreement. The determination of the exact structure of the nylon copolymers is difficult on the basis of IR alone (6). However, our spectrum for Elvamide 8061 appears to be identical with that shown in the literature (6) for a nylon 6:6/6:10; 40/30/30 terpolymer. Confirmation of this could be obtained by hydrolysis of the Elvamide and identification of the products.

A thin film of Elvamide 8061 was observed to form spherulites after melting at 160°C on the hot stage microscope and cooling to about 100°C. This raises the possibility of variable crystalline morphology in the uncured adhesive film and possibly in the cured material; alternatively, this agregation of the nylon prior to curing may result in heterogeneities in the cured material.

Figure 5 shows DSC heating curves (10°C/min) for the uncured commercial NE-A and the model adhesive compound. The curves both show a gradual endothermal fusion region with a peak at about 135°C followed by an exothermic peak at 220°C. The former transition corresponds to melting of the nylon crystallites and the latter is the cure reaction.

Lap shear specimens were prepared using the model adhesive formulation and tested at R.T. as described above. The results, shown in Table 1, indicate that the lap shear strength of the model nylon-epoxy adhesive is comparable to that of NE-A.

3.4 Time/Temperature Cure Study of NE-A (Nylon-Epoxy) Adhesive

The cure behavior of thermosetting resins (rate, degree and chemo-kinetic mechanism) is one of the most poorly understood areas of polymer resin science (Resinology). To this end, some useful studies in developing an understanding of thermosetting resin cure processes have been reported in the early work on the dynamic mechanical properties of supported polymers by torsional and flexural braid analysis by Lewis and Gillham (7,8).

In later work by Gillham and coworkers (9) the cure behavior of an epoxy resin/anhydride system was studied using torsional braid analysis (TBA) with reference to the gelation, vitrification, and rheological phase changes that occur during cure and characterize the thermal cure of the resin system. Collectively combining the general cure data and the concepts described in references (8) and (9), a time/temperature cure "phase diagram" (Figure 6) has been constructed which illustrates, schematically, the cure time/temperature behavior of a curing liquid epoxy resin (a Bisphenol A diglycidyl ether epoxy resin cured with diethylene triamine for example). At very low temperatures the resin/curative system "freezes" and little curing occurs. At higher

temperatures, where the resin/curative system becomes a viscous liquid, cure can proceed at a rate which increases as the temperature. At room temperature the cure proceeds or traverses the full range of polymeric, rheological state "phase" changes; from liquid through gelation point to rubbery phase and finally to the glassy state (this isothermal cure line is noted in Figure 6). At some higher cure temperature (above the Tg of the finally cured resin), the curing resin traverses from the liquid range through the gelation point and directly into the rubbery region; at a still higher "critical" cure temperatures time dependent degradation of the resin system will occur. The above scheme provides the basis for the study of the cure behavior of the NE-A adhesive system.

Uncured NE-A adhesive film was dissolved in a methanol/methylene chloride solvent mixture and coated onto glass yarn braids. After evaporating the solvent in the absence of moisture, isothermal cure experiments were performed (in a dry nitrogen atmosphere) on the NE-A coated braids using the dynamic mechanical torsional braid analysis technique (10).

Cure time/temperature dynamic mechanical property "phase" diagrams were sketched according to the data obtained. A summary of these data are presented in Figure 7 (log decrement) and Figure 8 (apparent torsional modulus*; see footnote below). These two Figures attempt to display a three-dimensional (contour mapping) profile of the experimental dynamic mechanical data and present a

---

*Footnote: In the present case, since all the braids were identically coated with approximately the same amount of NE-A the "apparent" shear modulus for each braid was estimated from the equation $\bar{G} = 8\pi f^2 I/r^4$ where $\bar{G}$ is the apparent shear modulus, π the length of the braid, f the vibration frequency, r the (averaged) radius of the coated glass braid and I the moment of inertia of the free vibration pendulum mass.

general time/temperature cure profile for the NE-A adhesive system; the gelation line separating the liquid and rubbery region is clearly illustrated. The latent nature of the curative in the NE-A system is also evident; there is no cure at lower temperatures.

Figures 7 and 8 uniquely display the time-temperature cure behavior of the NE-A thermosetting adhesive system; the data presented (although incomplete) illustrates the value of the TBA approach in describing the rheological state "phase diagramming" of complex resin systems.

3.5 Characterization of Cured NE-A

A. Differential Scanning Calorimetry (DSC)

The thermal behavior of cured adhesive films was studied with the Perkin Elmer DSC 1B scanning calorimeter. Scans at 10°C/min of NE-A and the model nylon-epoxy both cured for two hours at 175°C are shown in Figure 9 (curves A and B respectively). The transition at 30°C corresponds to a "glass transition" associated with the nylon polymer (c.f. curve D) shifted to a higher temperature presumably by the epoxide crosslinks. The exothermic peak at 60°C associated with crystallization of the nylon (c.f. curve C) is not observed in the cured material. This observation does not, however, eliminate the possibility of some form of microcrystallinity.

Subsequent observations suggested that the "glass transition" of the dried cured film as measured by DSC increases with storage (in a dessicator) at room temperature. Our preliminary interpretation of this phenomenon is that it is due to enthalpy relaxation. Similar effects are observed in other polymers annealed at temperatures up to 30°C below their glass transition temperatures (11,12). This effect has important practical consequences for the conditioning of materials prior to measurement of any properties.

B. Dynamic Mechanical Analysis

1. Rheovibron: Dynamic Tensile Modulus

The dynamic tensile modulus (E*) and loss tangent (tan δ) of cured and dried NE-A (0.05 mm thick) were measured on a Rheovibron (Toyo Instrument Co.) at 3.5 Hz and 110 Hz from 20°C to 200°C. The usual procedures for correcting the measurements for the specimen length effect were followed and the calibration of the instrument was checked using a standard Mylar (polyester film) specimen. From the corrected data shown in Figures 10 and 11, the value of the glassy modulus, 2.7×10^{10} dynes/cm^2, is in good agreement with the value of 2.6×10^{10} dynes/cm^2 reported by Butt and Cotter (13) for a commercial nylon-epoxy adhesive (NE-A) also determined on a Rheovibron instrument.

The glass transition at 62°C (3.5Hz) is higher than that from DSC results (40°C) because of the higher frequency. After exposure of the cured film to ambient conditions for several hours the Rheovibron measurements showed that the transition temperature had decreased by 15°C. The nylon polymers are notoriously sensitive to moisture absorption.

The value of the apparent molecular weight between crosslinks, $\bar{M}c$, was 2886 g/g-mole as calculated from the observed modulus in the rubbery region:

$$\bar{M}c = \frac{3\rho RT}{E} \qquad (1)$$

2. Shear Creep Compliance

A detailed study of isothermal creep and creep recovery properties of NE-A has been carried out using a sensitive creep apparatus which employs a frictionless levitation magnetic bearing. Isothermal creep measurements over a temperature range of 30-170°C and covering a time scale of 5 decades were made on the wet and dry state of the material. Following the usual time-temperature reduction scheme, master curves for each state were constructed from the

experimental data. The principal findings were that the moisture caused more than a simple plasticizer effect. The slope of the reduced curves in the transition region was determined and the distribution function of retardation times of the two states of the sample were calculated. The problem of predicting the physical state of the bulk adhesive at higher temperatures was found to be complicated, possibly due to the presence of nylon crystallites. These experiments are described in detail in the separate manuscript in Appendix A.

3.6 Conclusions

From the results of infra-red and DSC analyses and adhesive joint strength tests the model nylon-epoxy adhesive material with the formulation given in section 3.3 appears to be equivalent to commercial NE-A.

The main glass transition occurs at about 40^{o}C and is sensitive to moisture content so that the rheological properties of the adhesive will vary considerably over the range of expected operating conditions. The tests also suggest that the morphology and therefore the results of characterization tests will be sensitive to the thermal and processing histories of the material.

In view of the experimental difficulties in characterization of this class of nylon-modified epoxies portended by the above observation and the diminished interest in these materials for high performance adhesive applications work on the NE-A system was discontinued.

SECTION IV

ELASTOMER MODIFIED EPOXY RESIN - RE-A

4.0 Introduction

The current interest in rubber toughened epoxies centers on the use of a reactive prepolymer-carboxyl terminated butadiene-acrylonitrile copolymer (CTBN) which, when mixed with epoxy resin and cured, separates out as a rubbery phase (including some epoxy resin) as small ($\sim 10^3$ nm), roughly spherical inclusions. In their recent and comprehensive review of CTBN-epoxies Drake and Sibert (14) view this technology as an analogue of the much earlier nitrile rubber modified phenolic resins. Although CTBN is the usual choice for the elastomeric component, equivalent rubber toughening of epoxies has been accomplished (15) with carboxy terminated isoprene/acrylonitrile (CTIN), ethyl acrylate-butyl acrylate (CTA), and butadiene (CTB) copolymers. The criteria (14) for a significant rubber toughening effect appear to include:

1. a discrete second phase of rubbery inclusions
2. chemical bonding between rubber particles and matrix
3. the correct particle size

Similar criteria have been established for rubber toughening of glassy thermoplastics (16). Rubber toughened epoxy systems show improvements in fracture toughness, fatigue properties, and impact strength.

The main feature of this class of materials is the phase separation which occurs during cure and the advantageous mechanical properties thus conferred on the cured material. The thermodynamics of phase separation in rubber-epoxy resin mixtures has been discussed by Sultan (17) and by Bucknall and Yoshii (18) with reference to the Flory-Huggins theory. An initially homogeneous mixture will demix when the Gibbs free energy of mixing, ΔG_m, becomes positive; for the mixing of two polymer species ΔG_m is given by (19)

$$\Delta G_{mix} = \frac{RTV}{V_R}\left[\frac{V_A}{X_A}\ln V_A + \frac{V_B}{X_B}\ln V_B + \chi_{AB} V_A V_B\right] \qquad (2)$$

where V is tht total volume of the mixture, V_R is a reference volume which is taken as close to the molar volume of the smallest polymer repeat unit as possible, V_A and V_B are the volume fractions of polymer A and polymer B in the mixture, X_A and X_B are the degree of polymerization in terms of the reference volume, V_R, respectively, and χ_{AB} is the interaction parameter between the two polymers. χ_{AB} is related to the enthalpy of interaction of the polymer repeat units, each of molar volume, V_R, and is given by

$$\chi_{AB} = \frac{V_R}{RT} (\delta_A - \delta_B)^2 \qquad (3)$$

where δ_A and δ_B are the Hildebrand solubility parameters. In the more recent methods of toughening epoxy resins, carboxy terminated elastomer prepolymers are prereacted with an excess of diepoxide to form an adduct. In this case the two polymers A and B mentioned above would both be linear diepoxide species one of which would contain within it an elastomer moeity the other would not. The last term in Equation 2 is the enthalpy term and is always positive, the preceding terms represent the entropy of mixing which is always negative.

As each species increases in molecular weight the entropic terms in Equation 2 becomes numerically smaller until eventually ΔG changes from negative to positive and phase separation is thermodynamically favored and phase containing the elastomer is precipitated. Although these general principles provide a useful qualitative description, real polymer mixtures are far more difficult to describe in detail (20,21,22). This topic is discussed further in Section V in connection with some experimental compatibility studies.

From the initial mixture of ingredients in a typical resin mix the composition of the growing macromolecules is determined by the chemical selectivity and reactivity of each of the various molecular species present during the curing reaction; the chemistry of the CTBN-epoxy reactions has

been discussed in detail by Siebert and Riew (23) and provides considerable insight into the likely chemical compositions of the continuous and the dispersed phases.

The only published studies on structure-morphology of CTBN-epoxy systems and ultimate mechanical properties are by McGarry, et al. (24,25,26,27), Siebert, et al. at B. F. Goodrich (14,15,23) and more recently, Bucknall (18). Other mechanical studies of fracture behavior have been carried out by Bascom, et al. (29,30) and Mostovoy, et al. (31). The principal observations from their work may be summarized as follows:

1. Toughening as measured in crack propagation experiments is optimised by a certain concentration of rubber and a certain size range for the precipitated inclusions (24). Bucknall's work (18), however, shows that the fracture toughness is linearly proportional to the rubber phase volume (as distinct from the fraction of CTBN added in the formulation); the particle size was of secondary importance.
2. Yield behavior is also dependent on particle size (27). Very small (100 nm) inclusions reduce the yield stress whereas larger particles ($1\text{-}2 \times 10^3$ nm) reduce the yield stress but follow a different yield criterion under multiaxial loading. When both principal stresses are tensile a cavitational type of yielding occurs (the material stress-whitens); when one principal stress is tensile and the other compressive then the usual shear yielding occurs. The origin of this particle size effect is not known.
3. For a given fixed chemical composition of epoxy resin and rubber prepolymer (CTBN) mixture the size and volume fraction of the inclusions after curing the mixture is dependent upon the choice of curing agent and the cure temperature (24,18).

4. The fracture toughness of CTBN toughened epoxy resins is rate sensitive, e.g. the apparent K_c is a function of crack velocity (29,30).

5. The 'toughness' of a CTBN-epoxy adhesive bond is strongly dependent on the characteristic size of plastic zone at the crack tip in relation to the thickness of the adhesive layer (29).

One factor not accounted for in the above work is a possible variation in the mechanical properties of the inclusion itself as a function of its size, which is not unlikely since the particle size was controlled by varying the chemical kinetic parameters, e.g. temperature, curing agent, etc. The importance of the gel-cure conditions on morphology and properties has recently been elegantly demonstrated by Gillham (32) using the TBA technique.

The observation by Bascom that the toughness of adhesive joints formed from rubber modified epoxies is a function of the size of the crack tip plastic zone in relation to the bond line thickness suggests that the usual methods of measuring fracture toughness of adhesive joints based on linear elastic fracture mechanics are of limited applicability to more ductile materials (33).

4.1 Materials

Twenty-eight square feet of RE-A supported film (0.085 lbs/sq.ft. on mat carrier, unsupported film is not available) was obtained from the manufacturer. The material was wrapped and stored in a freezer at $0^{\circ}F$.

4.2 Acceptance Tests of RE-A

Adhesive joint specimens for lap shear and 180°T-peel tests were fabricated from RE-A and aluminum sheet according to MMM-A-132 specifications. The adhesive joints were formed in a jig to give the required bond line thickness and cured at 300°F for 1 hour as recommended by the manufacturer (another set was prepared at a cure temperature of 250°F). The test results, obtained under conditions given in the above specification, are shown in Table 2. The data were less than the manufacturer's specifications; some large void defects were observed in the adhesive layer and the bond line thickness was not uniform.

4.3 Analysis of RE-A

A. Infra Red Spectrum Analysis

RE-A adhesive was only available to us as supported film on polyethylene terephthalate scrim. In the initial work the resin was extracted from the as received film by soaking in chloroform overnight at room temperature. Subsequently, some discrepancies observed in the infra-red spectra of GPC fractions obtained from these extracts indicated polyester contamination. From the literature it is known that PET contains low molecular weight (mostly cyclized) oligomers extractable with hot chloroform (34) although the quantity, 1.5%, seemed too small to explain the observed discrepancies. From inquiries to Du Pont it was learned that Reemay, a Du Pont spun bonded non-woven PET mat, contains from 10 to 15% of polyethylene isopthalate which acts as a low melting point binding agent in the manufacturing process. Our examination of samples of Reemay showed that in a 24 hour soak in chloroform at room temperature there was a 5% weight loss. Toluene, methanol, methyl ethyl ketone and trichloroethylene were found to produce no measurable weight loss under similar conditions.

Films of adhesive resin, extracted from the carrier mat with toluene, were solvent cast on dry sodium chloride plates. Infra red spectra were obtained on a Beckman AccuLab 4 Spectrophotometer at a scan speed of 7.5 min/scan. The spectrum of RE-A, Figure 12, shows all the absorption bands characteristic of the bisphenol A diglycidyl ether (DGEBA) epoxy resins; e.g. hydroxyl (2.9 μm), aromatic ether (8.1 μm), aliphatic ether (9.6 μm) and the para substituted benzene nucleus (12.0 μm). The terminal oxirane (epoxy) group absorbs at 10.0 μm and at 11.6 μm (6), (35), (36), (see also spectra of commercial DGEBA resins shown in the Appendix). Noticeable additional absorptions compared to DGEBA epoxies are at 5.85 μm, characteristic of the carboxylic ester group; at about 6.2 μm; increased absorption at 10.35 μm; and a weak but definite absorption at 4.4 μm characteristic of nitrile. These comparisons can be made from Figures 12 and 13.

The absorption at 10.35 μm could be due to 1,4 trans unsaturation. This combined with the ester group immediately suggested the possible presence of a carboxy terminated butadiene polymer (Figure 14). It was found that conversion of the free carboxylic acid end group to ester by reaction with an epoxy resin shifted the carbonyl absorption to the same position as observed in the IR spectrum of RE-A. It is well known that "end group modification" of carboxy terminated elastomers improves their compatability with epoxy resins and generally improves properties of the cured resin mixtures (15).

It was learned from an independent study that the curing agent in RE-A was 2,4 tolylene-1,1-bis(3,3-dimethyl urea). Since this material was not commercially available it was synthesized in the laboratory: 2,4 toluene diisocyanate (Fisher Scientific Reagent grade) was added to dimethylamine (Fisher Reagent) in a small r.b. flask, the desired adduct immediately separated out as a white crystalline solid; its melting point was 184°C.

The IR spectrum of this material, Figure 15, shows a strong absorption at 6.0 μm coinciding with a band at the same wavelength in the RE-A spectrum.

B. Gel Permeation Chromatography

Epoxy resins based on bisphenol A can be manufactured by two different methods, both methods lead to products having the same structural formula, Figure 1. In the so-called "taffy" process, bisphenol A is reacted with epichlorohydrin in alkaline conditions. The molecular weight of the resin produce is controlled by the ratio of the two reactants:

The product of this process contains all the diepoxide oligomers. The exact distribution of oligomers depends of course on the ratio of reactants and the degree of reaction. In the "fusion" or "advancement" process the diepoxide oligomer k=0 is condensed in varying ratio with bisphenol A in a base catalysed reaction:

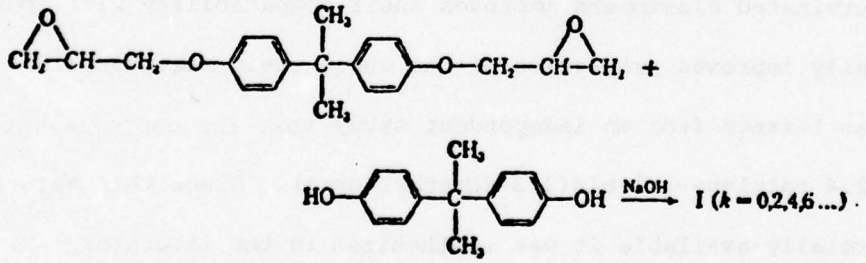

In this process only the even oligomers k=0,2,4,--- are produced.

The composition of a DGEBA epoxy resin in terms of the distribution of the various oligomers can be determined by gel permeation chromatography (GPC) where the usual general purpose instruments can separate oligomers corresponding to k=0,1,2 and 3 but the higher oligomers usually elute as a single broad peak. Higher resolution e.g. up to k=7 or 7 can be obtained with multiple columns (37), and with the gradient separation technique (38) resolution up to k=24 has been obtained. Results of GPC analysis of commercial epoxy resins have been published (3,38,39,40). The most comprehensive study was by Larsen but unfortunately there appears to have been an error in the peak assignments and an impurity peak was assigned as k=1. In Larsen's results reproduced here (Figures 16 and 17) this error has been corrected as indicated. In other results published by Dark, et al. (38) it was found that of two different lots (41) of Epon 1004 one contained even and odd oligomers (Figure 15, ref. 38) while the other contained only the even oligomers (Figure 16, ref. 38). Evidently even though the two resins carried the same product number they were manufactured by a process involving different chemistries and actually contained different molecular weight compositions. A detailed discussion of the molecular weight distribution for epoxy resins of the same epoxide equivalent weight made by the two processes is given in the studies of Batzer and Zahir (37,42). Furthermore we have found that the Epon 836 used in our work contained only the even oligomers and was evidently manufactured by the "fusion" process. This is in contrast to the earlier finding of Larsen (see Figure 17, c.f. Figure 19) where Epon 836 was made by the "taffy" process.

In our analysis of RE-A two different GPC units have been used. Figure 18 shows gel permeation chromatograms for RE-A and Epon 836 obtained on a Waters Model 200 Chromatograph (instrument A) with a bank of four Poragel columns with

pore sizes of 500, 250, 100 and 60 Å in series with toluene as a solvent; 1% w/v solutions were injected for two imnutes and the flow rate was 0.53 cc per minute for the sample side at a pressure of 35-40 psi. The detector was a differential refractometer. The peaks at counts 22.5 (and shoulder at 21.5), 24.6, 26.5, 30.2 and 32.0 correspond exactly in both resins. Differences occur at the low molecular weight end at count 37. These peaks in the epoxy resin are probably due to impurities such as epichlorohydrin. The enhanced peak at count 37 corresponds, however, to the elution count for acetone as determined in a separate run thus suggesting that acetone may be a solvent used in the processing of the RE-A. The additional peak at count 19.4 was found to correspond to the elastomer adduct. Further work to establish this was also done on a Waters Model 200 but a different instrument (instrument B): four columns of 50/80, 80/100, 700/2000, and $5 \times 10^3/1.5 \times 10^4$ Å pore sizes were used with tetrahydrofuran solvent. Solutions were 2% w/v and the detector was again a differential refractometer. Chromatograms of RE-A and Epon 836 are shown in Figure 19; the correspondence is excellent. The peaks beyond count 33 are due to THF impurities and inhibitors. In none of our GPC analyses of RE-A have we been able to identify a peak attributable to the curing agent. This is probably because in addition to its low concentration its effective molecular volume is not much different from the lowest molecular weight DGEBA oligomer. This point is discussed further in the Appendix B.

In order to identify the elastomer adduct in RE-A a careful fractionation of the extracted resin was performed on a Waters Model 200 GPC unit (Instrument B) with THF solvent. Solutions, 2% w/v, were injected for two minutes at a flow rate of 0.53 cc/minute for the sample side at a pressure of 35 psi. The chromatogram is shown in Figure 20; the fraction at count 21 corresponds to the

elastomer adduct. Three rounds of injections were applied to the column to collect, between counts 18 and 22, sufficient material for an IR spectrum analysis which is shown in Figure 21. The clear absorption band at 4.4 μm is confirmation for the presence of acrylonitrile in the elastomer component of RE-A.

Three model adduct materials were prepared by reacting Epon 836 epoxy resin with three different carboxy terminated acrylonitrile-butadiene copolymers at 1:1 ratio by weight for two hours at 170°C with 0.3% triphenyl phosphine catalyst. The reaction products, shown schematically in Figure 22, were then fractionated by GPC as described above; a typical chromatogram is shown in Figure 23. The higher molecular weight fractions, of the adduct type shown in Figure 22, were collected and IR spectra, Figure 24, obtained for each. Absorptions were calculated from the spectra for several different characteristic bands and the absorption ratios calculated for each adduct and compared, Table 3, with similar calculations on the IR spectrum obtained on the adduct material fractionated from RE-A itself. An excellent match was obtained with the adduct prepared from Hycar CTBN-1300 x 8, which contains 18 wt% acrylonitrile. Several model resins were prepared based on Epon 836 with varying amounts of CTBN (18% AN) epoxy adduct). Based on comparison of IR spectra of some model compositions with that of RE-A resin the estimated composition of the latter is:

Epon 836	90 parts
CTBN (1300 x 8)	10 parts
Curing agent	5 parts

4.4 Time/Temperature Cure Study of RE-A Adhesive

A time/temperature cure study of the rubber modified epoxy adhesive RE-A was conducted employing the Torsional Braid Analysis (TBA) technique. The dynamic mechanical damping (log decrement) and moduli (apparent modulus) of adhesive coated glass fiber braids (braids coated from MEK solution of the adhesive) were determined at several temperatures in a dry nitrogen atmosphere. The changes in damping and modulus that occurred were followed for over one week (∿10,080 minutes) at the various temperatures (50°C, 75°C, 100°C, 125°C, and 149°C). The data obtained are presented in Figures 25 and 26 where the changes in rheological state during cure are indicated. At the lower temperatures (50° to 100°C) the adhesives are clearly observed to traverse the various rheological states: fluid polymer, gel phase, rubber and finally to the glassy state. At 125°C and 149°C, the adhesive polymer shows a cure profile indicating that the system does not enter the glassy state during cure. Such behavior indicates that the dynamic glass transition temperature for the RE-A adhesive material is between 100° and 125°C. As a check on this, the dynamic mechanical properties of a film of the adhesive cured for 2 hours at 165°C were measured (Figure 27) using the Rheovibron and a dynamic glass temperature of 130°C (3.5 Hz) was observed.

The commercial literature on RE-A specifies a cure temperature between 225°F (107°C) to 300°F (149°C). Reviewing Figures 25 and 26, one can rationalize that the commercially recommended cure schedules specify reasonably proper cure temperatures although the cure time might be somewhat short for the lower specified temperatures. Figures 25 and 26 provide a useful guide for the processing engineer planning to employ RE-A for aircraft fabrications. The data in these experiments raise an

interesting materials question regarding the nitrile-epoxy adhesive cured at say 100°C vs. the same system cured at 149°C. Do the distinct differences in cure history effect the functional and/or terminal behavior (environmental durability, fracture toughness) of adhesive joints fabricated from these materials?

4.5 Characterization of Cured Re-A

A. Differential Scanning Calorimetry

A sample of uncured resin was solvent extracted from the mat supported film and examined in the Perkin-Elmer DSC 1B Scanning Calorimeter. DSC scans, shown in Figure 28, show an exothermic curing peak in the range from 120°C to 220°C with a maximum at 175°C when the sample was heated up at 10°C/min. No transition was detected when the sample was cooled at a rate of 5°C/min. In the cured sample a transition was observed at 90°C at a heating rate of 10°C/min. This is consistent with the 130°C transition observed in the Rheovibron data (see below).

B. Dynamic Mechanical Analysis - RE-A

1. Rheovibron

The dynamic mechanical analysis was carried out on the Rheovibron Viscoelastometer following the standard procedures for machine calibration and correction of the data for the specimen length effect. The first task was to investigate the effect of sample cure hisotyr on the dynamic mechanical 'spectra'. From Figure 25 a cure time of two hours at 300°F would be sufficient but at 225°F it would appear that 'full cure' would require more than ten hours. Accordingly samples of commercial RE-A (extracted from the supporting polyester resin cloth) were cured at the following different cure schedules: 165°C for two hours, 120°C

for two hours, 75°C for thirty hours without and with a post cure of two hours at 150°C. Rheovibron data (dynamic tensile modulus and loss tangent) are shown in Figure 27. For the first two cure histories the dynamical mechanical properties are not significantly different, although the lower temperature cure gives slightly broader loss peaks. The slow cure at 75°C gives a much lower Tg at 100°C but which subsequently rises significantly higher, to 138°C, after post cure at 150°C (2 hours) than the Tg obtained for a straight cure of two hours at 165°C (Tg-125°C). The 'undercure' also only shows one low temperature damping peak at -70°C in contrast to the double peak in all the high temperature cured specimens. One peak is characteristic of the epoxy network and the other of the elastomer; further discussion of these observations is deferred until the experiments on the model materials described in Section V.

4.6 Morphology of RE-A Resin

The morphology of RE-A neat resin (extracted with acetone) cured under different conditions has been examined with optical, transmission (TEM) and scanning (SEM) electron microscopy.

A. Optical Microscopy

Specimens of extracted resin cured at different temperatures were embedded into a disk of room temperature curing epoxy casting resin and the specimens metallographically polished. Estimates of the volume fraction of inclusions were made by drawing radii from the center of each micrograph, shown in Figures 29 and 30, at 15° intervals, four representative micrographs (4" x 5" @ 500X) were used for each specimen, and the linear fraction (equal to the volume fraction) of intercept lying on the inclusions was measured. The mean values for each specimen are listed in Table 4. The total volume fraction of inclusions visible on the optical micrographs remains surprisingly

constant over the range of curing temperatures. The apparent particles sizes range from the limit of resolution (about 0.5 microns) up to 10 microns. The morphology of the material cured at 120°C is anomalous; the major inclusions are about 20 microns or greater and show subinclusions presumably of the matrix phase, and many much smaller particles of ∿ 0.5 microns are also evident.

B. Transmission Electron Microscopy

Specimens were prepared for transmission electron microscopy by casting resin films from chloroform solution directly onto copper grids. The dried films were then cured at different temperatures. The cured films and their supporting grids were then exposed to osmium tetroxide vapor for 48 hours in a dessicator.

Representative micrographs are shown in Figures 31 and 32. It should be noted that the apparent morphology results from the projections of inclusions embedded in a film a micron or so thick; the volume fraction of inclusions may be exaggerated. It should also be noted that since the cure is carried out in a thin film, diffusion is partially restricted to two dimensions with respect to the larger inclusions and it is possible that the resulting morphology could differ from that which would occur in the bulk at the same cure temperature. Large inclusions seen in all micrographs are of the order of 2-8 microns apparent diameter and smaller particles ranging continuously from 0.1 microns up to 1 micron. In Figure 31a, it seems that larger droplets separated first and that further cure causes precipitation within the inclusion of smaller sub-inclusions, which, since they are darker stained, would appear to contain a higher concentration of elastomer.

In Figure 31c, on the other hand, it seems that in some regions there is a tendency for the smallest particles to be unstained, i.e. epoxy, and the stained or rubbery phase to be continuous. The compatibility of the two resin components decreases during the reaction as the molecular weight increases. The high viscosity imposes kinetic restraints on the demixing process and the final morphology is arrested by the gel and cure which may not, of course, occur simultaneously in both phases. This is discussed in more detail in a later section.

C. Scanning Electron Microscopy

The dynamic mechanical analysis of RE-A cured at various conditions showed that the major glass transition temperature for the matrix rises from 100°C to 125°C as the curing condition is changed from 75°C to 165°C (Figure 27). The low temperature damping peak at -70°C to -50°C range also shows differences between the single peak of the specimen cured at 75°C and the double peak in all the high temperature cured specimens. The degree of phase separation of the cured rubber modified epoxy adhesive systems was studied by scanning electron microscopy of the morphology of the surfaces formed when specimens were broken after cooling in liquid nitrogen. The surface of fracture was coated by vapor deposition of carbon and platinum films. As expected, the existence of a two-phase material (rubber particles included in a glassy matrix) was easily observed (Figure 33).

Since the size of the particle is also believed to be an important factor in the toughening efficiency of the second phase (27), we notice the sizes of the large particles are similar for all specimens but the number of the particles with size range from 5-8 microns is greatest for the specimen cured at 150°C. The degree of phase separation, the particle size distribution and consequently the mechanical behavior of specimens with the same composition

are dependent on the curing conditions. The fracture surface texture of the epoxy matrix is also different from one specimen to another. The one cured at 75°C shows a smooth fracture surface which suggests a low toughness of the undercured matrix. As the curing temperature increases, the roughness of the fracture surface of the matrix increases up to a cure temperature of 150°C. When the curing temperature is higher, (e.g. 165°C), the general features of the fracture surface of the matrix are similar except there appear to be fewer large rubber particles; perhaps the fast curing conditions limit the aggregation of the precipitated phase. Even if the degree of crosslinking were the same for two matrix resins cured at different conditions, the toughening effect may not be the same since the conditions for the phase separation differ.

D. Correlation of the Adhesive Joint Strength and the Morphology of Variously Cured Systems

Three sets of lap shear specimens are prepared for adhesive joint strength tests cured at various conditions: 100°C for one and half hour, 100°C for 20 hours, and 150°C for one hour. Representative data of the adhesive joint strength tests (run at 21°C) are given in Table 5. At a lower temperature and shorter cure time (100°C for one and half hour), according to the time/temperature curing study of the material by TBA (Figure 25), one would expect this adhesive to be "under-cured". Even for the system cured for 20 hours at 100°C, where no further reaction is taking place, the material is still not fully cured. The reaction is "quenched" by vitrification of the resin and the joint strength was found to be measurably lower than when the adhesive was cured for one hour at 150°C.

The scanning electron micrographs of the fracture surface of these three adhesive joint test specimens are shown in Figure 34. The matrix texture and the size of the rubber particles in the adhesive cured at 100°C for 90 minutes and 100°C for 20 hours were quite different. The material under-cured at 100°C

for 90 minutes shows a smooth fracture surface against a rough surface for the one cured for 20 hours at 100°C. A difference in fracture surface texture and morphology was also observed with the adhesive material cured at 150°C for one hour. Here, a rougher fracture surface was observed and while the rubber inclusions were still about 5-8 microns in diameter their shape was more irregular perhaps because of superior interfacial adhesion between matrix and inclusion.

SECTION V

MODEL EPOXY-CTBN RESIN SYSTEM

5.0 Introduction

Based on the analysis of the commercial rubber modified epoxy adhesive the following model formulations were selected for further study:

Epon 836	90 parts	and	Epon 836	100 parts
CTBN 1300x8	10 parts		'Bis urea' curing agent	5 parts
'Bis urea' curing agent	4.5 parts			

It has previously been mentioned that the rubber particles responsible for the toughening effect in these epoxy systems are precipitated out as liquid globules in the earliest stage of the cure reaction prior to gelation. The latter event fixes the primary matrix-inclusion morpholgoy. The compatability of the epoxide resin with a particular CTBN elastomer prepolymer is very sensitive to the molecular weight of the epoxide resin. Compositions of 10% by weight of CTBN 1300x8 (18% acrylonitrile) with a series of epoxide resins with epoxide equivalent weights of 190, 240, 310 and 400 had cloud point (demixing) temperatures ranging from below room temperature up to 180^{o}C. Similarly wide variations in behavior are observed in mixtures of a particular epoxide resin with the several CTBN prepolymers commercially available.

5.1 Materials

The epoxide resins used in this study were commercial resins of the bisphenol A type and were characterized by gel permeation chromatography on a Waters 200 instrument using THF solvent (see Section 4.3B). The elastomer prepolymers, CTBN series, were obtained from B. F. Goodrich Corp. No characterization tests were run on these materials; specifications from the

manufacturer's data sheets are reproduced in Table B-3. The curing agents used were 2,4 tolylene-1,1'-bis (3,3-dimethyl urea) previously mentioned (Section 4.3A), which was prepared in the laboratory, and piperidine (Fisher Reagent Grade).

The CTBN elastomers were reacted with epoxide resins (excess) to form an adduct with a diepoxide molecule added to each carboxyl group terminating the butadiene/acrylonitrile copolymer (Figure 22). The reaction was carried out at 170°C in a closed r.b. flask, under nitrogen and catalysed with 0.30% of triphenyl phosphine (Fisher Reagent Grade) for from one to three hours. It was observed that the length of reaction time had a noticeable effect on the cloud point temperature of the resulting resins, as shown in Figure 35.

The 'bis urea' curing agent was a white crystalline solid which was not soluble in the epoxide resins at low temperatures. The curing agent was ground into a fine powder using a ball mill and dispersed, as a solid, in the liquid resin at about 80°C. It was observed that on heating to about 120°C the curing agent reacted, presumably forming some sort of adduct, since, as it went into solution, the resin underwent a color change at the same time. Although this catalysed resin could then be cooled before gelation this process was difficult to control. After addition and mixing of the curing agent ('bis urea' compound or piperidine) the resin was degassed in shallow pans in a vacuum oven at 80°C. The resin was then poured into casting cells formed from 0.25" glass plates coated with a release agent (Frekote 34) and separated by a Teflon gasket. The castings were then cured using a 16 hour programmed temperature cycle of 50°C → 150°C at 0.2°C/min and 2 hours at 150°C. The casting cell was then separated and the castings annealed for 1 hour at

150°C between the glass plates and cooled slowly at 0.2°C/min to room temperature.

5.2 Epoxy-Elastomer Compatibility

The usual criterion for the determination of compatibility is that the Gibbs free energy (free enthalpy) of mixing, ΔG, must be negative for a stable or homogeneous system:

$$\Delta G = \Delta H - T\Delta S \rightarrow 0 \tag{5.1}$$

In long chain polymers the number of arrangements in a lattice model is small compared to a mixture of small molecules although the total of interatomic interactions between neighboring molecules is not much different. The entropy of mixing per unit volume for a pair of polymers is negligible and a small positive heat of mixing will be sufficient to ensure demixing or incompatibility. In fact most pairs of compatible polymers show endothermic heats of mixing (43). However, Slominskii, et al. concluded that the simple lattice model for the entropy was not sufficient and that non-combinatorial entropy terms related to the molecular packing must be important, as manifested by volume changes which occur on mixing.

Figure 36 shows the Gibbs free energy of mixing for a binary liquid system as a function of concentration (22). Mixtures can and often are unstable at negative ΔG (but not relative to the pure components) and can diminish ΔG still further by phase separation. The stability of the mixture to small amplitude fluctuations in composition is determined by the curvature of the $\Delta G(\psi_2)$ curve (Figure 36) and the stability limit, the spinodal, is defined by

$$\left(\frac{\partial^2 \Delta G}{\partial \psi_2^2}\right)_{P,T} = 0 \tag{5.2}$$

The boundary between stable and metastable compositions, at which there is equality of the chemical potential of each component in the two phases, is the binodal; it defines the compositions of the phases into which an unstable mixture separates.

Expressions for the free enthalpy of mixing of polymers have been derived for the lattice model of the liquid state by Flory (44) and by Huggins (45). In the simplest case:

$$\frac{\Delta G_\psi}{RT} = \Sigma \frac{\psi_{1,i}}{M_{1,i}} \ln \psi_{1,i} + \Sigma \frac{\psi_{2,j}}{M_{2,j}} \ln \psi_{2,j} + \Gamma(p,T,\psi_2) \qquad (5.3)$$

where ΔG_ψ is the free enthalpy of mixing per mole of lattice sites, $\psi_{1,i}$ and $\psi_{2,j}$ are the volume fractions of species i in polymer 1 and species j in polymer 2, and $M_{1,i}$ and $M_{2,j}$ are the relative chain lengths of the two polymers expressed in terms of the number of lattice sites they occupy. For a system which obeys equation (5.3) the stability limit (equation 1) is defined by

$$-\left(\frac{\partial^2 \Gamma}{\partial \psi_2^2}\right)_{P,T} = \frac{1}{Mw,1\psi_1} + \frac{1}{Mw,2\psi_2} \qquad (5.4)$$

so that for a binary mixture the stability limit is determined by the concentration dependence of the semi-empirical interaction parameter Γ. Although the simple lattice theory supplies expressions for Γ in terms of concentration and chain lengths it cannot predict how it will depend on pressure and temperature. In this respect the "equation of state" approach by Flory is potentially more useful.

Equations for the binodal are more complex and implicit, and must be solved by numerical methods. However, knowledge of the spinodal alone is indicative of the miscibility gap in a binary liquid system. Figure 37

shows some stability limits (spinodals) calculated by Koningsveld, et al. (22) for model binary polydisperse polymer systems with varying ratios of $M_{w,1}/M_{w,2}$. The lower set of curves ($1/M_{w,2}$) shows the well known asymmetry of the miscibility gap and the shift of the critical point towards the solvent axis with increase in the molecular weight of the polymer. All curves show an upper critical solution temperature (UCST) above which all compositions are compatible. A similar but less pronounced effect occurs when species 1 is a polymer with molecular weight much lower than species 2. This is the situation in the epoxy-elastomer systems where the molecular weight of the epoxide is typically an order of magnitude lower than that of the rubber modifier.

The compatibility behavior of the epoxy rubber systems was investigated by preparing an adduct of the CTBN 1300x8 (18% acrylonitrile), 1 mole, with a pure diglycidyl ether of bisphenol A (DER 332), 2.4 moles, by reaction at 170°C for two hours with 0.3% triphenyl phosphine catalyst. This material was then blended off at several different concentrations with each of a series of epoxy resins with increasing molecular weights: DER 332 (360), DER 337 (∿540), Epon 836 (∿600) and CIBA 6060 (∿900). A gram or so of each resin was then placed in a small glass vial and placed in an air oven. From a high temperature at which the resins were all transparent the temperature was slowly decreased (∿0.5°C/min). The cloud point temperature was recorded when turbidity was clearly recognized in the resin samples. The results, shown in Figure 38, indicate how sensitive the miscibility gap is to the molecular weight of the epoxy resin. It has already been mentioned that for a particular epoxide resin equivalent weight the distribution of the molecular weights of the constituent oligomers may vary according to its method of manufacture, i.e. the taffy versus the advancement process. From Figure 38 it could be anticipated that resins with identical epoxy equivalent weight could have different compatibility characteristics if they were made by different processes (i.e. different molecular

weight distributions).

When an epoxy resin is cured the molecular weight increases so that the miscibility gap would also increase. For example a resin based on DER 337 and containing 10% elastomer (as an adduct) and cured at 95°C would be initially incompatible. The compositions of the two phases would be given by the ends of the tie line AB. As the reaction progressed the molecular weight of the epoxide resin and that of the elastomer adduct species would both increase. The equilibrium compositions of the two phases would then be given by another tie line, A'B', corresponding to the spinodal of the current molecular species in the reaction mix. Although the increasing molecular weights of the reactants would not be identical to those corresponding to the set of spinodals (or more precisely cloud point curves) shown in Figure 38 we would expect the effect to be qualitatively similar. The right hand branch of the curve should move upwards and to the right. While the composition of the epoxy rich phase (the continuous phase) would not change much, that of the precipitated phase could vary very much indeed. Its composition would continue to change (as far as the viscosity would allow) as the reaction progressed until the gelation of the matrix phase. Thereafter the quantity of epoxide and elastomer in the precipitated globules, which may not yet be gelled, would be fixed but phase separation could progress further. In fact, depending upon the ratio of epoxy to elastomer in the globules, it would be possible for either epoxy or elastomer to form subinclusions within the globule with the other being the continuous phase. In view of Figure 38 it could be expected that the volume fraction of the precipitated phase would be significantly larger than the actual volume fraction of elastomer in the formulation as has in fact been observed by Bucknall (18).

Although the elastomer-Epon 828 system was compatible over the whole composition range above about 40°C it was observed that at still

higher temperatures a liquid-liquid phase transition occurred and the composition became incompatible. The existence of a lower critical solution temperature is not a fundamental feature of the Flory-Huggins model but the Prigogine-Flory equation of state theory does predict that most polymer pairs should exhibit a decrease in mutual solubility with increasing temperature. The latter theory (46-48) is derived from considerations of the number of ways that particles of volume, v*, can be placed into a configurational space whose cells have a volume, v. The volume, v*, is the hard core volume of the polymer segment and is always less than the actual molecular volume. Additional volume in phase space is therefore available for the segment and contributes to the configurational integral for the system.

McMaster (21) has shown how the equation of state model can be used to give qualitatively correct predictions of the effect of chain length on compatibility and the marked sensitivity of the latter upon the thermal expansion and pressure coefficients. By equating the expressions for the chemical potentials from the two theories McMaster also derived an expression for X_{12}, the Flory-Huggins interaction parameter, in terms of the equation of state theory. These equations are very complex and will not be discussed here. Some of the general results from McMaster's calculations on model binary polymer systems are shown in Figure 39. A change in the average chain length of one component by a factor of two will shift the cloud point by more than 100°C. In our study of the rubber-epoxy system (Figure 37) the cloud point curves for the Epon 828-rubber and Epon 836-rubber mixtures are separated by just about 100 to 140°C over the range of compositions from 0 to 50% rubber and the nominal epoxy equivalent weights are 176 and 300 respectively for these two resins.

When 1-2 interactions dominate over 1-1 and 2-2 interactions the interaction parameter assumes negative values, e.g. in the case of hydrogen bonding (which occurs in the epoxy resins). With the introduction of negative X_{12} the theory predicts that the critical temperature (UCST) is raised and the binodal and spinodal tend to flatten out. It is also predicted that for certain limited conditions; molecular weights, interaction parameter, etc., that both UCST and LCST will be observed; as is the case with the epoxy rubber system. The equation of state theory is consistent with the observed compatibility characteristics of the epoxy-rubber system and provides a basis for relating the position of the miscibility gap with molecular parameters.

5.3 Gel-Cure Characterization

A. Experimental

The gel-cure behavior of the base epoxy resin, Epon 836, and a rubber modified version were studied by the Torsional Braid (TBA) technique. The experiments were carried out by *Plastics Analysis Consultants*, Princeton, New Jersey. The rubber modified resin was prepared by "prereacting" Epon 836 (90 pph) with a carboxy terminated butadiene/acrylonitrile copolymer (10 pph), CTBN 1600 x 8 (B.F. Goodrich Corp.) at 170°C for three hours and using 0.30% triphenyl phosphine as a catalyst. Known weights of both resins were dissolved separately in chloroform solution to which was then added weighed amounts of a curing agent, 2,4 tolylene-1,1' bis 3,3 dimethyl urea (in chloroform solution) equal to 5 wt% based on the weight of epoxy. The solutions were then impregnated into the glass fiber braids used in the TBA apparatus. The equipment is fully described in references (10,49). The main purpose of the study was to determine how the properties (e.g. dynamic thermomechanical spectrum) of a cured epoxy resin depend on the detailed thermal cure history. Isothermal cures were run at 52°C, 80°C, 103°C, 127°C, and 152°C each for over

200 hours during which time the change in modulus and damping with time were recorded. Transitions which characterize the dynamic thermomechanical spectrum were then observed by monitoring the rigidity and damping characteristics during "temperature scanning" as follows

(a) decreasing from T_{cure} down to -190°C or room temperature (RT), then

(b) increasing temperature from -190°C or RT up to +200°C, followed by

(c) decreasing temperature from +200°C down to -190°C (or RT)

Temperature scans were run at approximately 1.5°C/min.

As will be discussed the temperature scanning of isothermally cured specimens in the interval $T > T_{cure}$ causes further reaction and amounts to "post curing". Other curing experiments were carried out with varying linear heating rates starting from RT up to a maximum of +200°C at 0.05°C/min, 0.25°C/min, 0.75°C/min, 1.5°C/min, and 5.0°C/min. At the slowest rate the cure cycle took 60 hours and at the fastest about 30 minutes. A temperature scan was then obtained by decreasing the temperature from +200°C down to -190°C. On some specimens additional 'cycles': -190°C → 200°C → -190°C were carried out.

B. Results and Discussion

1. Gel-cure phase diagram

Any resin which is not completely crystalline has a glass transition temperature; a resin which is liquid at room temperature is above its Tg. A resin undergoing cure is a material with a molecular structure which changes continuously so that its characteristic glass transition temperature also changes; it increases as the molecular weight and crosslink density increases and reaches some terminal value when the chemical reactivity of the resin is exhausted. During isothermal cure in the TBA experiment a thermosetting

resin usually exhibits first a damping peak and increasing rigidity as the liquid resin gels. This is probably an isoviscous state when the individual fibers in the braid cease to move independently; for practical purposes this is probably very close to the gelation point (50) which in network theory corresponds to a fixed chemical conversion (44) in any given system. A plot of apparent gel times versus reciprocal absolute temperature is shown in Figure 40. The epoxy resin shows reasonable agreement with a simple Arrhenius equation except at the lower temperatures. Activation energies, ΔH, for these two resin systems were calculated according to

$$\log \frac{t_1}{t_2} = \frac{\Delta H}{2.303R} \left(\frac{1}{T_1} - \frac{1}{T_2}\right)$$

where t is the gel time, T the isothermal cure temperature, and $R = 1.98 \times 10^{-3}$ kcal/deg C-mole is the gas constant were 12.3 kcals/gram mole and 9.3 kcal/gram mole respectively.

As polymerization and crosslinking proceed the glass transition of the material gradually increases and eventually rises to or a little above the cure temperature; the material then passes from a rubbery to a glassy state. On the TBA plot this is seen as another damping peak and an increase in relative rigidity, as shown in Figure 41. If the temperature of cure is above the glass transition of the fully cured material the resin during cure, passes from a liquid through gelation into a rubbery state. This is shown as steadily increasing rigidity (crosslink density) and decreasing damping in the TBA plot (Figure 42) for the 152.5°C isothermal cure. Figure 43 shows the gelation-vitrification phase diagram constructed from the isothermal cure data.

In the other series of cure experiments it was observed that at the slower heating rates the curing material passed through the gel point and rubbery state into the glassy state and then, as the cure temperature continued to rise, back into the rubbery state. This is shown very clearly in Figure 44, the TBA plot of the 0.05°C/min cure. At the highest temperature programmed

heating rates the material did not enter a glassy state at all during cure. A gelation-vitrification phase diagram, shown in Figure 45 was constructed from the linear heating rate cure data. Since the various rheological states, as they appear in two dimensional t-T space on the "phase diagram", are determined by the kinetics of the curing reaction the boundaries between the 'phases' are not independent of the thermal cure path. Nevertheless, the diagrams provide a useful guide to the probable rheological states which may occur during any practical cure cycle.

2. Cure history and crosslink density

The location of the glassy state during cure is of particular importance since the rate of reaction drops drastically and for all practical purposes stops (50) once the curing material vitrifies. This is evident (Tables 6 and 7) from the isothermal cures at 52°C, 80°C, and 102°C where, although the Tg is above T_{cure}, it is well below the final Tg, even after 200 hours cure, which was obtained by raising the cure temperature (i.e. a post cure at 200°C). For isothermal cures carried out at or above the Tg/max., e.g. 125°C and 152°C a high temperature post cure had little or no effect. On the other hand when a high temperature post cure (which occurs during the temperature scan to 200°C) is added to a long isothermal cure below Tg_{max} the final Tg is highest for the isothermal cure at the lowest temperature. This general trend is also observed for the linear heating rate cures (Tables 8 and 9); the highest Tg is obtained for the slowest cure rate. Evidently, if the cure reaction is too rapid the resulting network is less highly crosslinked; a characteristic which cannot be corrected by post curing. Presumably, competing network reactions lead to different networks when the temperature is changed. In the rubber modified epoxy system cured at 5°C/min up to 200°C the Tg increases only about one degree even after four temperature scans 200°C → -190°C → 200°C. The Tg of a epoxy-rubber specimen cured 213 hours at 52°C was 118°C on decreasing

the temperature after a temperature scan up to T_{max} = 150°C, and 121°C after a scan up to T_{max} = 200°C; and was still only 125°C after a 4.5 hour post cure at 200°C (see Table 7). Thus the usual temperature scan up to and down from 200°C causes almost complete reaction; prolonged post curing at 200°C raises the Tg but a few degrees. The rubber modified specimen cured at 0.047°C/min showed no change in Tg after repeated temperature scans to +200°C (see Table 7). It is possible that maximum crosslinking could be achieved under rapid cure conditions by changing the concentration of curing agent; we have not investigated this possibility.

3. Modulus and crosslink density

It is interesting to note that specimens cured isothermally at lower temperatures show a rise in Tg on 'post curing' and a decrease in elastic modulus immediately below the Tg as shown in Figure 46; in addition the secondary damping peak (∿ -103°C) in the undercured material broadens after post curing, shifting to -84.5°C, merging with and obscuring another, weak, damping peak at 47°C observed in the undercured material. The modulus of the post cured sample rises to the original level at temperatures below that of the secondary transitions.

This behavior seems to parallel the effects of low molecular weight oligomers, phenol end-capped bisphenol A diglycidyl ether resins, which act as antiplasticizers in crosslinked epoxy resins (51). The Tg was decreased, the modulus increased and the lower temperature secondary transition was narrower and shifted to lower temperatures. There was also a decrease in specific volume with addition of the antiplasticizer and an increase in (upper) compressive yield stress. For this reason the practice of measuring the degree of cure by an indentation hardness test (e.g. Barcol Hardness) could give misleading results for this resin.

In comparing the dynamic thermomechanical spectra of the unmodified epoxide resins cured at increasing heating rates and after post cures it is seen that in parallel with lowering of the final Tg the rubbery modulus decreases (this assumes that the cross sectional areas of the different braid specimens are not much different), the damping above Tg is increased and the lower temperature damping peaks become narrower. This same effect is observed in the rubber modified material where the $5^{o}C$/min specimen was temperature scanned up to $200^{o}C$ several times (i.e. post cured); confirming that there were permanent differences in the molecular networks.

4. Effect of elastomer adduct

Referring to Figure 47 and Table 7 it is particularly striking that the Tg of the rubbery phase remains essentially constant at 49.5 $\pm$ $1.5^{o}C$ for all thermal cure histories. This suggests that the precipitated phase, which contains elastomer, must have a more or less constant composition. Comparison of the measured Tg_{max} of the epoxy matrix, with and without the elastomer modifier, as a function of cure history shows a more or less constant difference in the linear programmed temperature cures while there is a definite trend, a decreasing difference, ΔTg, for the higher temperature isothermal cures. This suggests that at the lower cure temperatures less elastomer precipitates out and remains very well dispersed in the epoxy phase. The programmed temperature cure data does not show any definite trend.

5.4 Fracture Toughness of Model Rubber Modified Epoxy

The two experimental resins previously described, based on Epon 836/bis urea curing agent with and without 10% elastomer modifying agent, were tested for fracture toughness at room temperature using the conventional double torsion (DT) method (52). Plates 1/8" thick were cast between 1/4" glass plated coated with

Freekote 34 release agent and separated by a Teflon gasket (1/8"). In all DT specimens an unstable "stick-slip" behavior was observed as has been frequently reported by others in many different epoxy systems (53,54,55). K_{ic} values calculated at initiation of crack propagation and at arrest are given in Table 8. A typical load trace from the double torsion tests is shown in Figure 48. We observed in the rubber modified version "stress whitening" on the surface of fracture at the crack initiation position only; the toughness is evidently highly rate sensitive. These observations are consistent with those of others who have measured fracture toughness of rubber modified epoxy resins.

Table 1

Acceptance Test Results of Commercial

NE-A Adhesive and Model Resin

	Lap shear at R.T., psi	Lap shear at 180°F, psi	T-peel at R.T., lbs/in
NE-A cured at 350°C for 1 hour	6850 ± 99 S.d. (7090)	3710 ± 167 (3670)	60 ± 11 (60)
(Specification MMM-A-132)	(5000)	(2500)	(50)
Synthetic Film cured at 350°C for 1 hour	6100 ± 185		
Synthetic film with Cabosil cured at 350°C for 1 hour	6200 ± 50		
Synthetic film with Cabosil and Dicy cured at 350°C for 1 hour	7190 ± 50		

Table 2

Acceptance Test Results of Commercial RE-A Adhesive

	Lap Shear at R.T., psi	Lap Shear at 180°F, psi	T-peel at R.T., lb_f/in
RE-A cured at 300°F for 1 hour	5030 ± 50	3290 ± 40	20 ± 2
Commercial Specification	(6700)	(4500)	
Mil. Spec.	(5000)	(2500)	

TABLE 3

IR ABSORBANCE
CTBN - ADDUCTS

Epoxy-Elastomer \ Frequency cm^{-1}	3070	2240	1740	1640	1610	$1610/1640$	$3070/2240$	$2240/1740$
RE-A Elastomer Fraction	0.12	0.15	0.27	0.09	0.18	2.0	0.80	0.56
CTBN 1300 x 15 10%	0.68	0.31	1.32	0.56	0.82	1.5	2.2	0.23
CTBN 13 x 18% AN	0.29	0.33	0.59	0.21	0.41	1.9	0.89	0.56
CTBN 1300 x 13 27% AN	0.29	0.64	0.85	0.18	0.56	3.1	0.45	0.75

3085 cm^{-1}	C-H stretch, pendant vinyl, R-CH=CH_2
2240 cm^{-1}	nitrile, -C N
1740 cm^{-1}	C=O stretch, alkylester, R-COOR'
1640 cm^{-1}	C-C stretch, pendant vinyl, R-CH=CH_2
1610 cm^{-1}	C-C stretch, 1:4 disubstituted benzene (e.g. bisphenol epoxy)

Table 4

Inclusion volume fractions* from
Optical and Scanning Electron Microscopy

Cure Conditions	Optical of Polished Surface	SEM of Fracture Surface
75°C/30 hrs.	11.0%	15%
100°C/1 1/2 hrs.	10.5%	16%
100°C/20 hrs.	13.5%	10%
120°C/2 hrs.	10.0%	10%
150°C/2 hrs.	12.0%	14%
165°C/2 hrs.	9.5%	15%

*These observations refer only to the larger diameter inclusions. Smaller particles (~5000 Å) were only observed using transmission electron microscopy.

TABLE 5

Lap Shear Tests (ASTM D1002)
on RE-A

Cure	Strength
1 hour/150°C	40.7 MPa
1.5 hour/100°C	29.0 MPa
20 hour/100°C	33.8 MPa

Table 6

Glass Transition Temperature of Model Epoxy Resin versus Isothermal Cure Temperature

T_{cure} (t_{cure})	T_g after $T_{max} \approx T_{cure}$ Decreasing Temp/Increasing Temp	T_g after T_{max} = 200°C (Decreasing Temp)
52°C (209 hr)	($>T_{cure}$) / 69°C	126.5°C* + 134.5°C
80°C (200.3 hr)	($>T_{cure}$) / 111°C	136°C
102.6°C (163 hr)	($>T_{cure}$) / n.a.	n.a.
127°C (144 hr)	($>T_{cure}$)+119°C* / 118°C* + 130°C	122°C
152.5°C (154 hr)	121.5°C / n.a.	n.a.

*damping shoulder

Table 7

Glass Transition Temperature of Model Epoxy-Rubber Resin versus Isothermal Cure Temperature

T_{cure} (t_{cure})	E^{Tg} after $T_{max} = T_{cure}$ Decreasing Temp/Increasing Temp.	E^{Tg} after T_{max} = 200°C (Decreasing Temp.)
52°C (213 hr)	(> T_{cure}) / 71°C	121°C
80°C (218 hr)	(> T_{cure}) / 110.5°C	125°C
102.6°C (172.5 hr)	n.a. / n.a.	n.a
125°C (124.3 hr)	114°C / 114.5°C	115°C
152.3°C (109.25 hr)	113.4°C / n.a.	n.a.

n.a. = not available (no experimental data)

Table 8

Glass Transition Temperature of Model Epoxy Resin versus Linear Temperature Programmed Cure

Heating Rate (°C/min)	Increasing Temp. from RT (°C)	Decreasing Temp. from 200°C (°C)
0.05	74.5/81/137	140
0.25	90/∿104*/∿117°C*	132
0.75	105/123	124.5
1.5	119	118
5	156	109

*damping shoulder

Table 9

Glass Transition Temperatures (Epoxy Matrix and Rubber Inclusions) of Model Epoxy-Rubber Resin versus Linear Temperature Programmed Cure

Heating Rate (°C/min)	Increasing Temp. from RT (°C)	Decreasing Temp. from 200°C	
		$_{E}^{Tg}$	$_{R}^{Tg(\Delta)}$
0.047	73/78/123.5	130.5	-48 (0.1174)
0.1409	84/92.5/114.5	126	-47 (0.1225)
0.25	91/∿97*/∿115*	125	-49 (0.1207)
0.75	116/126*	113	-49.5 (0.1050)
1.5	119.5	109	-50 (0.0938)
5	?	100.5	-50 (0.0917)

*Damping shoulder

$_{E}^{Tg}$ epoxy glass transition

$_{R}^{Tg}$ rubber glass transition

Table 10

Fracture Toughness of Model Resins (Double Torsion Test)

	Base Epoxy	Epoxy + 10% CTBN
K_{1c}) initiation, ksi$\sqrt{in}$	2.2	2.8
K_{1c}) arrest	1.0	1.3

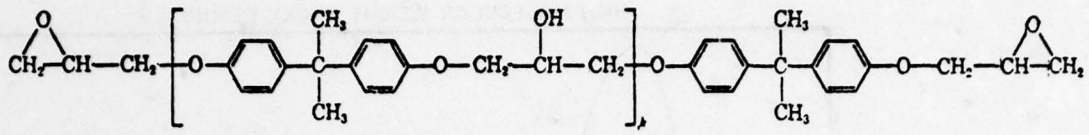

I

k = 0,1,2,3, . . . "taffy" process
k = 0,2,4,6, . . . "advancement" process

Taffy Process

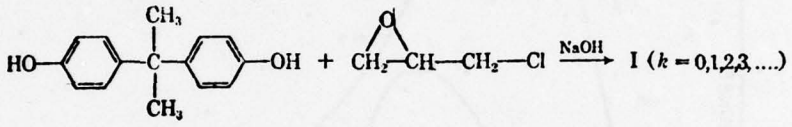

Fusion or Advancement Process

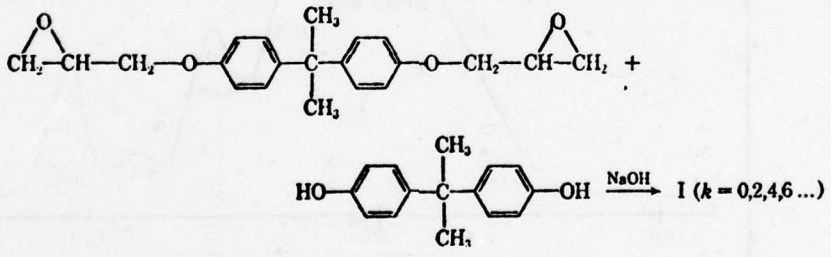

Figure 1 **Molecular Structure of Bisphenol A Diglycidyl Ether (DGEBA) Epoxy Resins.**

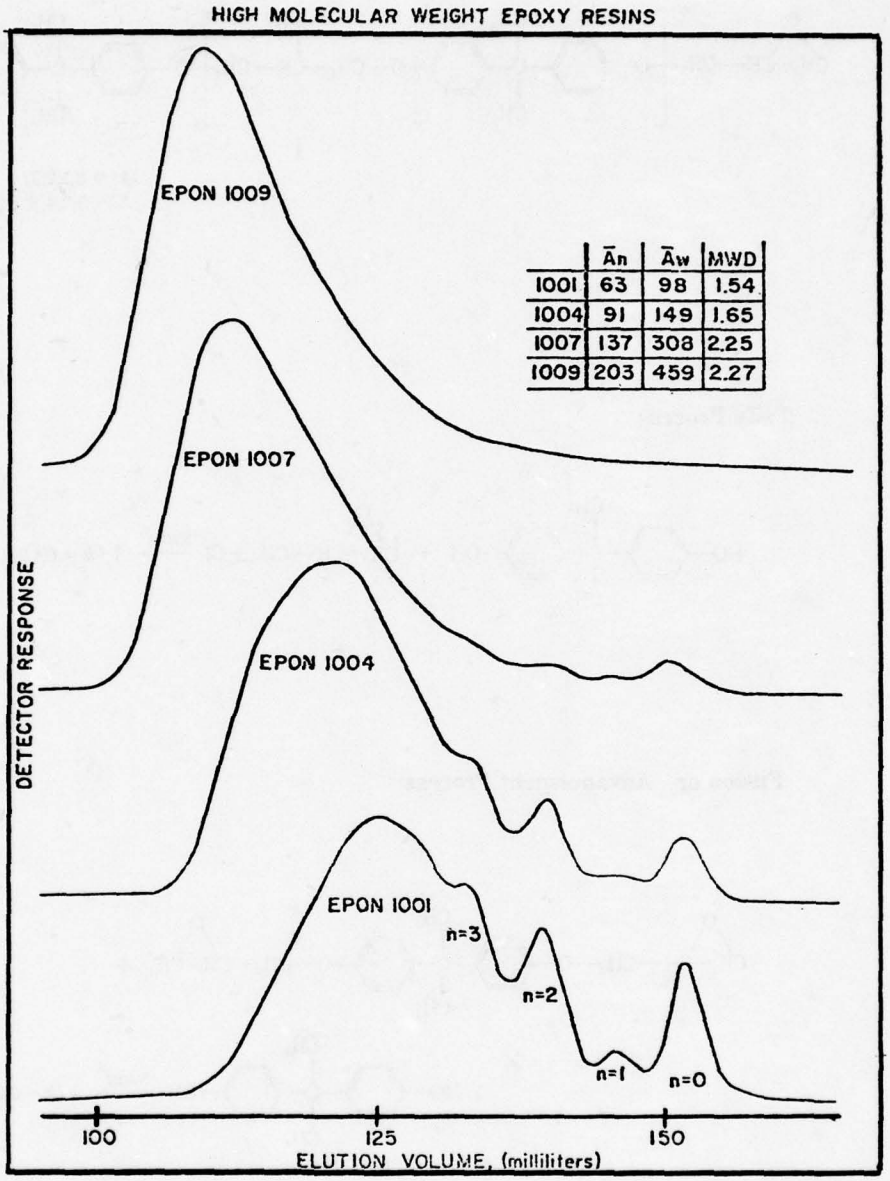

	$\bar{A}n$	$\bar{A}w$	MWD
1001	63	98	1.54
1004	91	149	1.65
1007	137	308	2.25
1009	203	459	2.27

Figure 2 **Gel Permeation Chromatograms of Selected Commercial DGEBA Epoxy Resins**

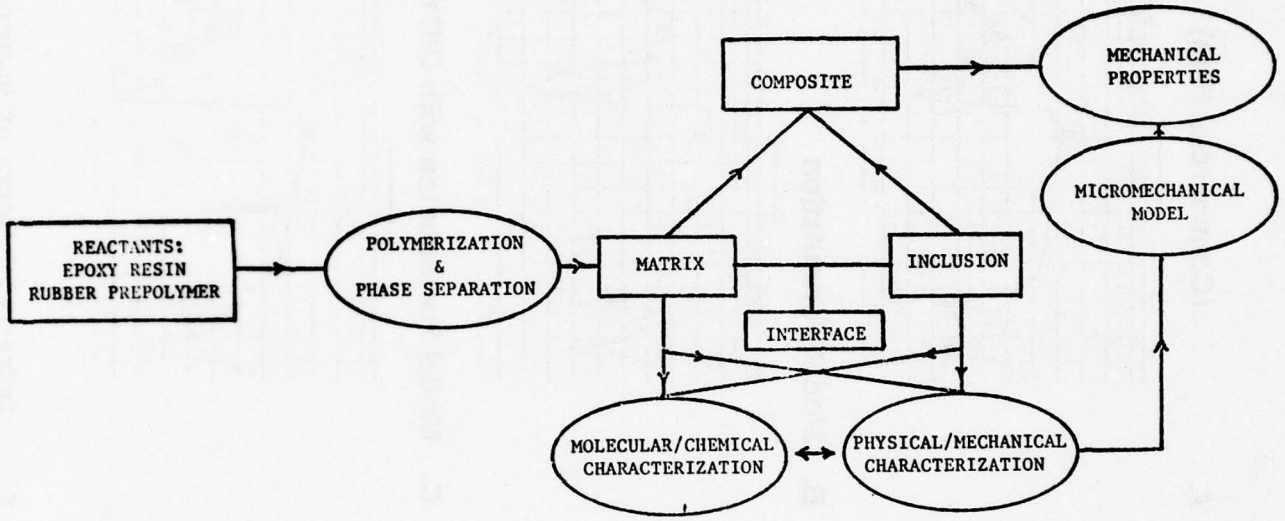

Figure 3 Program Schematic

INFRARED SPECTRA OF NYLON-EPOXY ADHESIVE

A. (Commercial Film)

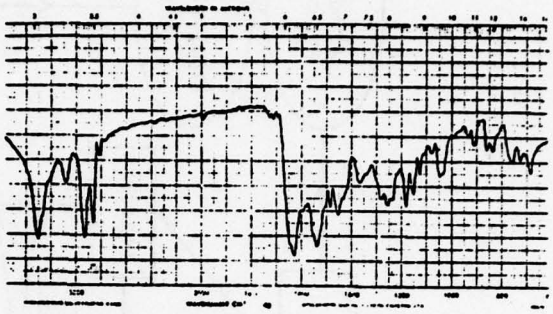

B. Model Formulation

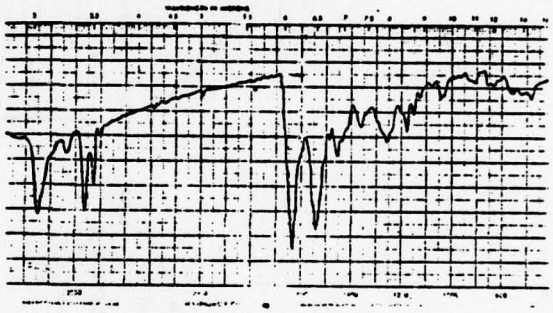

C. Model Formulation with DICY

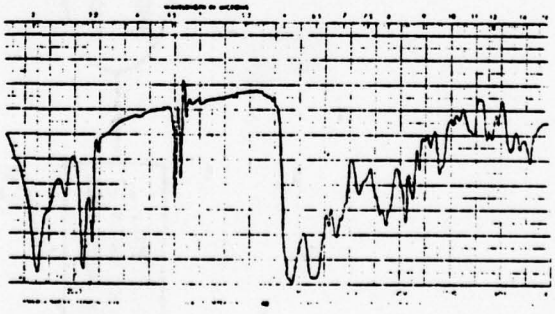

Figure 4 Infra-red Spectra of Uncured NE-A and Model Adhesives

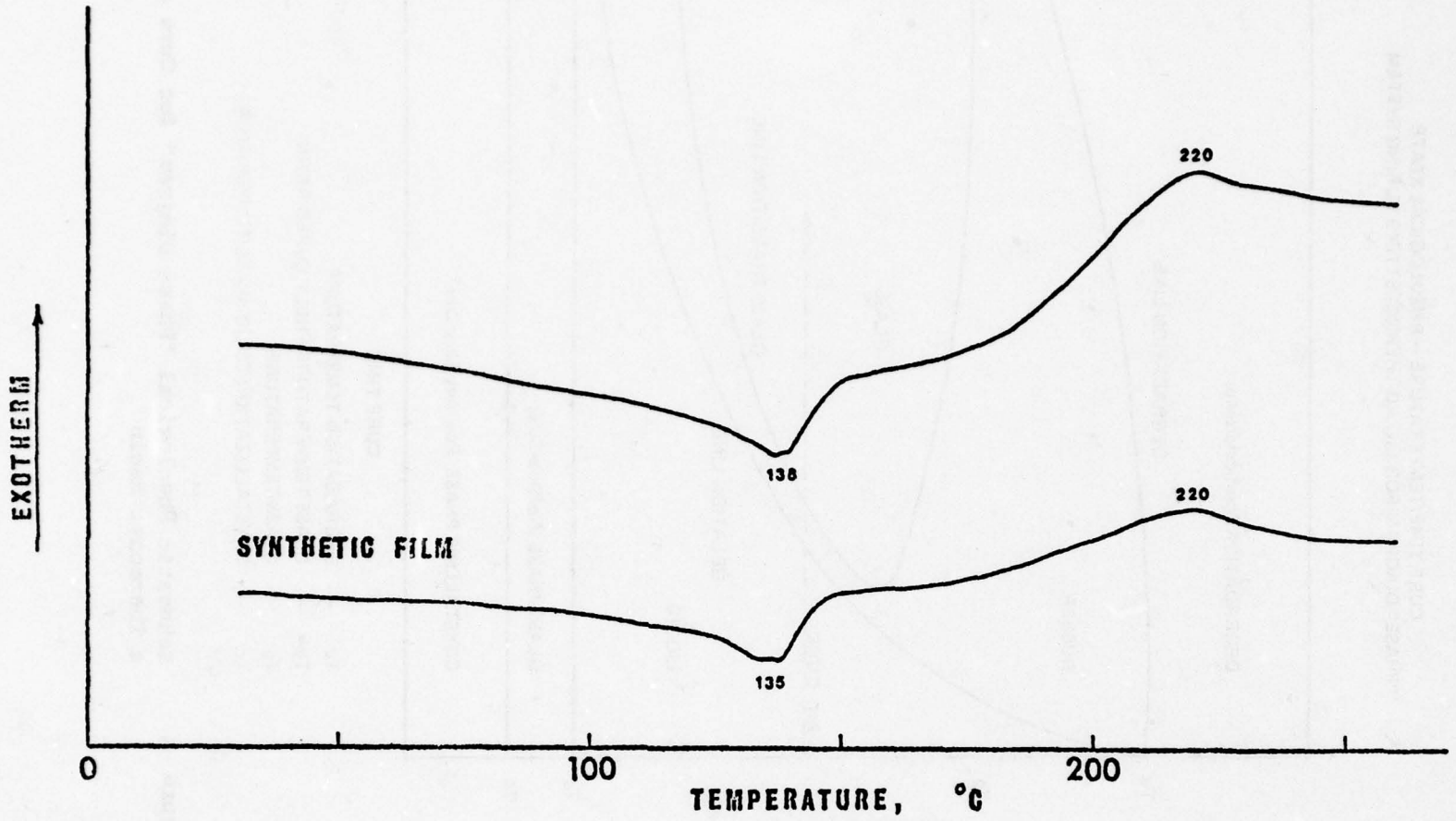

Figure 5 DSC Scans of Uncured NE-A and Model Adhesives

CURE TIME/TEMPERATURE – RHEOLOGICAL STATE
"PHASE" DIAGRAM FOR LIQUID THERMOSETTING CURING SYSTEM

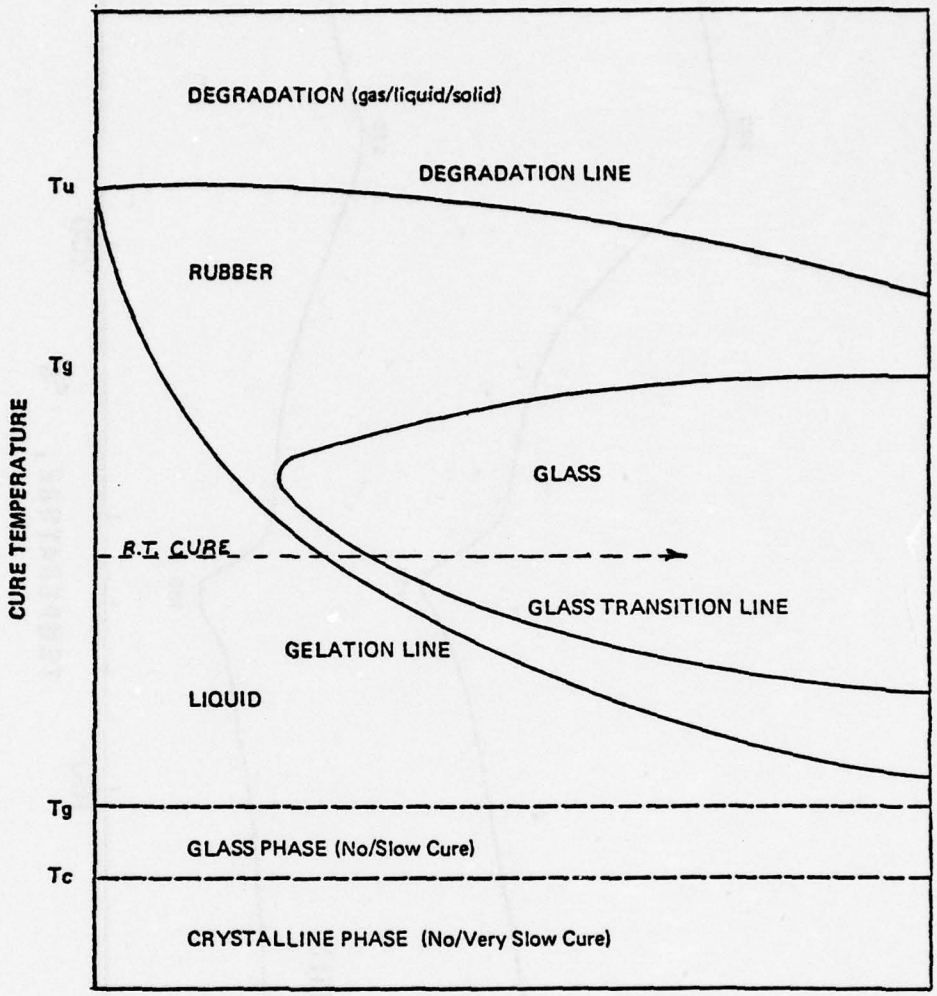

Tu – DEGRADATION TEMPERATURE
$T_{g\infty}$ – GLASS TEMPERATURE FULLY CURED RESIN
Tg – GLASS TEMPERATURE
Tc – CRYSTALLIZATION/SOLID PHASE TEMPERATURE

Figure 6 Schematic Rheological "Phase Diagram" for Cure of a Thermoset Resin

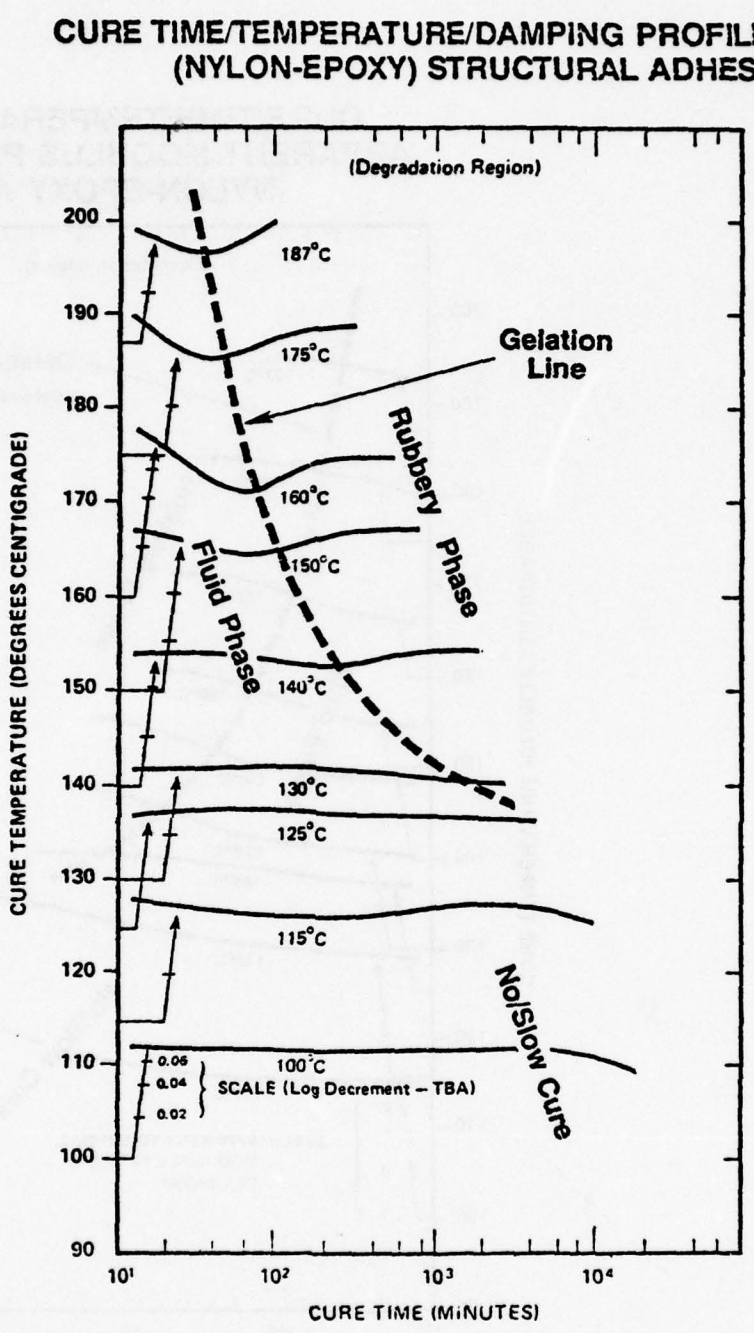

Figure 7 Cure Time-Temperature-Damping Profile for NE-A

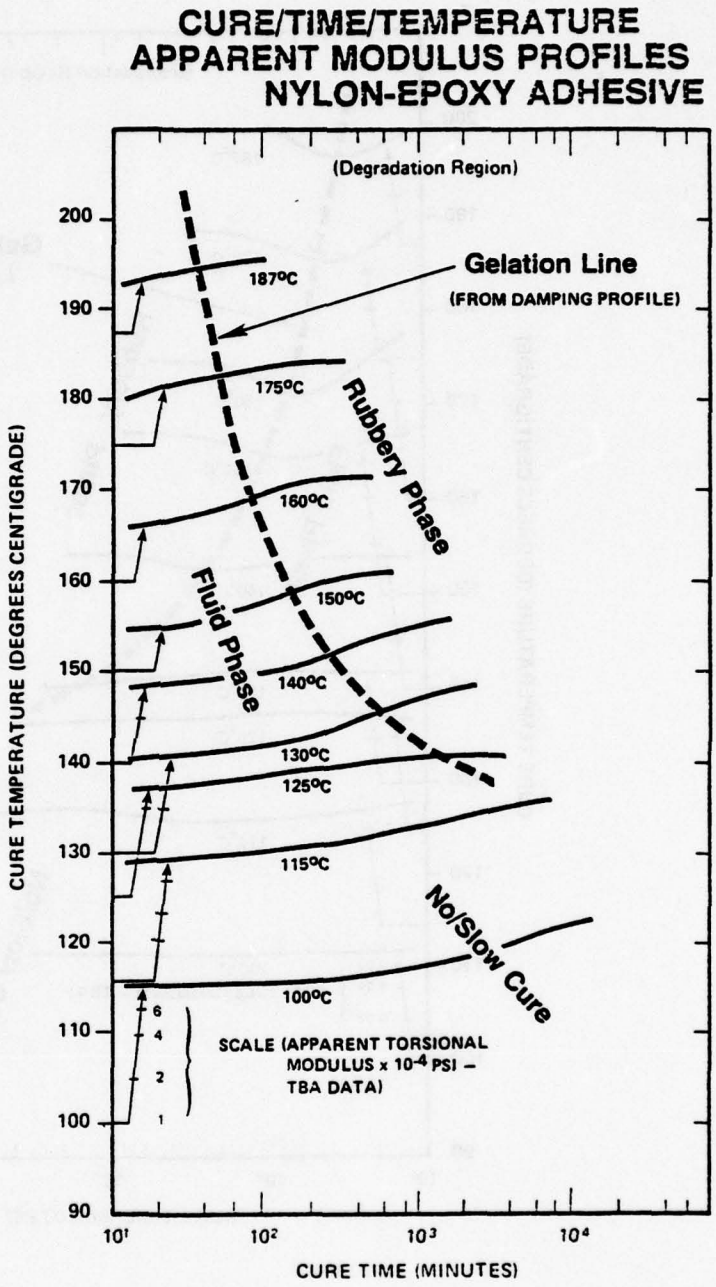

Figure 8 **Cure Time-Temperature-Modulus Profile for NE-A**

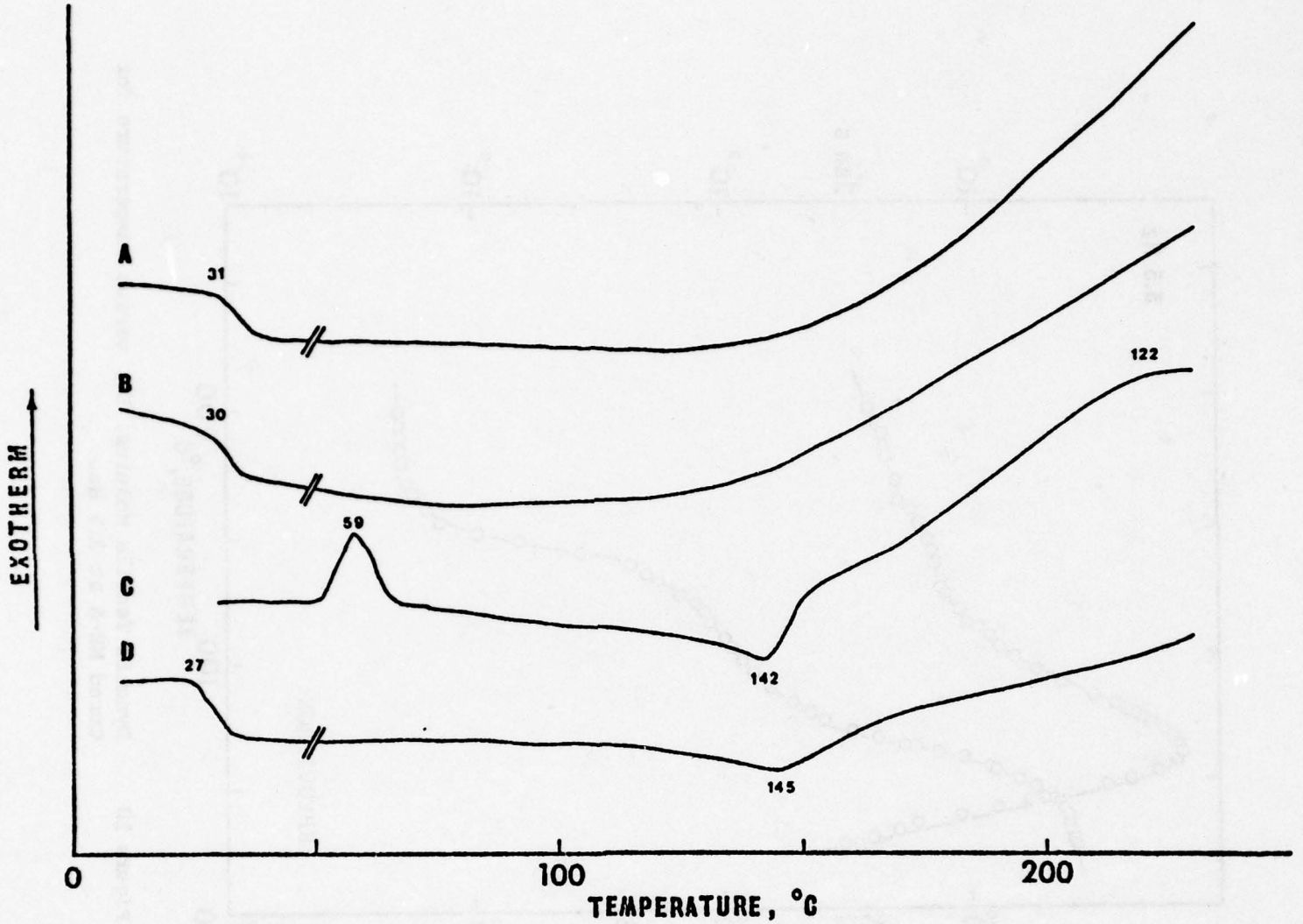

Figure 9 DSC Scans of Cured NE-A, A; and Model Adhesive; B; Partially Cured NE-A; C; and Elvamide 8061 (nylon), D.

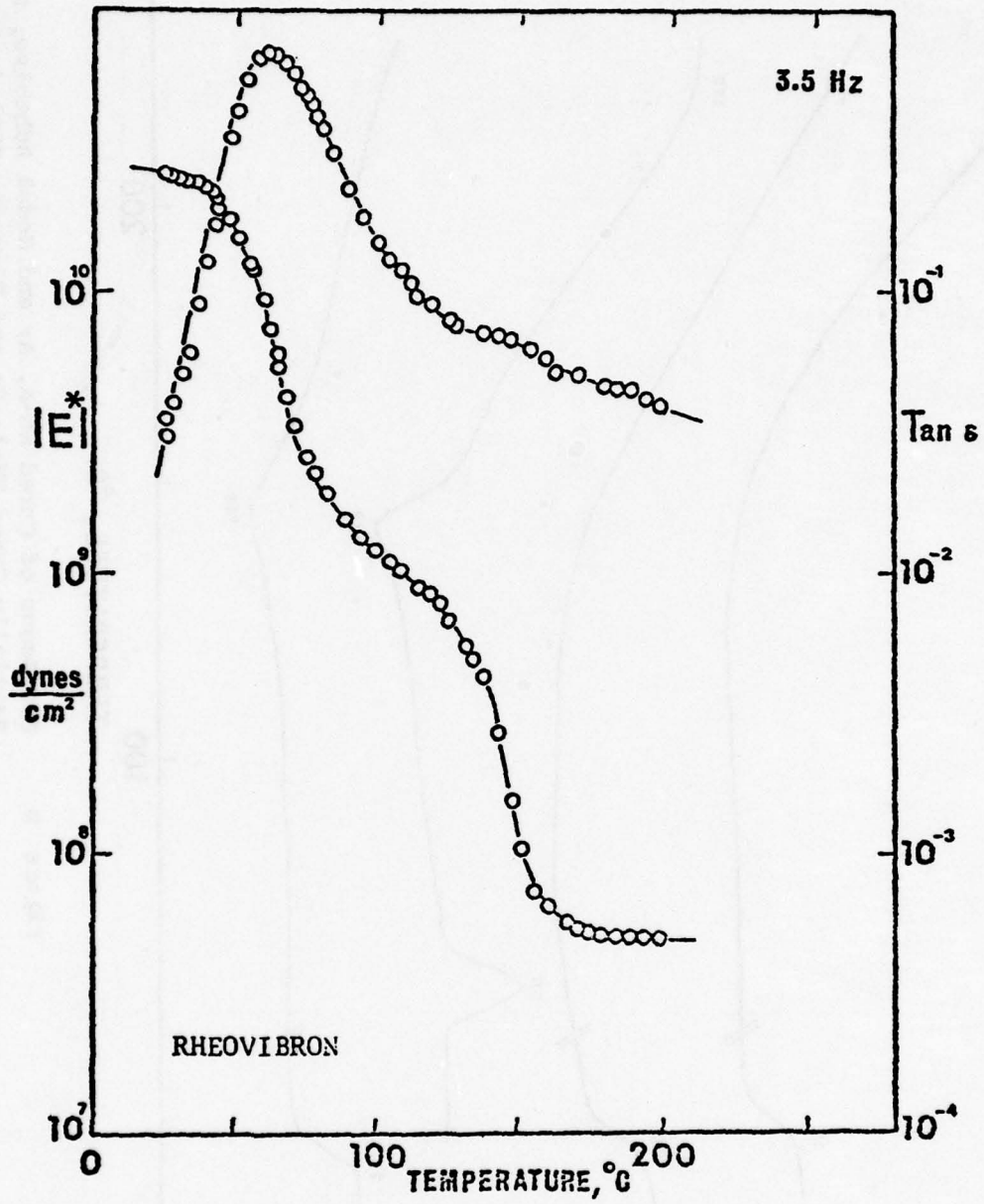

Figure 10 Dynamic Tensile Modulus, E', versus Temperature for Cured NE-A at 3.5 Hz.

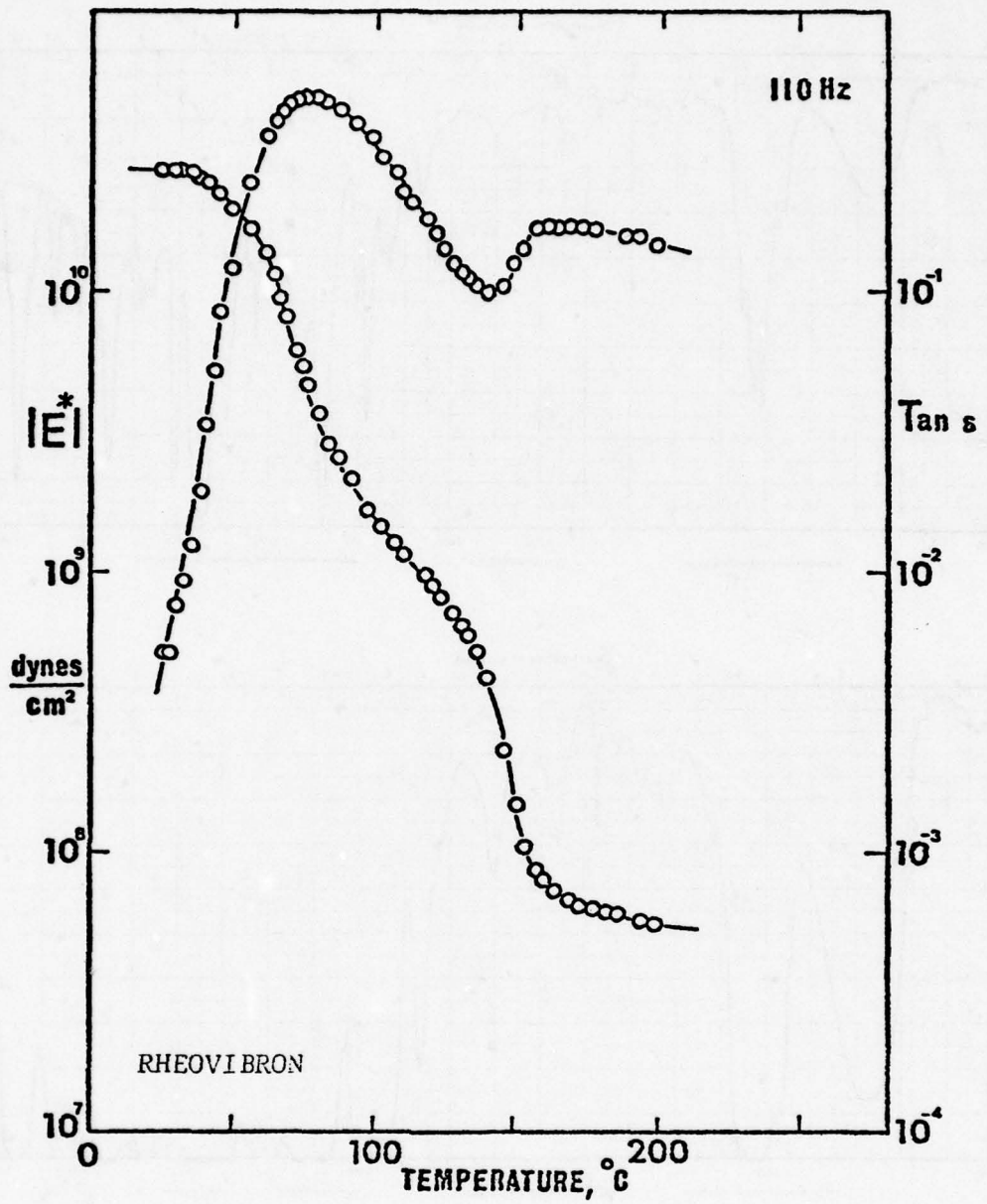

Figure 11 **Dynamic Tensile Modulus, E', versus Temperature for Cured NE-A at 110 Hz.**

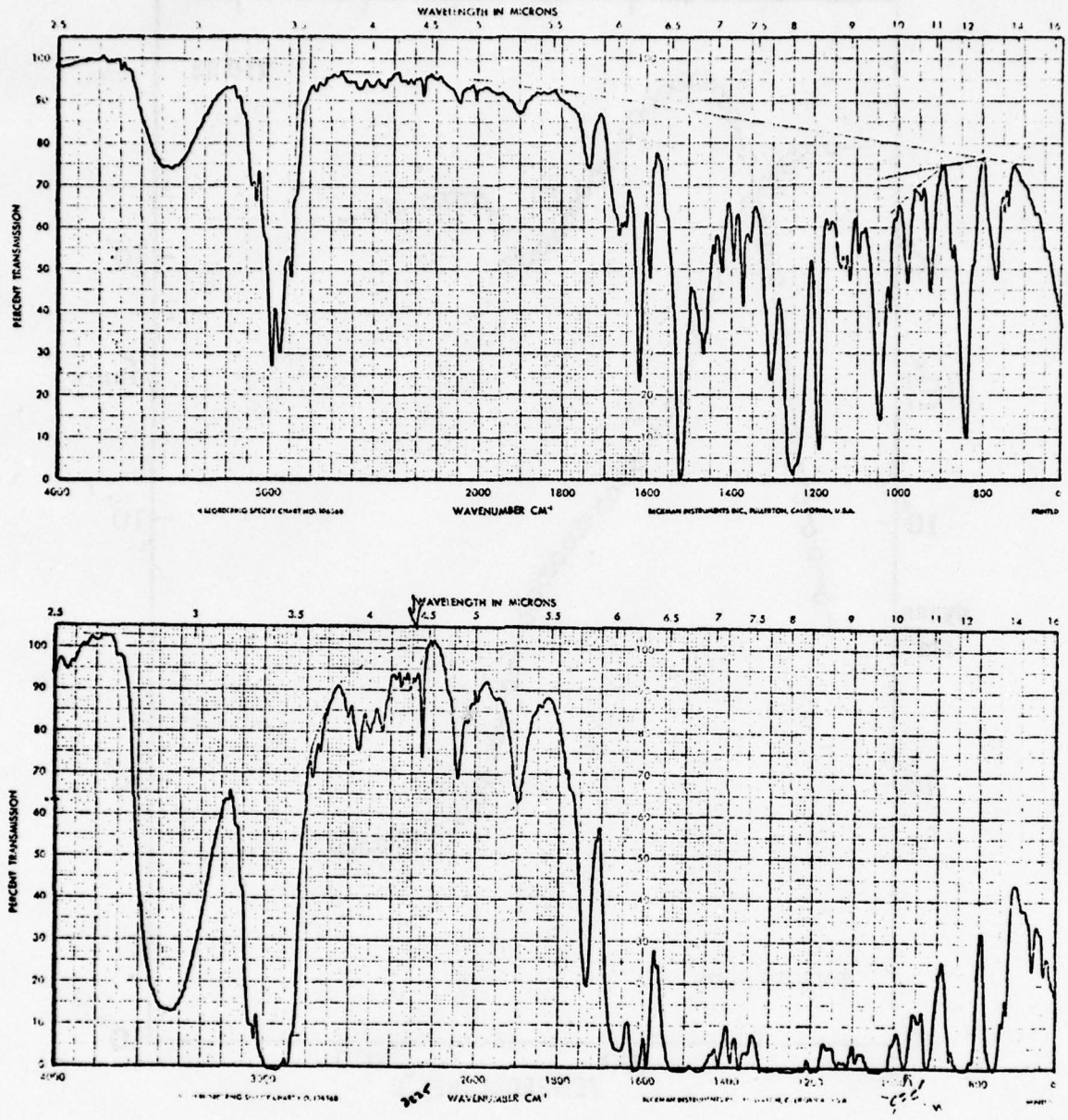

Figure 12 Infra-red Spectrum of RE-A, Extracted Resin

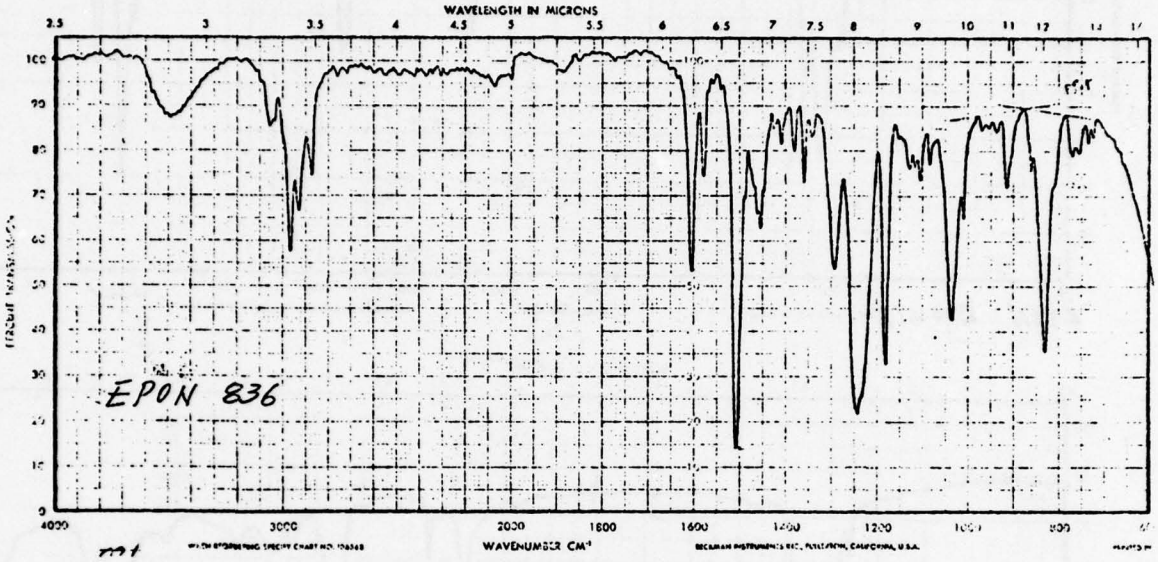

Figure 13 **Infra-red Spectrum of Epon 836, Diglycidyl Ether of Bisphenol A Resin, Epoxy Equivalent Weight 290-335**

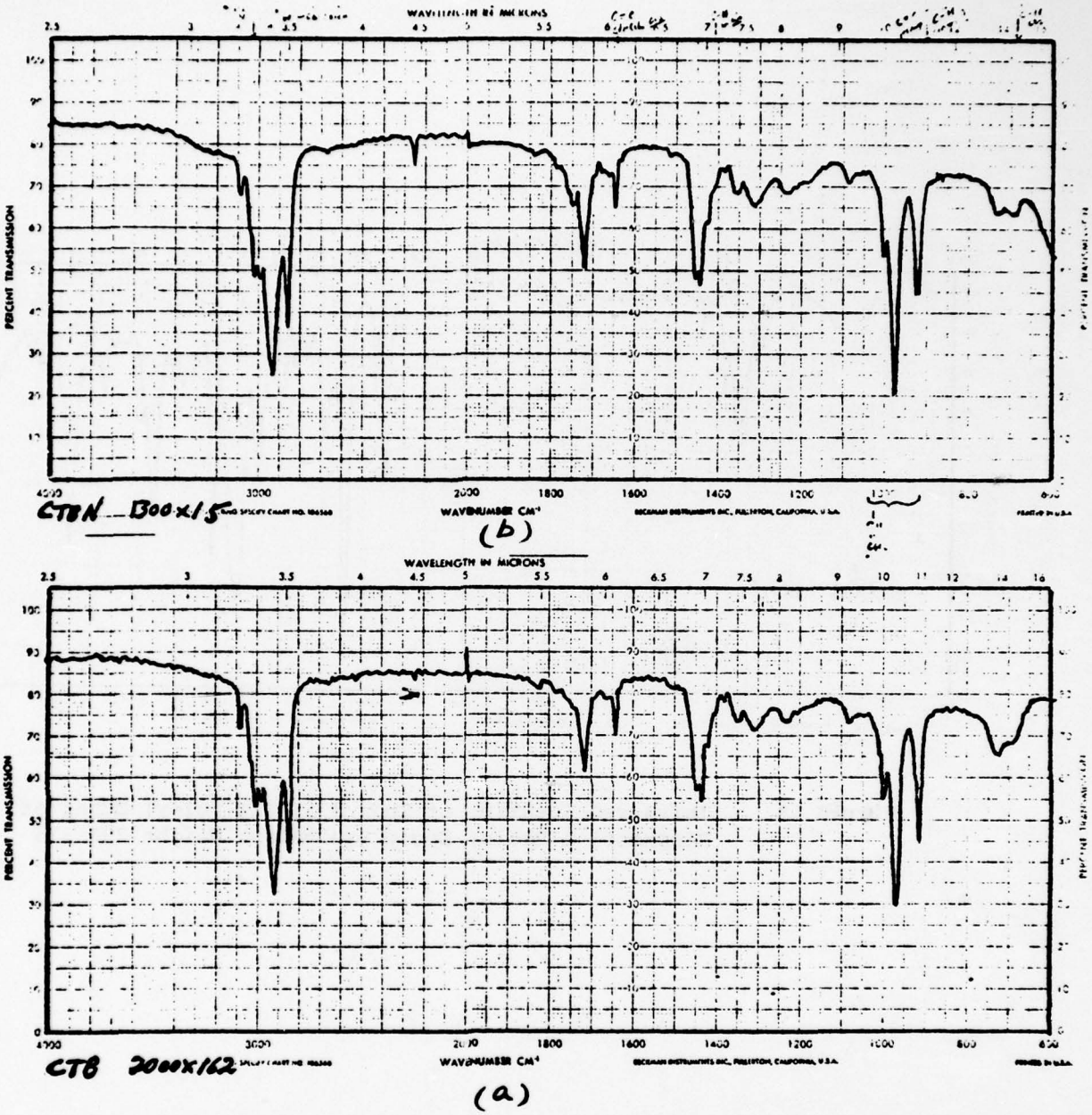

Figure 14 Infra-red Spectra: (a) Carboxy Terminated Polybutadiene (B.F. Goodrich, CTB 2000 x 162), (b) Carboxy Terminated Polybutadiene-Acrylonitrile Copolymer (B.F. Goodrich, CTBN 1300 x 15)

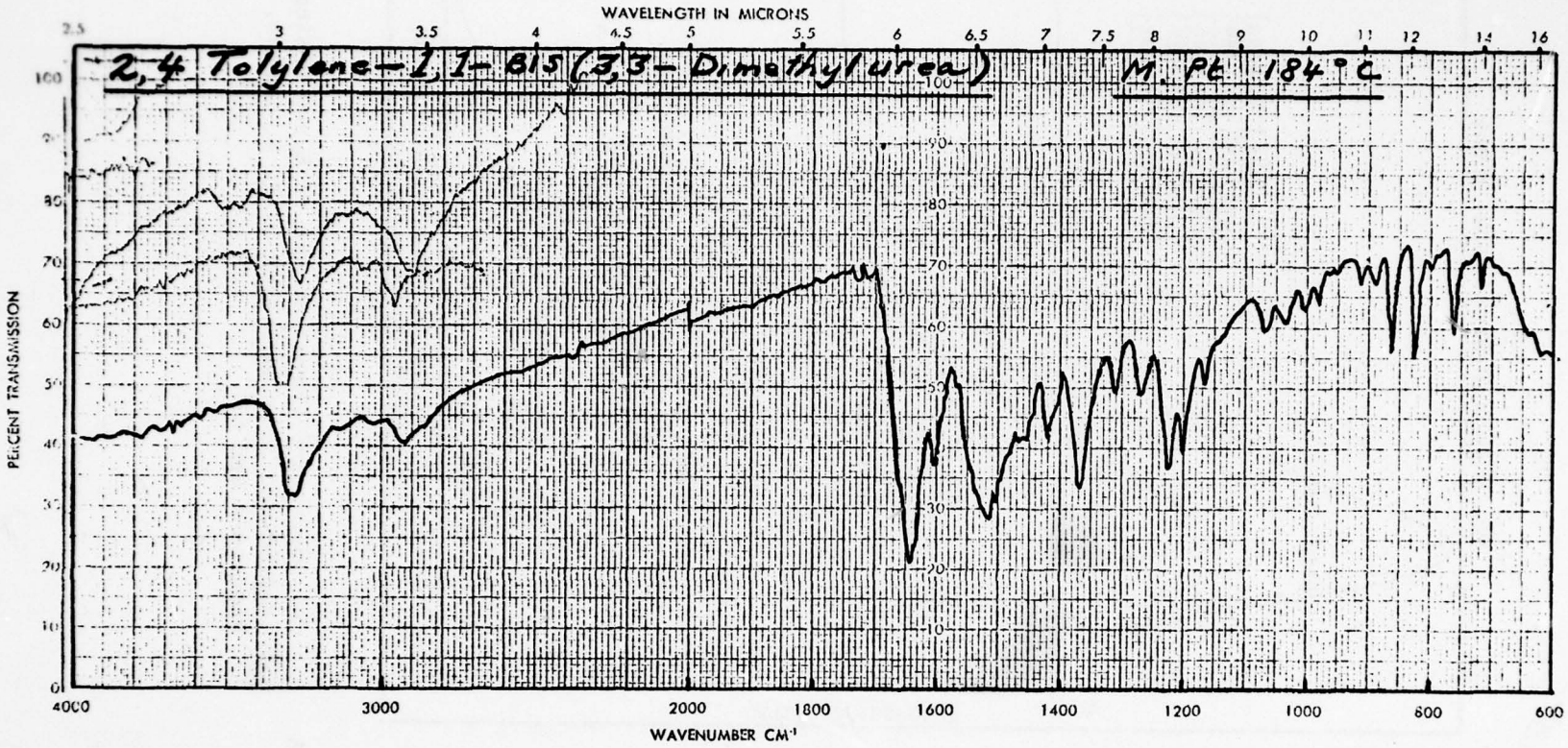

Figure 15 Infra-red Spectrum of 2,4 Toluene 1,1' bis (3,3 Dimethyl Urea). Laboratory Preparation, Melting Point 184°C.

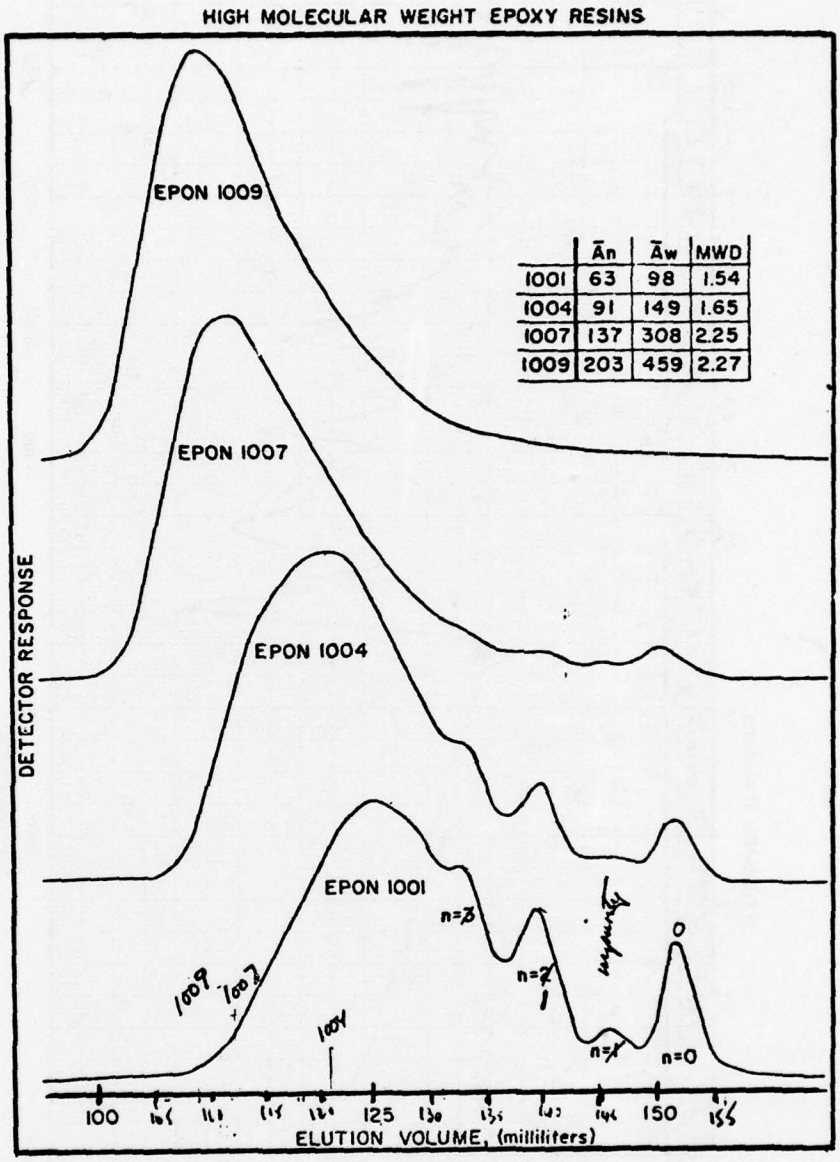

	$\bar{A}n$	$\bar{A}w$	MWD
1001	63	98	1.54
1004	91	149	1.65
1007	137	308	2.25
1009	203	459	2.27

Figure 16 Gel Permeation Chromatograms of Epoxy Resins. (Reproduced from Reference 3, F. N. Larsen, Figures 4 and 6)

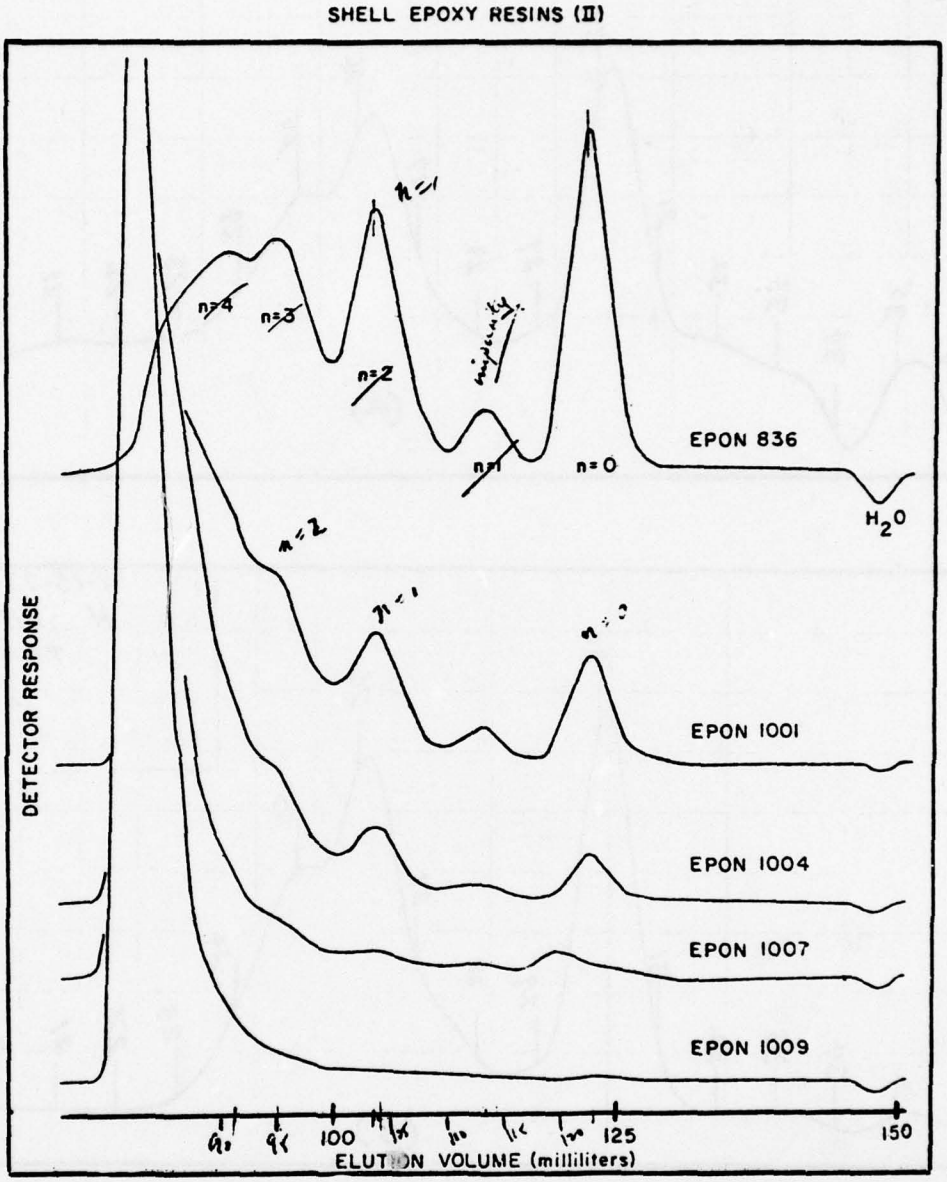

Figure 17 Gel Permeation Chromatograms of Epoxy Resins. (Reproduced from Reference 3, F. N. Larsen, Figures 4 and 6)

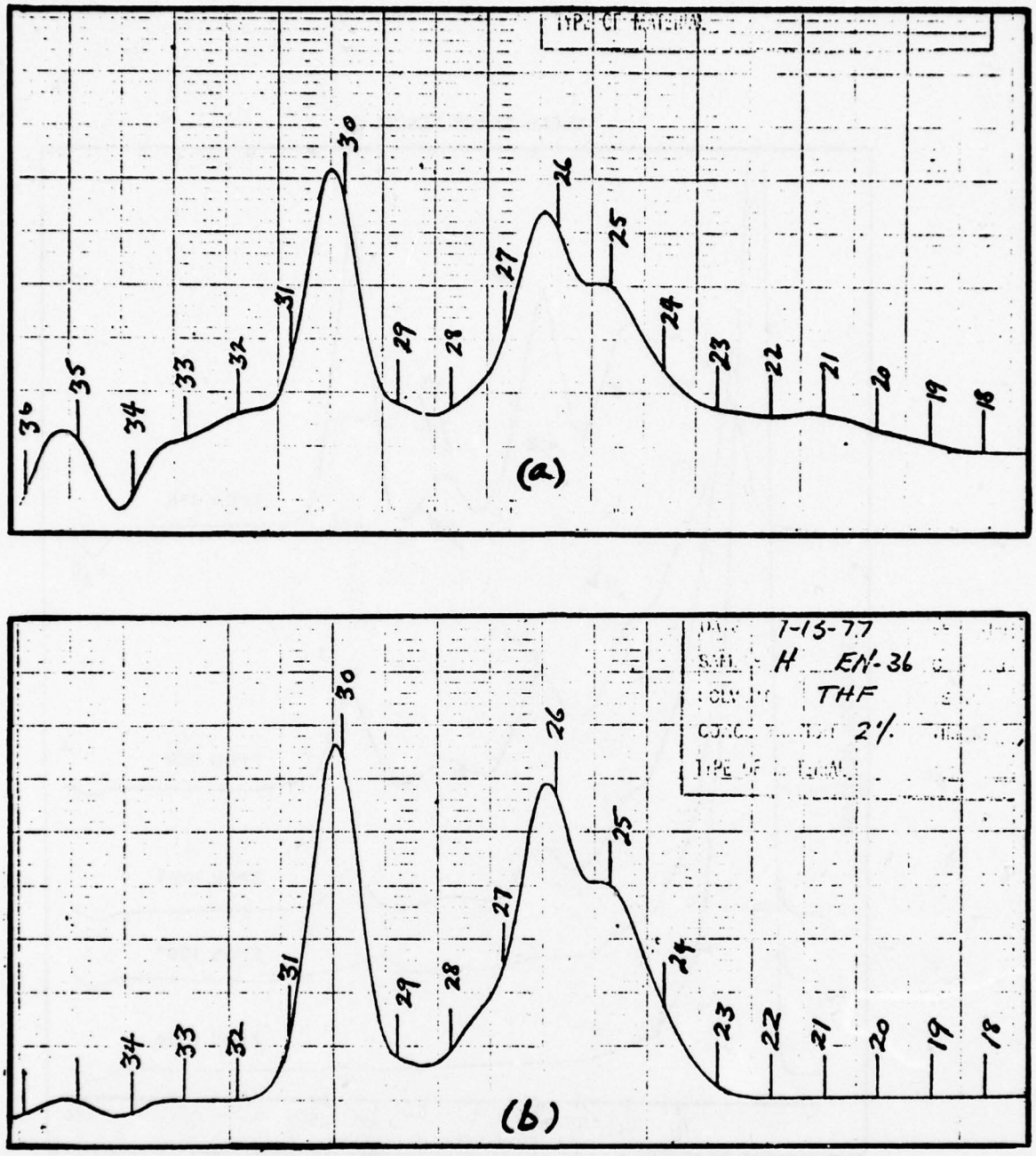

Figure 18 Gel Permeation Chromatograms (a) RE-A, (b) Epon 836, (c) Epon 1001 Waters Model 200, Instrument A, Solvent: Toluene

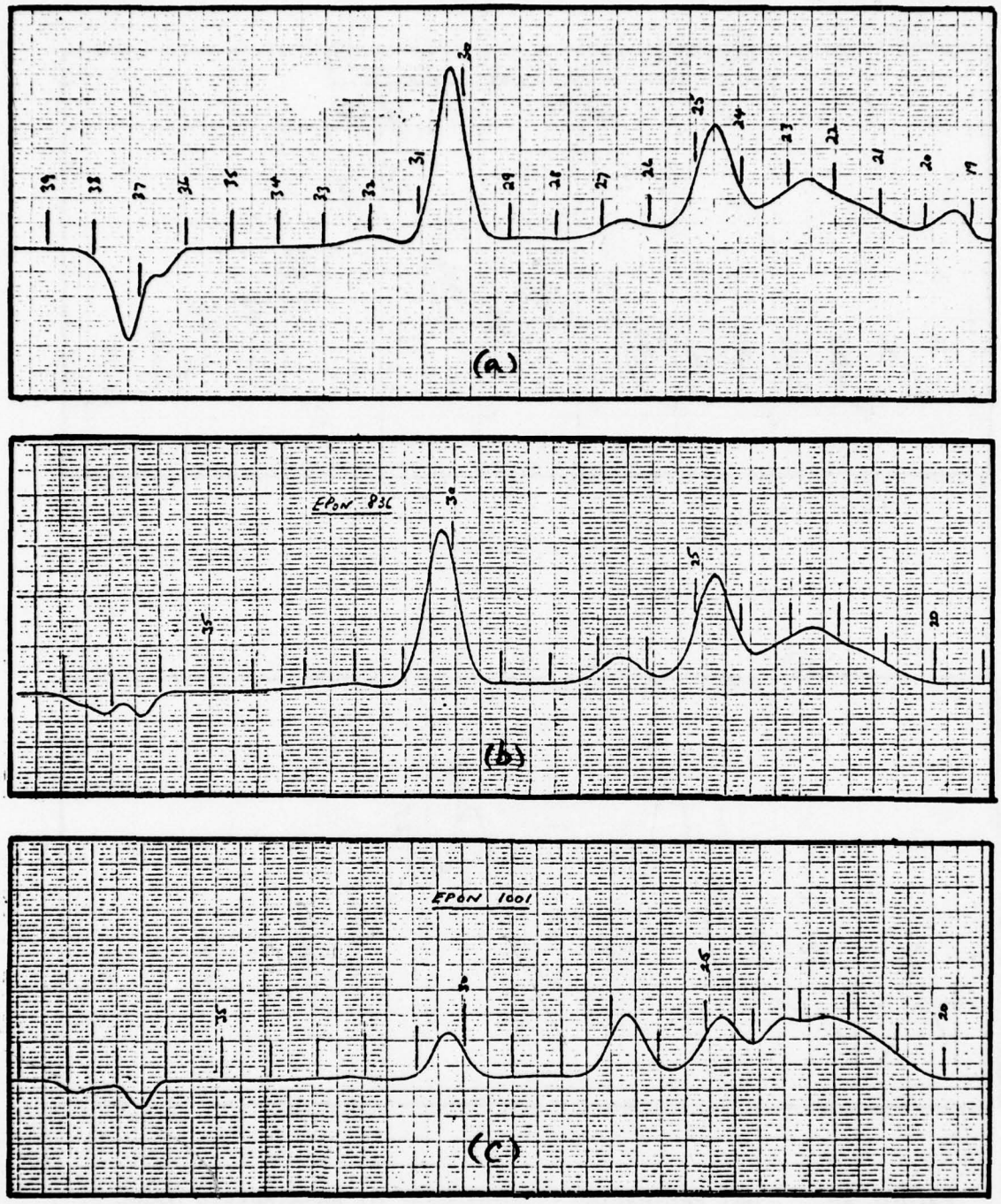

Figure 19 Gel Permeation Chromatograms (a) RE-A, (b) Epon 836 Waters Model 200 Instrument B, Solvent: THF

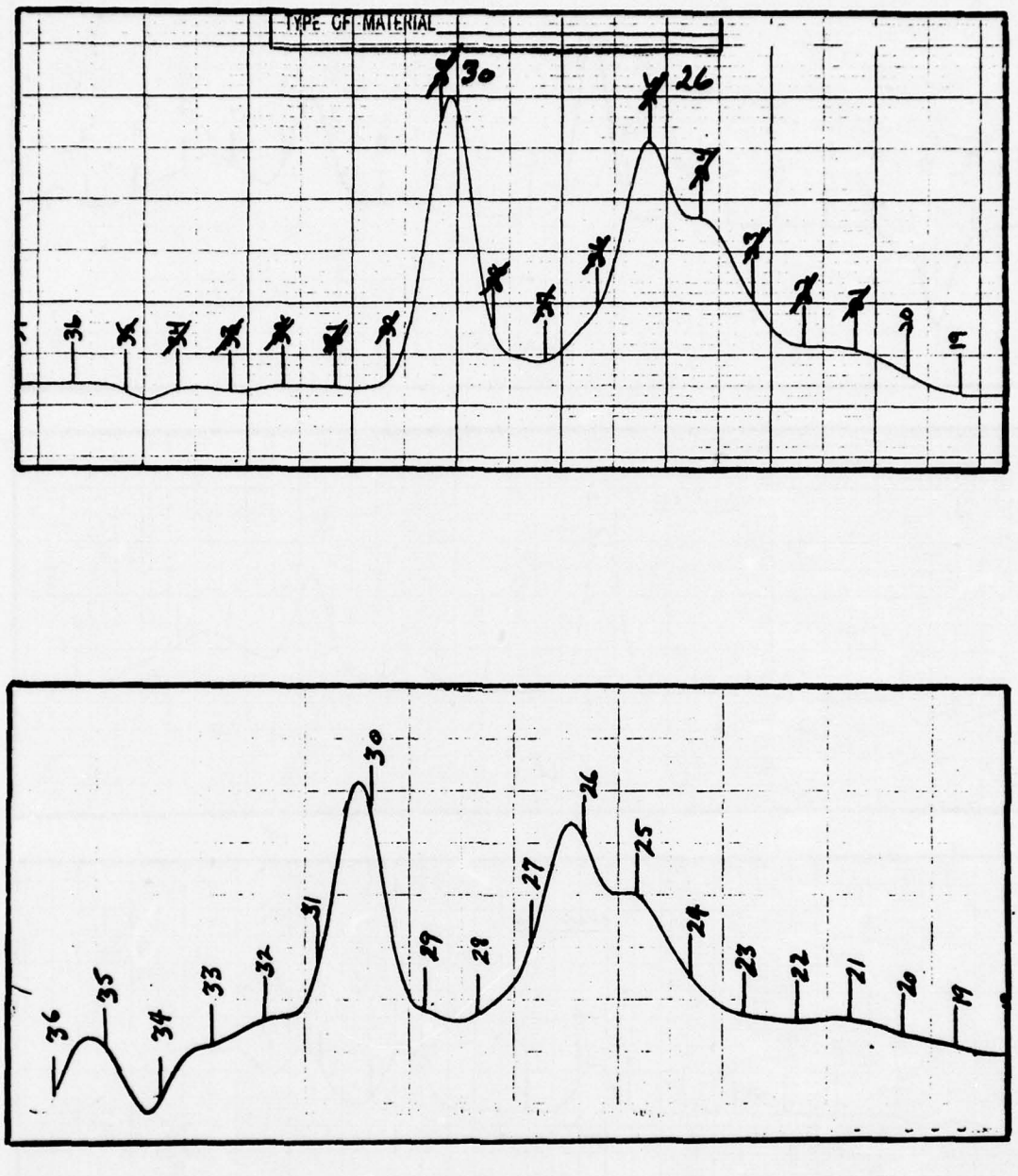

Figure 20 Gel Permeation Chromatogram of RE-A, Waters Model 200, Instrument B, Solvent: THF

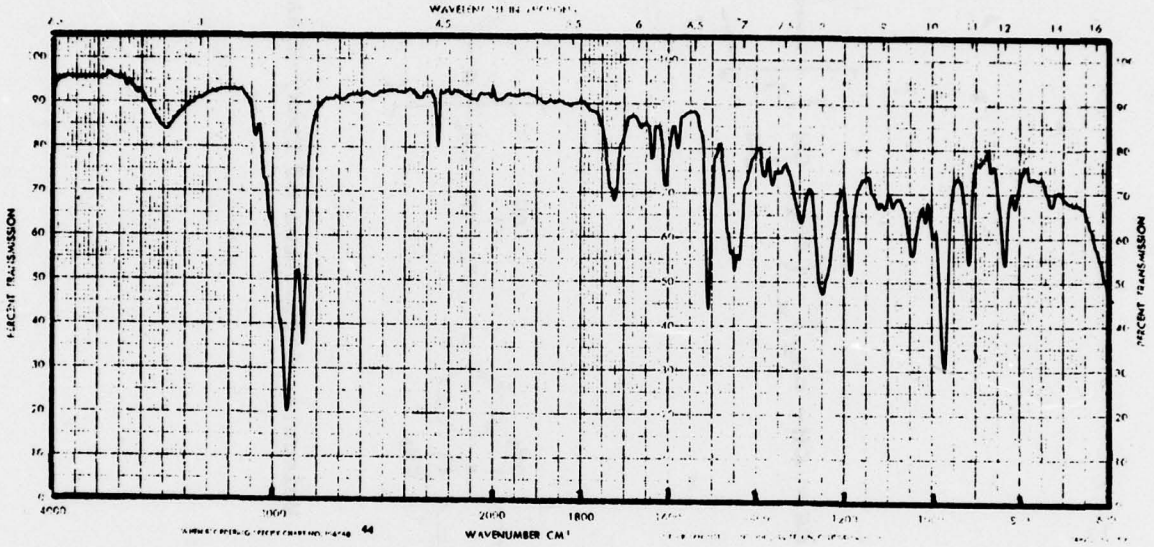

Figure 21 **Infra-red Spectrum of the High Molecular Weight Fraction Separated by GPC (see Figure 20)**

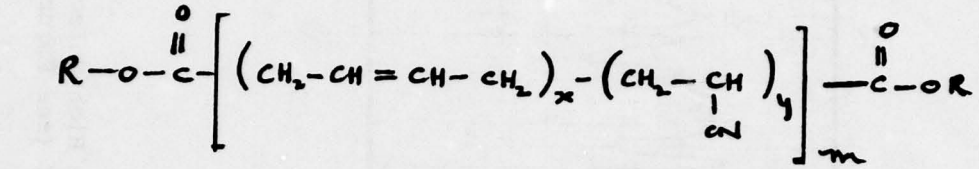

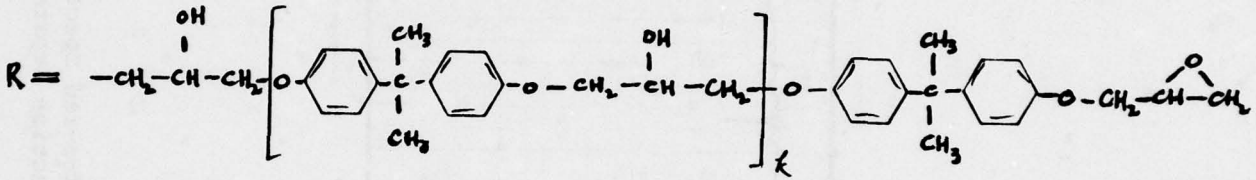

Figure 22 Molecular Structures of Epoxy-Elastomer (CTBN) Adducts

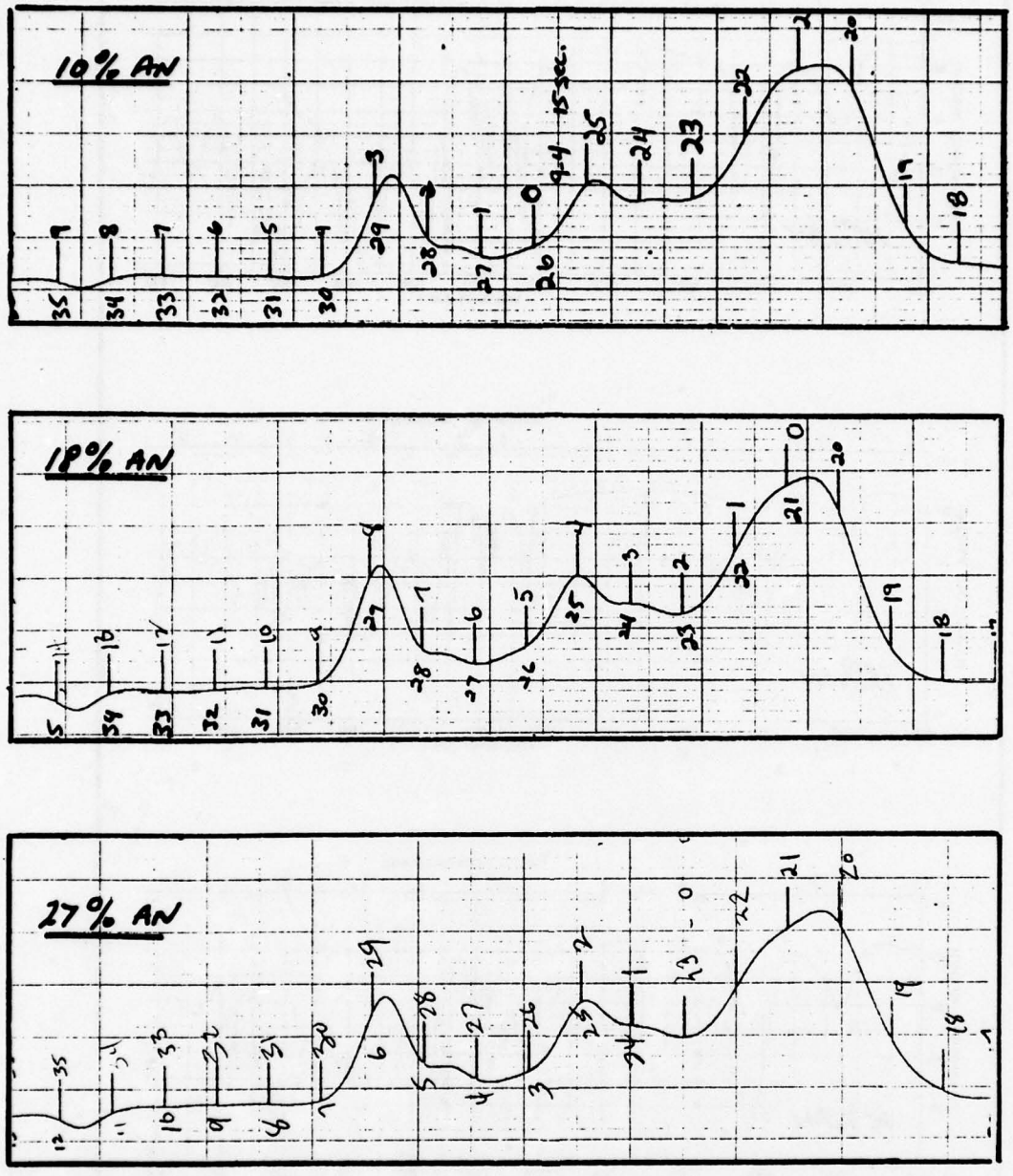

Figure 23 Gel Permeation Chromatograms of CTBN Adducts

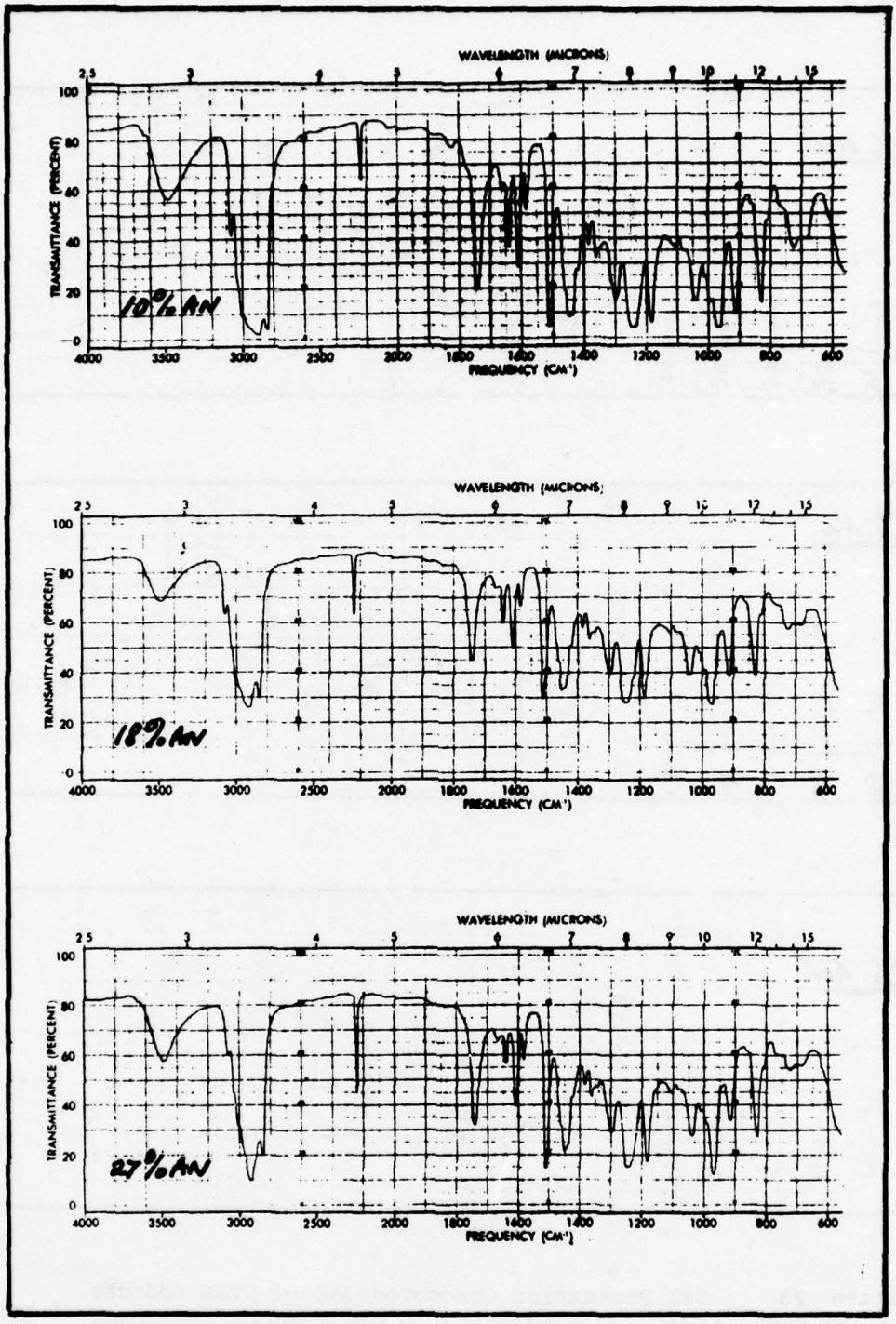

Figure 24 Infra-red Spectra of CTBN Adducts

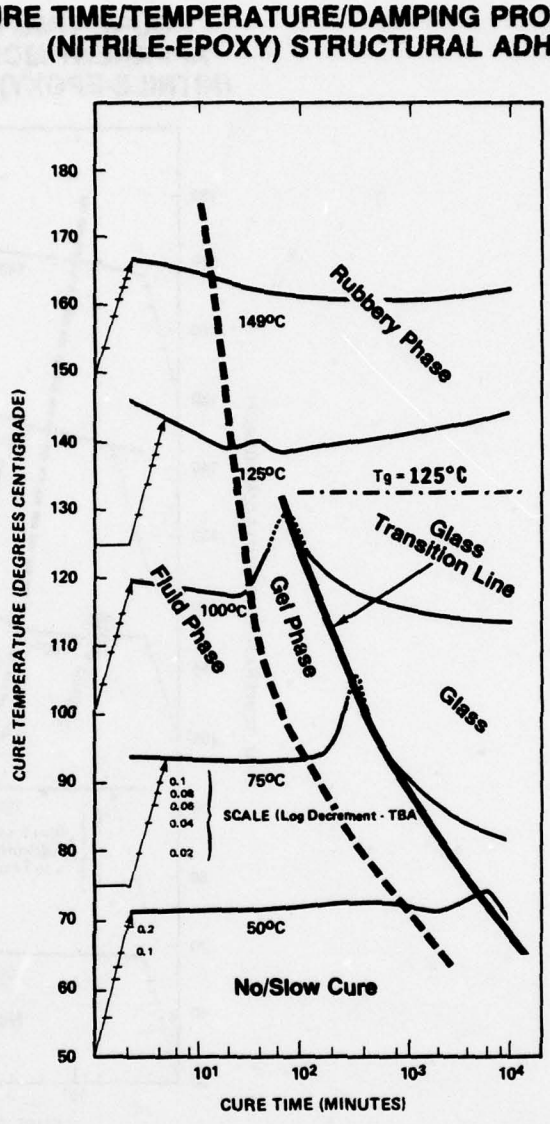

Figure 25 Log Decrement (Damping) versus Time at Different Cure Temperatures for RE-A Adhesive Resin

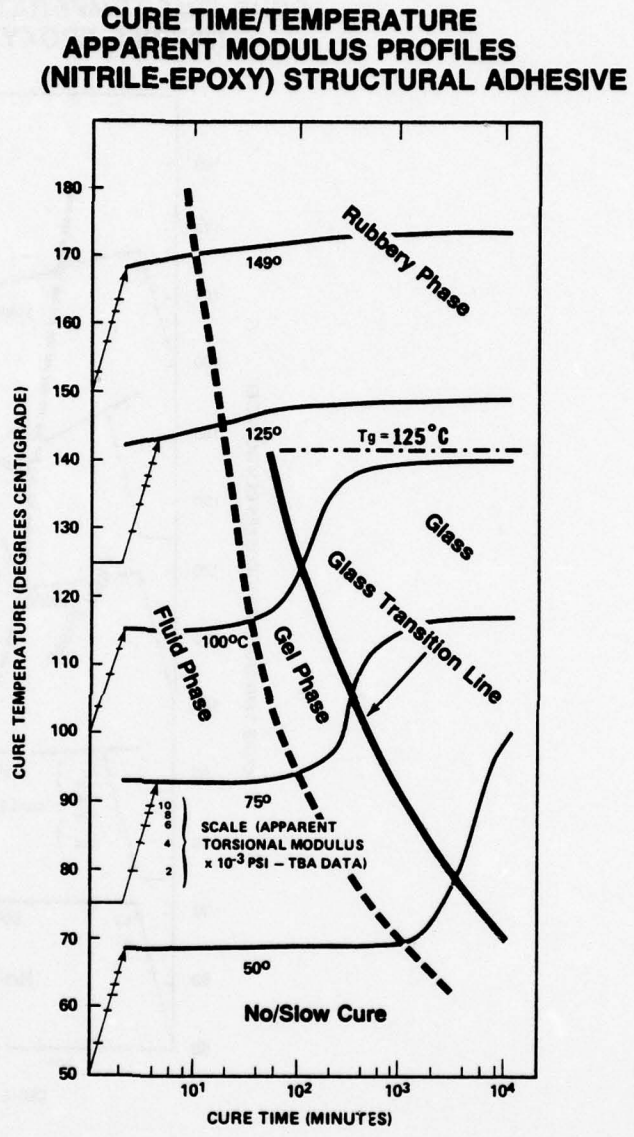

Figure 26 Dynamic Modulus versus Time at Different Isothermal Cure Temperatures for RE-A Resin

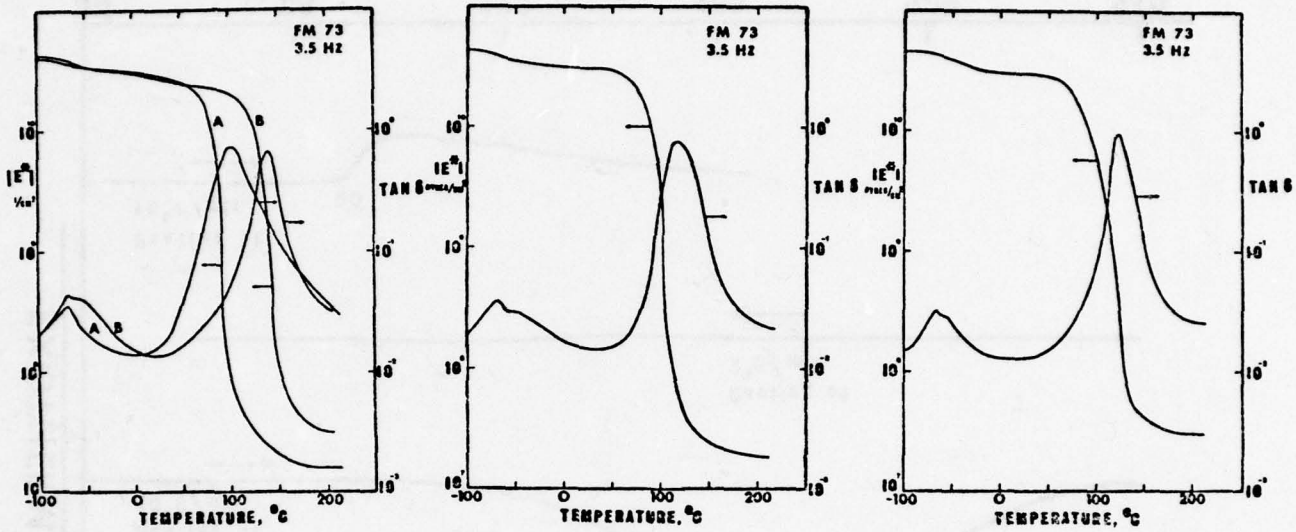

Figure 27 Dynamic Mechanical Properties, E' and Tan δ, versus Temperature for RE-A Cured at Different Temperatures: (a) 75°C for 30 Hours (A) and then Post Cured for 2 Hours at 150°C (B); (b) 120°C for 2 Hours; (c) 165°C for 2 Hours

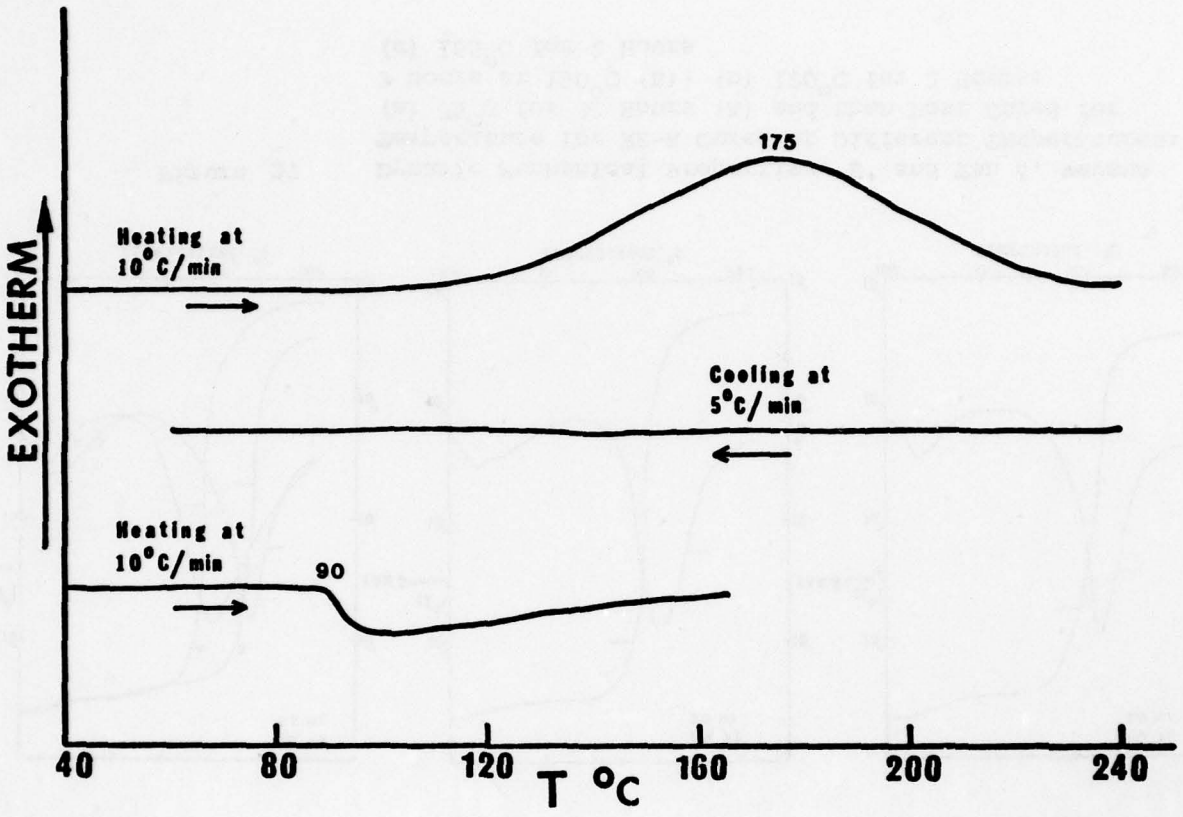

Figure 28 DSC Scan of RE-A Adhesive Resin. Heating (and Curing) at 10°C/min Followed by Cooling at 5°C/min then Heating at 10°C/min

AD-A069 517 PITTSBURGH UNIV PA DEPT OF MECHANICAL ENGINEERING F/G 11/9
MOLECULAR STRUCTURE AND COHESIVE PROPERTIES OF POLYMERIC ADHESI--ETC(U)
NOV 78 M J DOYLE F33615-76-C-5108

UNCLASSIFIED AFML-TR-78-117 NL

2 OF 2
AD
A069517

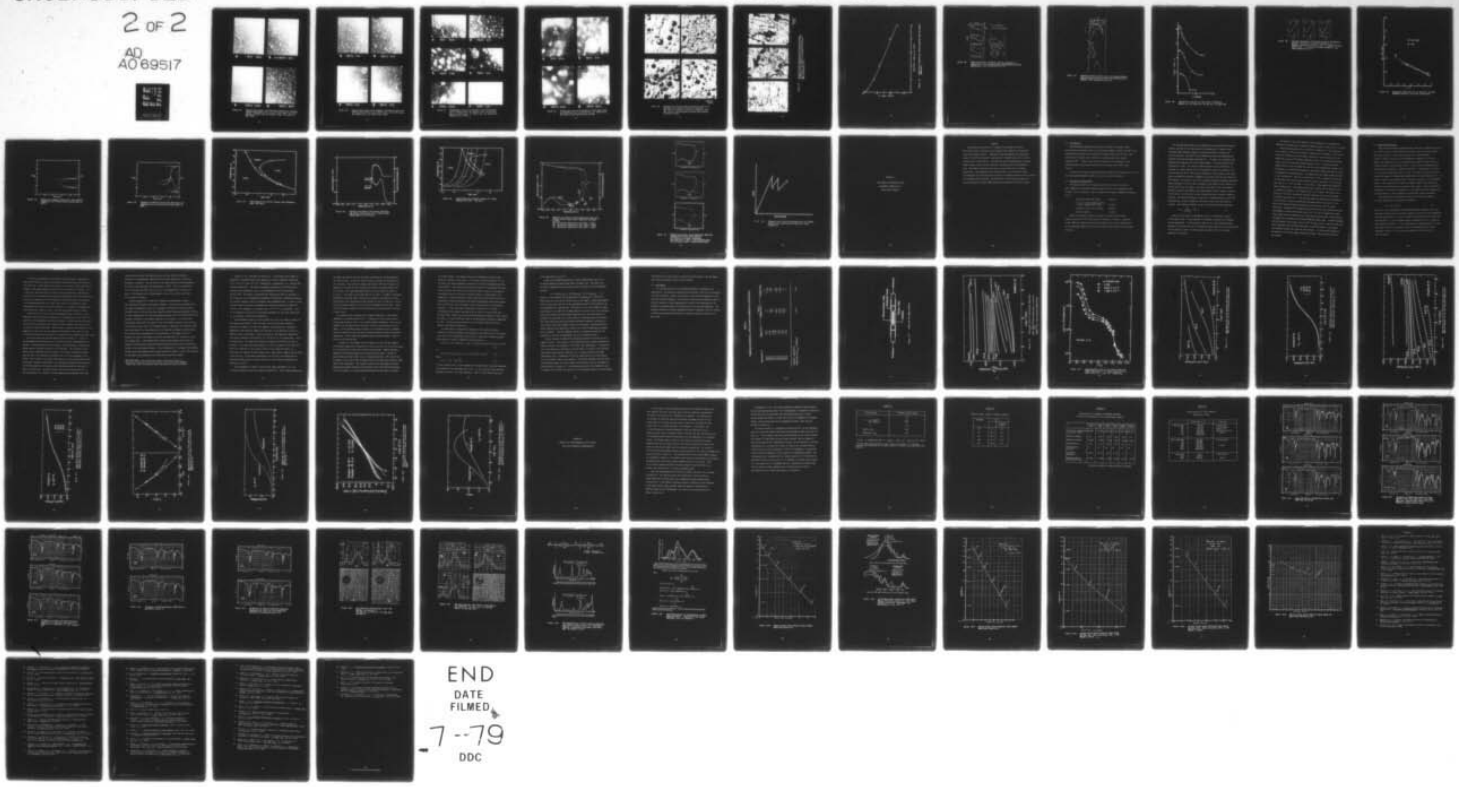

END
DATE FILMED
7-79
DDC

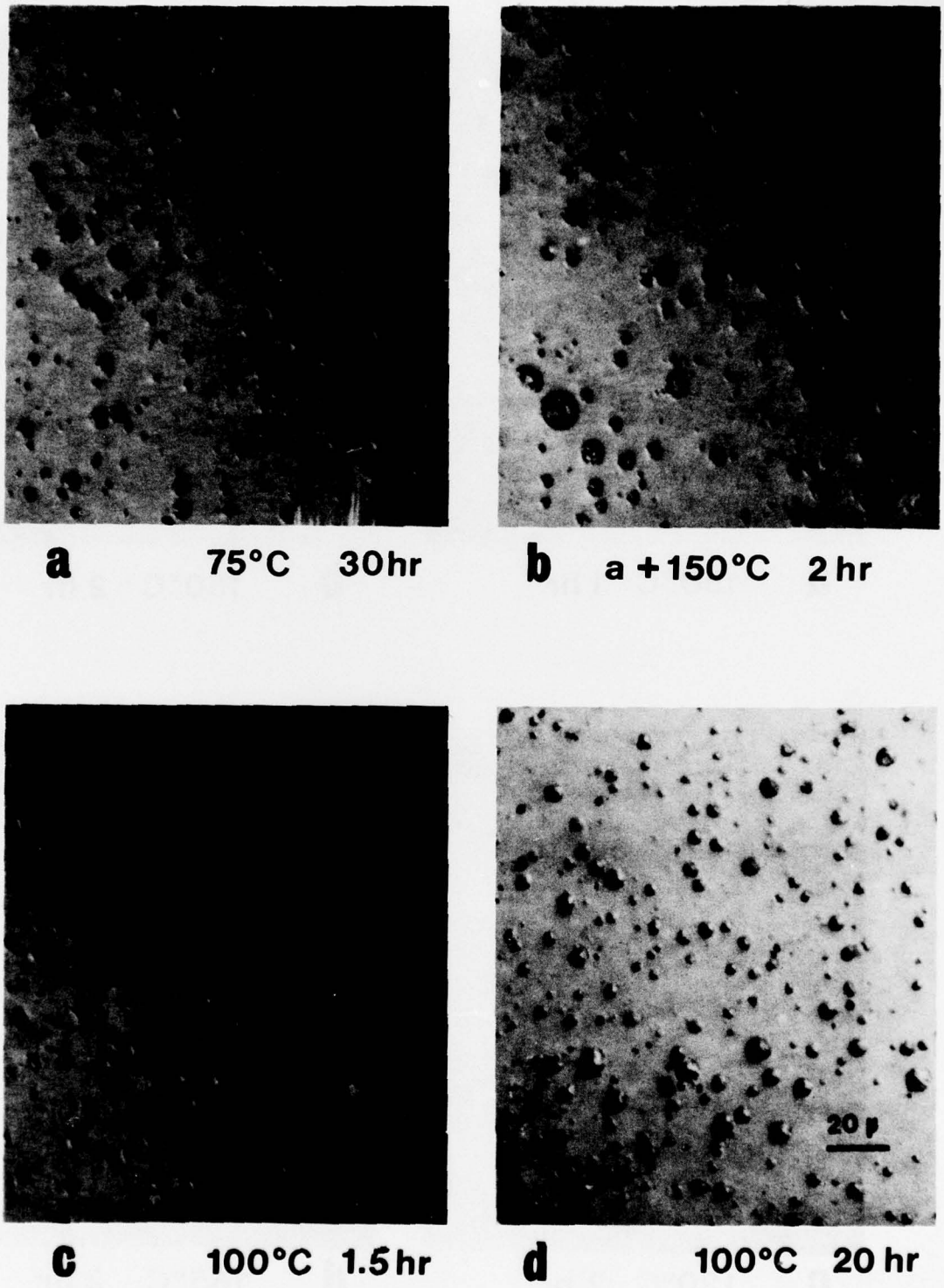

Figure 29 Optical Micrographs (with Nomarski Interference Contrast) of RE-A Neat Resin Cured at (a) 75°C/30 Hours, (b) 75°C/30 Hrs + 150°C/2 Hrs, (c) 100°C/1.5 Hrs, (d) 100°C/20 Hrs, 500X.

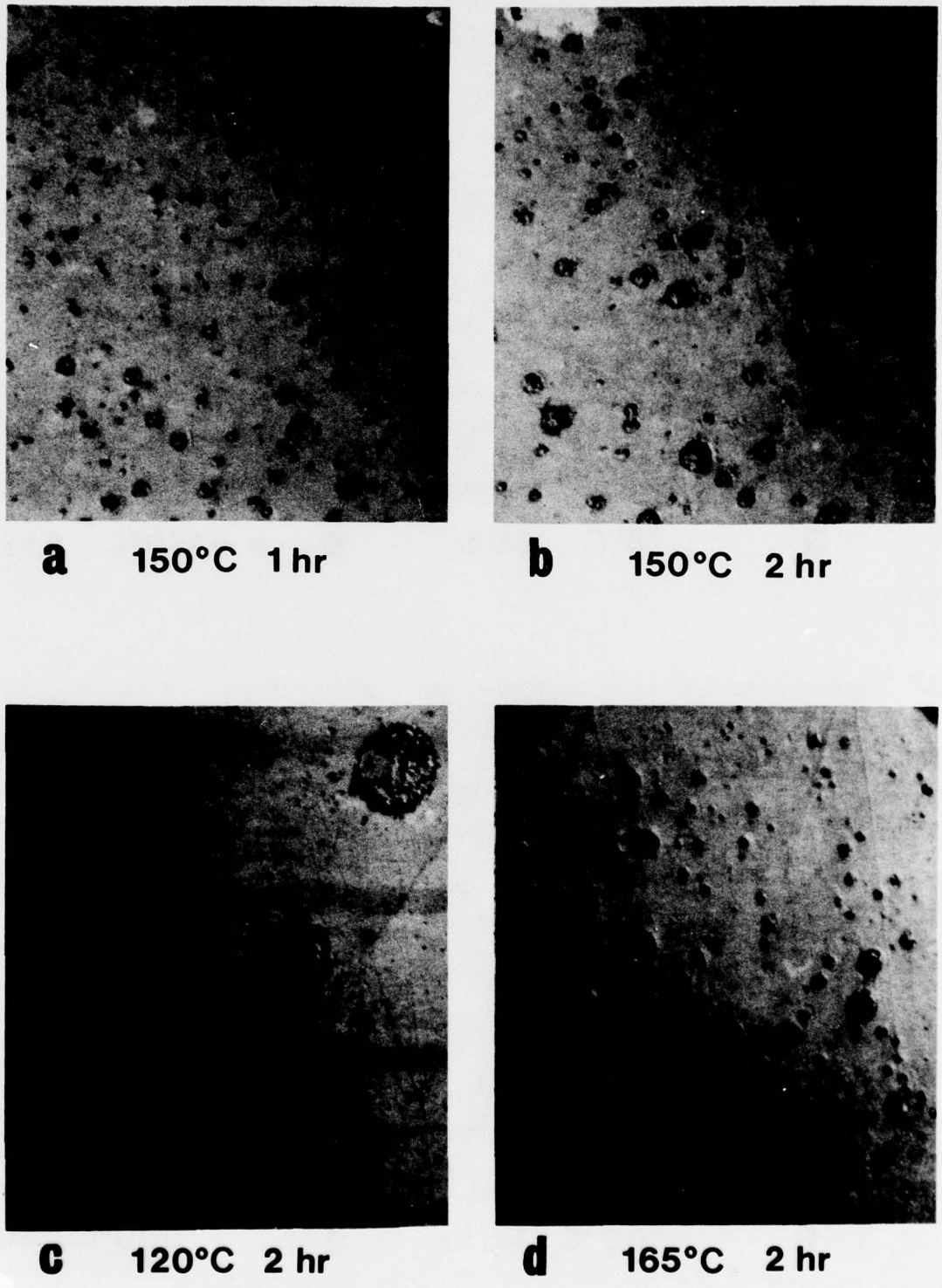

Figure 30. Optical Micrographs (with Nomarski Interference Contrast) of RE-A Resin Cured at (a) 150°C/1 Hour, (b) 150°C/2 Hrs, (c) 120°C/2 Hrs, (d) 165°C/2 Hrs, 500X.

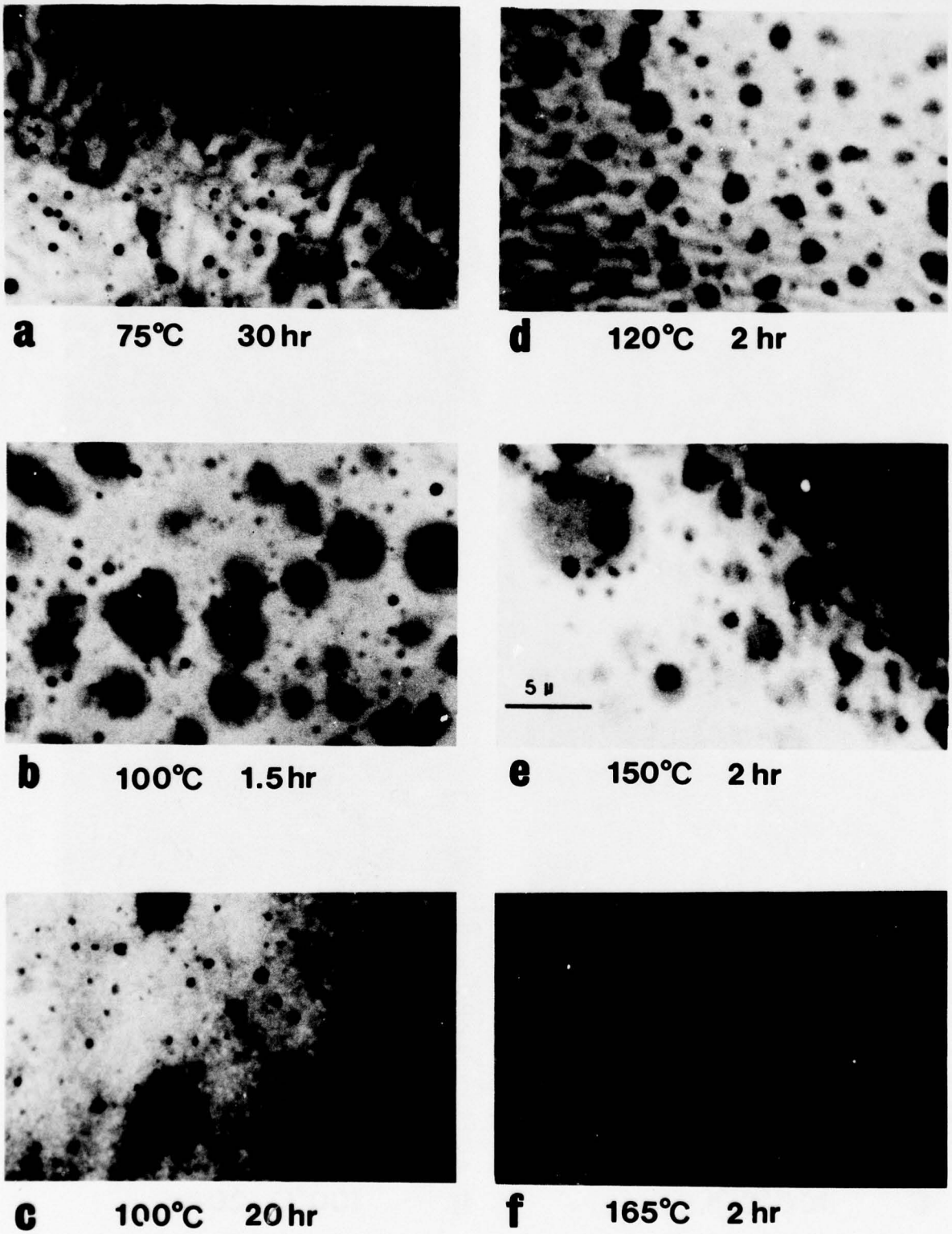

Figure 31 Transmission Electron Micrographs of RE-A Resin Cured at (a) 75°C/30 Hours, (b) 100°C/1.5 Hrs, (c) 100°C/20 Hrs, (d) 120°C/2 Hrs, (e) 150°C/2 Hrs, (f) 165°C/2 Hrs. Magnification 3,200X

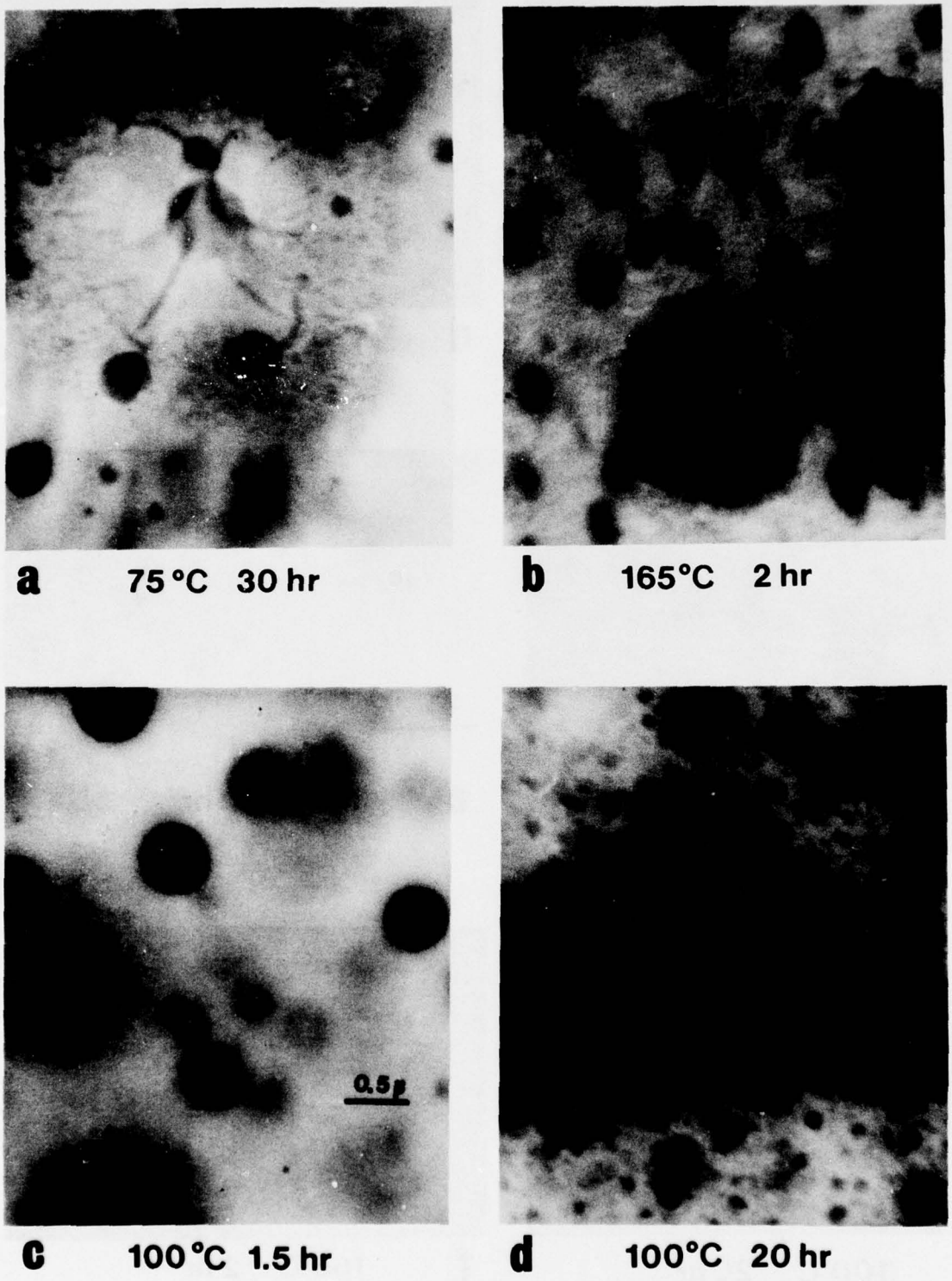

Figure 32 Transmission Electron Micrographs of RE-A Resin Cured at (a) 75°C/30 Hrs, (b) 165°C/2 Hrs, (c) 100°C/20 Hrs, (d) 100°C/20 Hrs. Magnification 20,000X

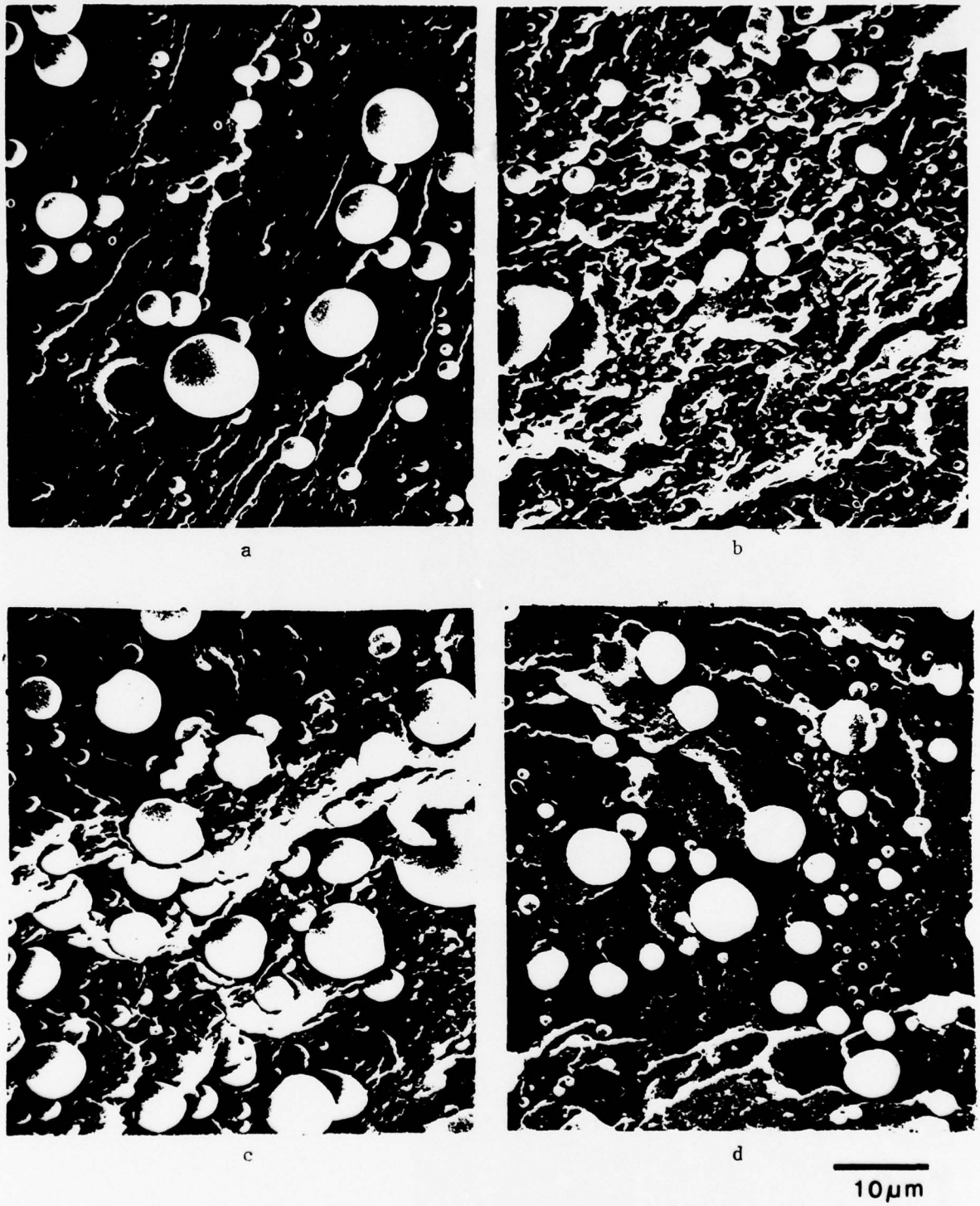

Figure 33 Scanning Electron Micrographs of Fracture Surfaces of RE-A Neat Resin Cured at (a) 75°C for 30 Hours (b) 120°C for 2 Hours (c) 150°C for 2 Hours (d) 165°C for 2 Hours. Cured Specimens Fractured After Cooling in Liquid Nitrogen

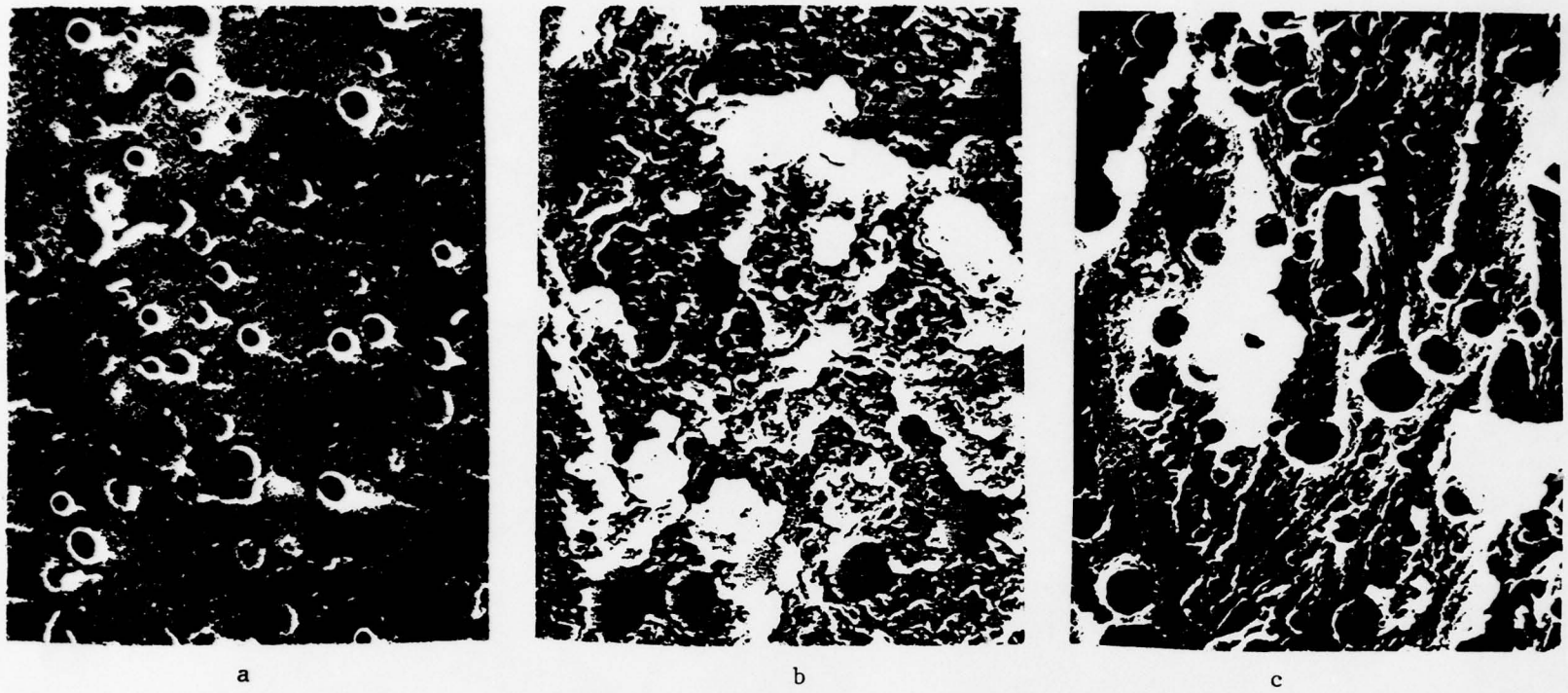

Figure 34 Scanning Electron Micrographs of Fracture Surfaces of RE-A Lap Shear Adhesive Joints Cured at (a) 100°C for 90 mins. (b) 100°C for 20 Hours (c) 150°C for Hour. Fractured at R.T.

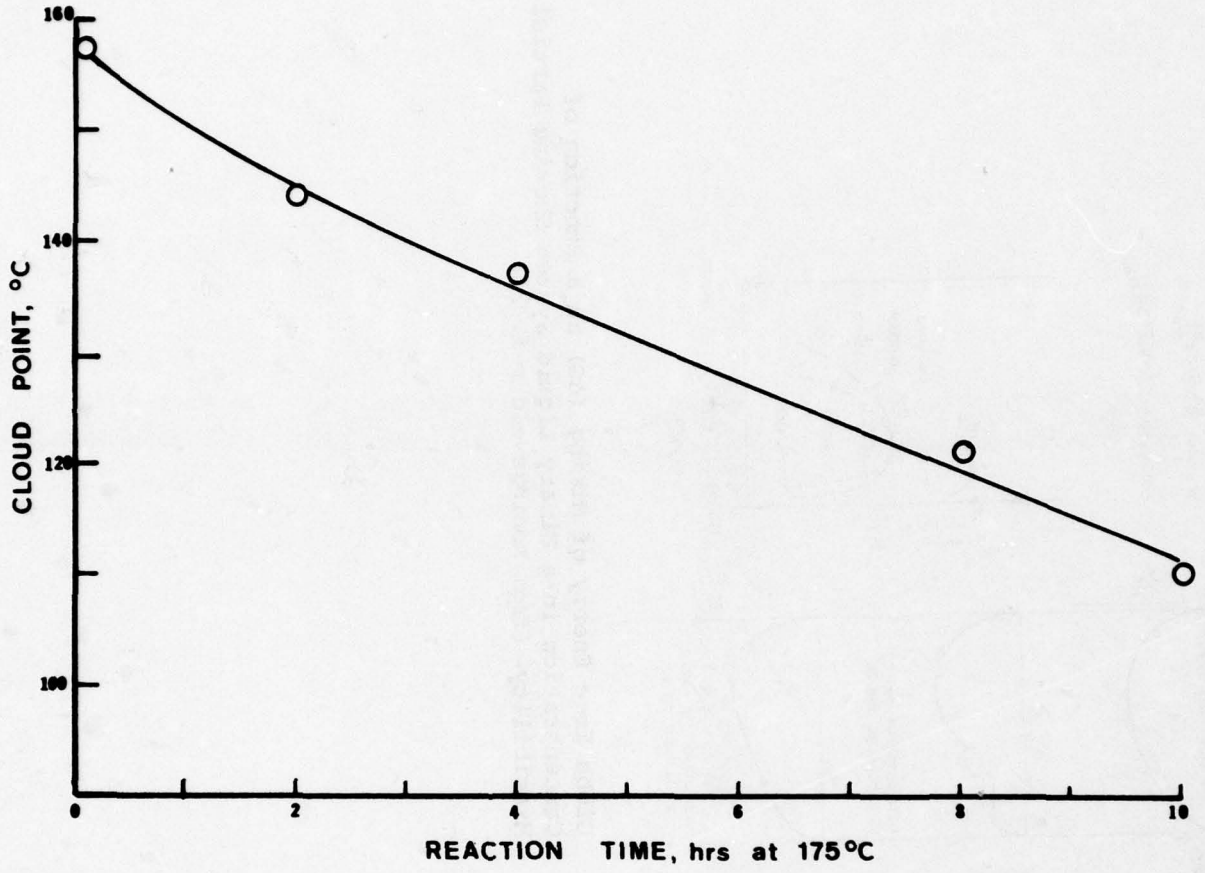

Figure 35. Cloud Point Temperature versus Reaction Time for Epoxy-CTBN Resin

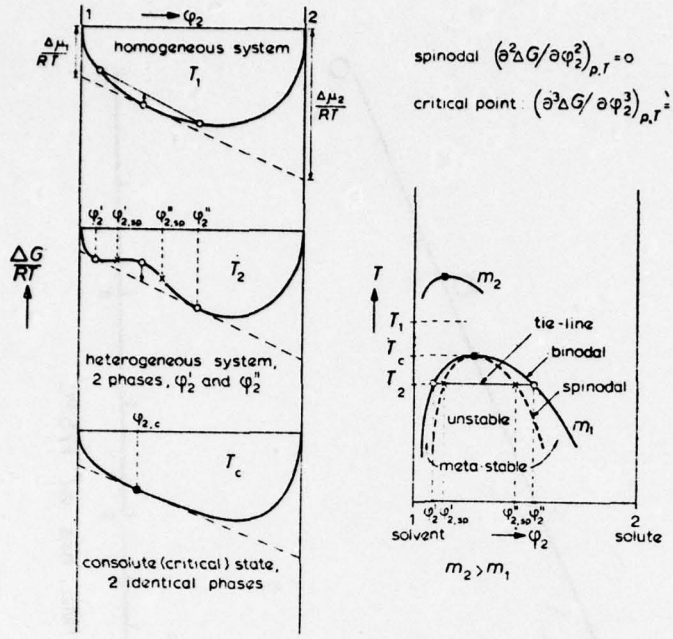

Figure 36 **Gibbs Free Energy of Mixing (ΔG) as a Function of Concentration in a Binary Liquid System Showing Partial Miscibility** (from Koningsveld ref. 22)

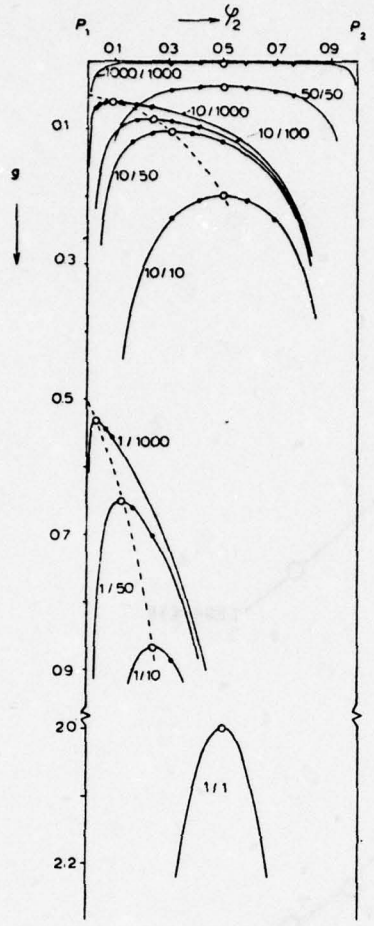

Figure 37 **Computed Stability Limits for a Two Polymer Mixture with Different Ratios of Weight Averaged Molecular Weights (from Koningsveld ref. 22)**

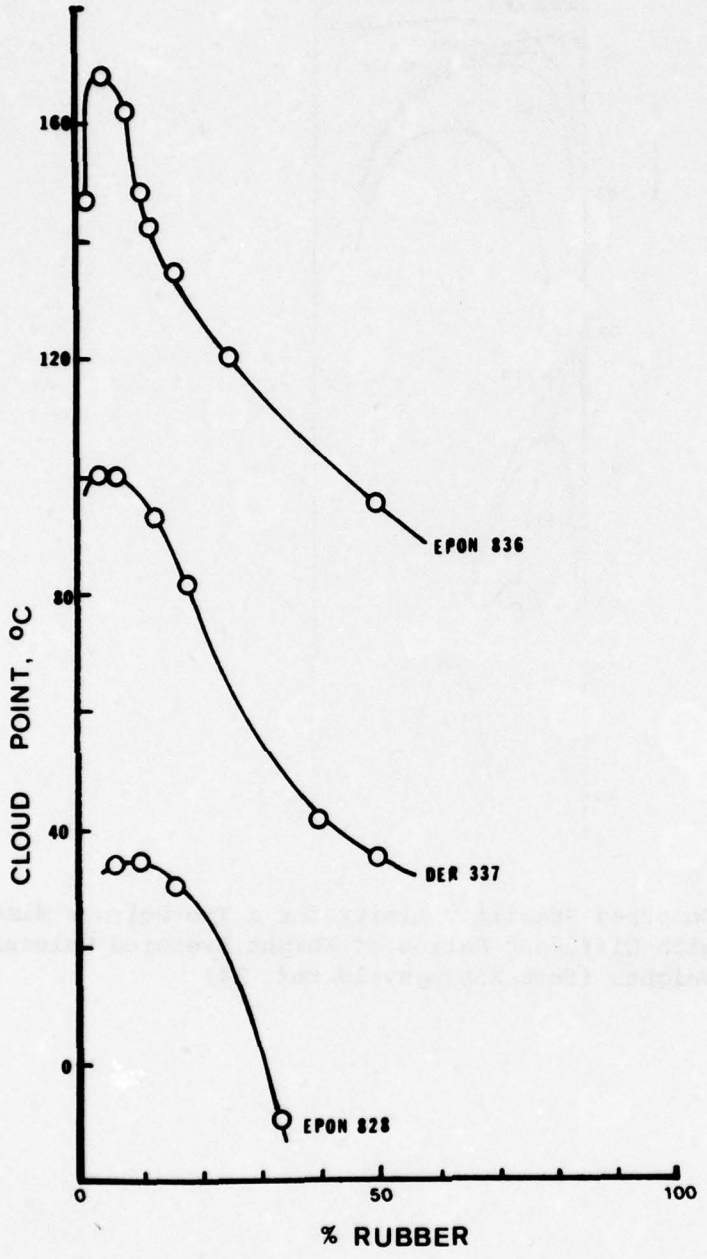

Figure 38 Miscibility Diagram for CTBN 1300 x 8 Elastomer Adduct with (a) Epon 828, (b) DER 337, (c) Epon 836

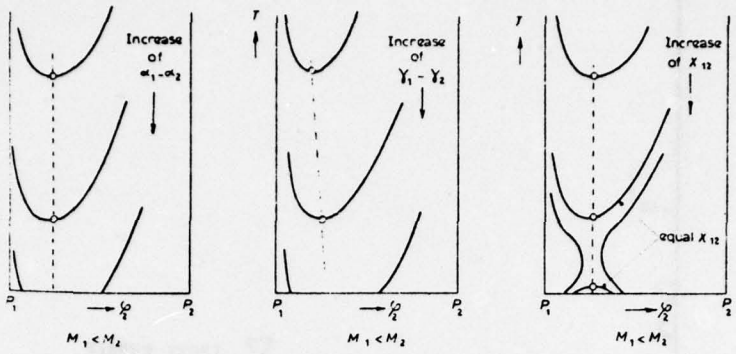

Figure 39 Computed Dependence of Miscibility Gap in Two-Polymer Mixtures on Equation of State Parameters (a) α = Thermal Expansion Coefficient, (b) γ = Thermal Pressure Coefficient, (c) Interaction Energy Parameter, X_{12}. (From McMaster ref. 21)

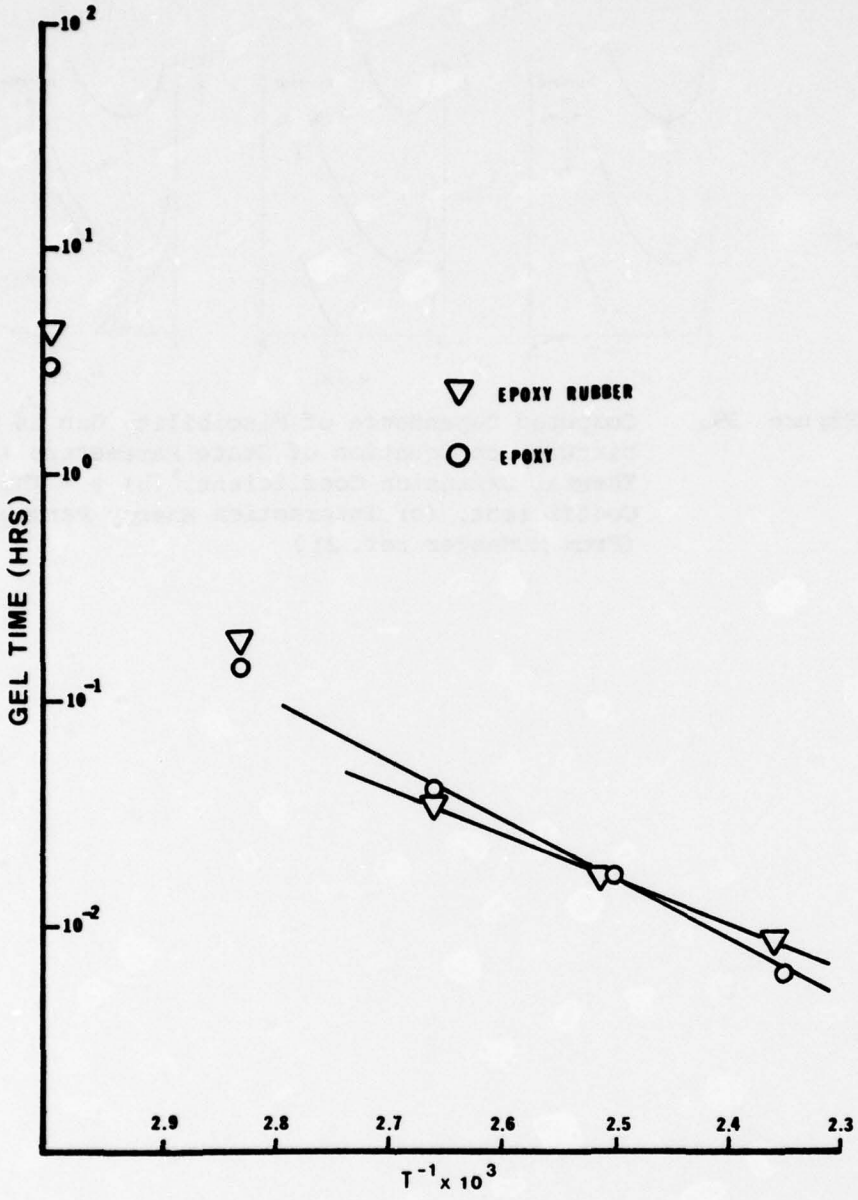

Figure 40 Activation Energy Plot for (a) Epon 836, (b) Epon 836/CTBN Cured with 'Bis Urea' Curing Agent

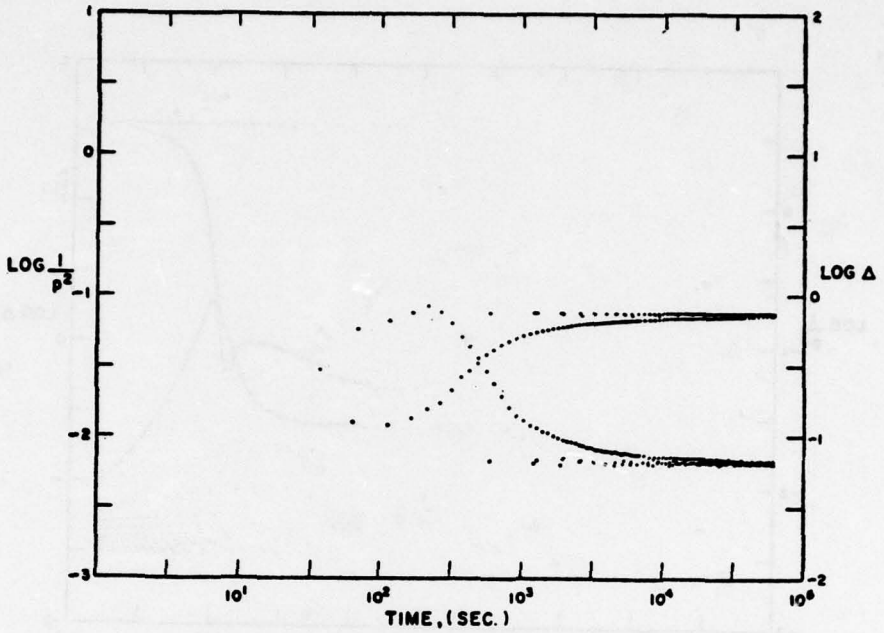

Figure 42 Rigidity and Damping versus Time (TBA plot) for Isothermal Cure of Epon 836/5% Curing Agent at 152°C.

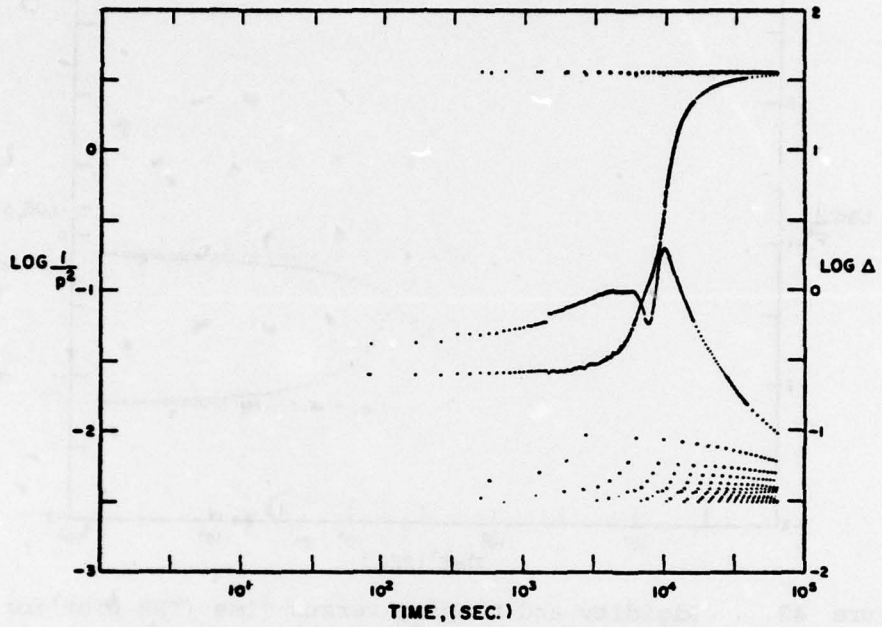

Figure 41 Rigidity and Damping versus Time (TBA plot) for Isothermal Cure of Epon 836/5% Curing Agent at 80°C.

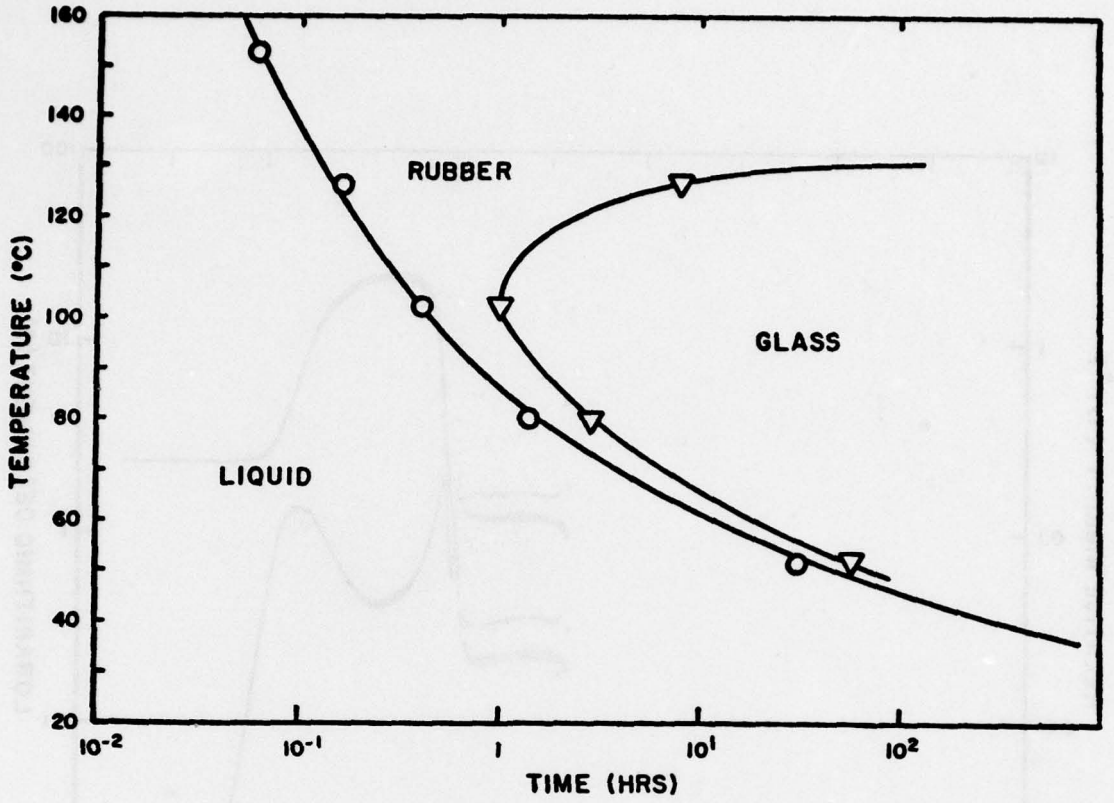

Figure 43 Time-Temperature Gel/Cure Diagram from Isothermal Cure: (TBA Data)

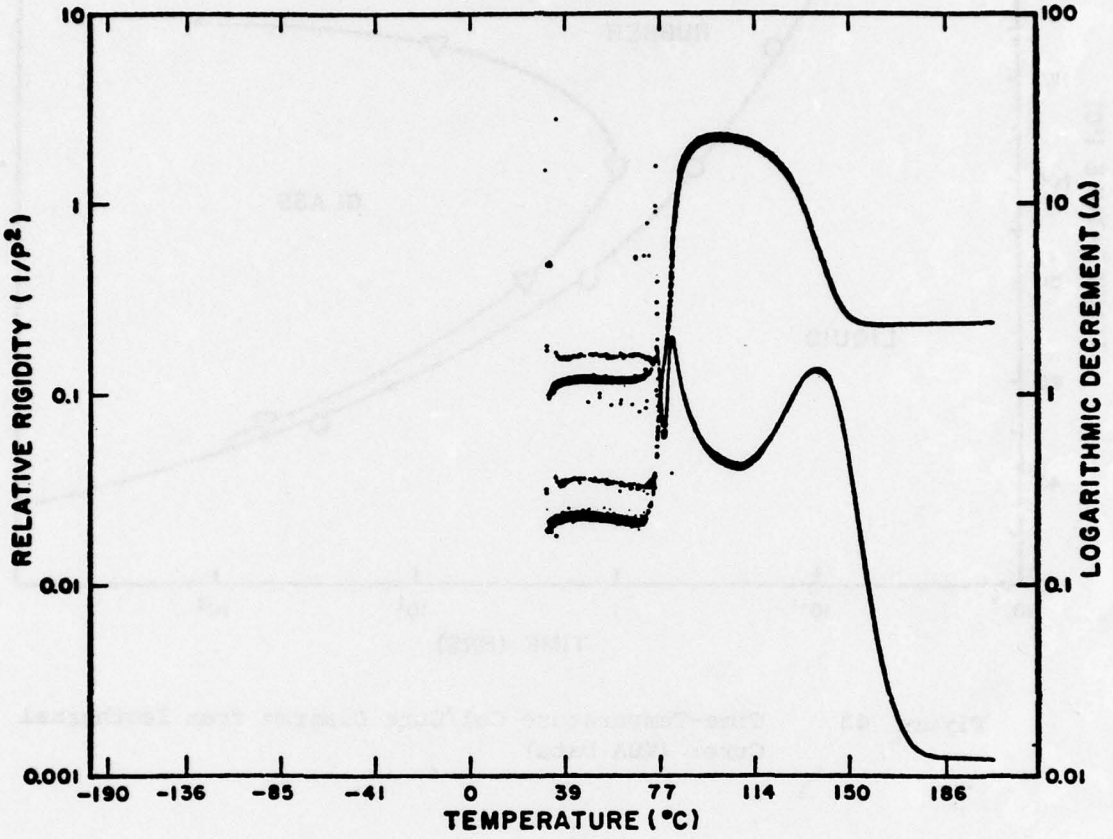

Figure 44 Rigidity and Damping versus Time (TBA plot) for Linear Heating Rate Cure of Epon 836/5% Curing Agent at 0.047°C/min.

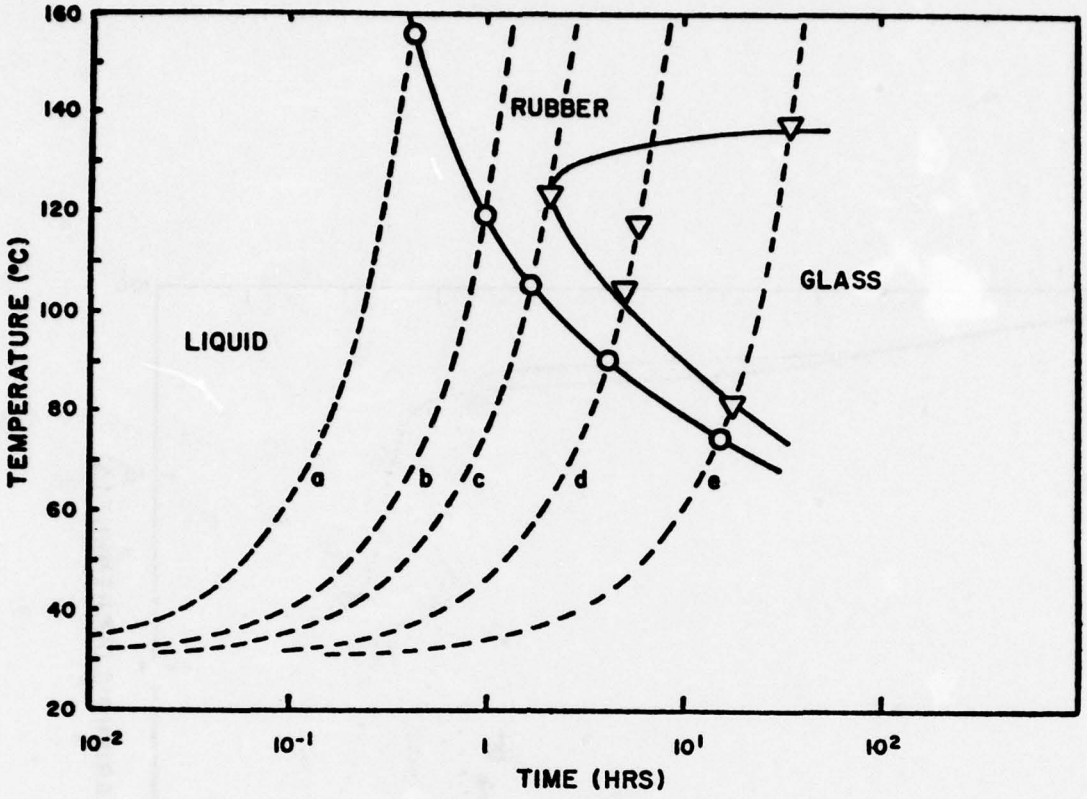

Figure 45 Time-Temperature Gel/Cure Diagram for Linear Heating Rate Cure, (TBA Data)

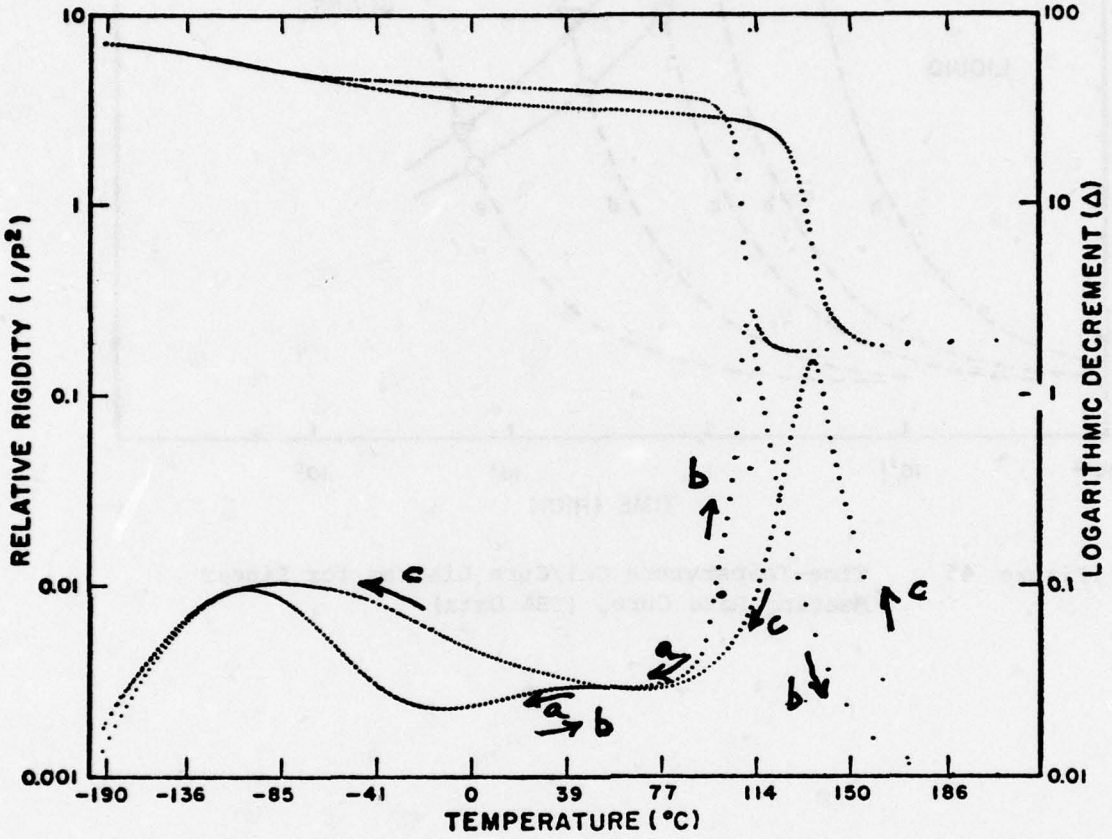

Figure 46 Rigidity and Damping versus Temperature (TBA plot) of Epon 836/5% Curing Agent Cured for 200 Hours at 80°C.

(a) Decreasing Temperature from 80°C → -190°C
(b) Increasing Temperature from -190°C → 200°C
(c) Decreasing Temperature from 200°C → -190°C

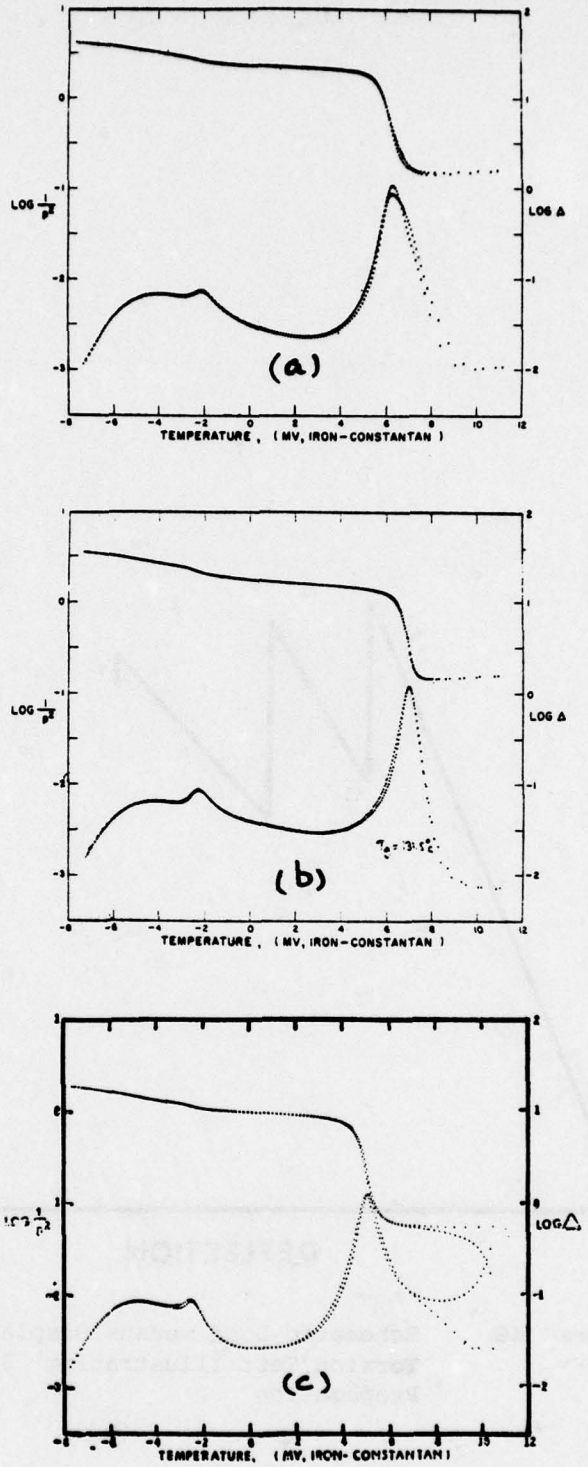

Figure 47 Rigidity and Damping versus Temperature (TBA plot) of Epon 836/5% Curing Agent Cured at
(a) 125°C for 124 Hours, (Isothermal)
(b) 0.047°C/min to 200°C, (Linear Heating Rate)
(c) 5.0°C/min to 200°C, (Linear Heating Rate)

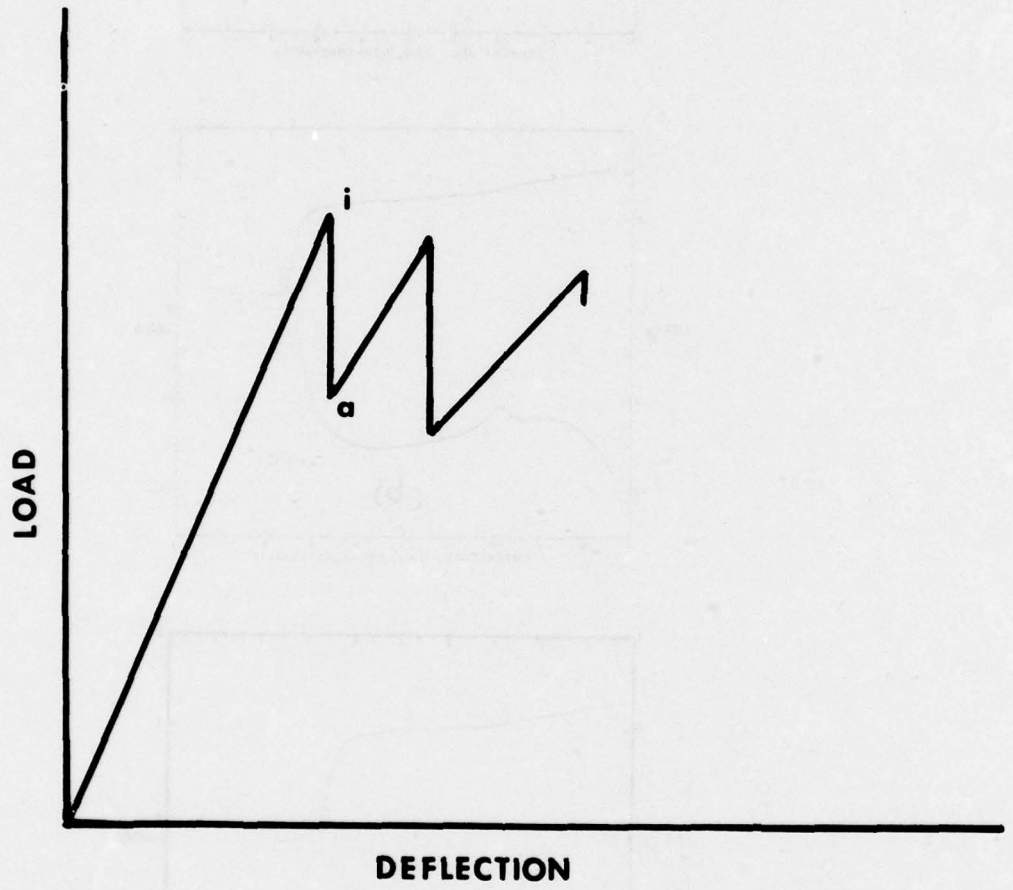

Figure 48 **Schematic Load versus Displacement Plot for Double Torsion Test Illustrating "Stick-Slip" Crack Propagation**

APPENDIX A

THE EFFECT OF MOISTURE ON THE MECHANICAL BEHAVIOR OF A NYLON EPOXY ADHESIVE

SYNOPSIS

The mechanical properties of a commercial nylon-epoxy resin have been studied using a sensitive creep apparatus which employs a frictionless levitation magnetic bearing. Isothermal creep measurements over temperature range of 30-170^{o}C and covering a time scale of 5 decades were made on the wet and dry state of the material. Following the usual time-temperature reduction scheme, master curves for each state were constructed from the experimental data. The effect of moisture was found to be more than that of a simple plasticizer. The steepness of the reduced curves in the transition region was determined and the distribution function of retardation times of the two states of the sample were calculated. The prediction of the mechanical behavior of the bulk adhesive at higher temperatures was not possible with simple theory.

A.1 Introduction

The nylon-epoxy adhesives since their discovery in the early 1960's have acquired a prominent place in the aircraft industry, because of some of the exceptional properties such as high peel strength (more than 175 psi), high tensile shear strength (up to 8000 psi), and high impact and fatigue properties (56) However loss in peel strength at low temperature, poor creep resistance and extreme sensitivity to moisture have limited their use (67).

In this note we report some experimental studies of the rheological state of the cured epoxy-polyamide adhesive in the dry and wet conditions.

A.2 Materials and Experiments

The adhesive used for the present study (which we will call NE-A) was a commercial nylon-epoxy adhesive supplied to us as an unsupported film of about 10 mil thickness. From our analysis the chemical composition appeared to be:

Resorcinol diglycidyl ether	25 parts
1,1',2,2' tetra p-hydroxylphenyl ethane tetraglycidyl ether	10 parts
Alcohol soluble nylon copolymer	65 parts
Diallyl melamine	4 parts

During cure several chemical reactions can occur and the final chemical structure of the cured resin is difficult to predict. According to Bell **(58)** the carboxyl and amine end groups as well as the amide groups of the polyamide chains react with the oxirane group forming the crosslinked structure.

All the measurements made on the sample were of creep and creep recovery and were confined to the linear range of viscoelasticity. Plazek's creep instrument which employs a magnetic levitation bearing to eliminate the friction was used. The details of the operating principle and experimental procedure have been described previously (59). In brief, the instrument uses parallel plate geometry with a disc shaped sample. The bottom plate of the instrument is fixed. The torque is applied through the top plate which is attached to a freely hanging rotor in the magnetic field of a solenoid. The vertical position of the rotor is kept constant by radio frequency coils which sense its height and activate a feedback circuit which controls the current of the solenoid. The torque in the rotor is applied through an aluminum conductive sleeve attached to the rotor and it resides in the annulus of the central core and the field coils of a motor. The poles of the field coils are connected through a capacitor and produces a rotating magnetic field. During a creep run the current in the field coil is kept constant and hence a constant torque is produced. The angular deflection of the rotor is monitored with a light lever reflected from a mirror attached to the rotor, to the light following pen recorder. The following equation is used to calculate the creep compliance.

$$J(t) = \frac{m^2}{2\pi h^2 \rho^2} \cdot \frac{\theta_o}{\tau} \cdot \Delta \qquad \text{A.1}$$

Where m is the weight of the sample in gms, h is the height (length) of the sample in cm, ρ is the density of the sample in gm/cm^3 at the temperature of measurement, τ is the torque in dyne-cm, θ_o is the calibrated angle constant of the light lever arm in radians per chart space and Δ is the deflection of the recorder at time t in chart spaces and finally J(t) is the creep compliance in cm^2/dyne.

The density of the cured sample at room temperature, as determined by floatation technique using a calibrated density gradient column, was 1.156 gm/cm^3.

From past experience with the instrument capabilities it was calculated that a sample of about one centimeter in length would be needed in order to get sufficient deflection on the recorder (especially at short times and at low temperatures; below 10^{-8} cm^2/dyne compliance level) with the maximum available torque and with the smallest diameter platens (1/8"). The existing sample chamber design of the instrument was such that only thermoplastic samples could be measured; a few small modifications in the sample holding were made in order to accommodate crosslinked resins. The samples for the present study were made in the following way. About 60 to 80 eyelets of 1/8" in diameter were punched out from the 10 mil film and were stacked on top of each other in a true glass bore tube of I.D. 1/8" and about 1 cm in length. (Some samples were prepared using a Teflon tube.) Two aluminum plugs each of about 3/8" in length by 1/4" in diameter and having a 1/8" diameter step of 1/8" length, were placed one in each end of the tube, the smaller diameter side being on the inside touching the sample (see Figure A.1). The aluminum plugs were previously acid etched in a 10% solution of sulfuric acid/sodium dichromate solution at about 75°C for about 15-20 minutes followed by washing and oven drying at 80°C for about 20 minutes. Alignment of the sample and the metal 'grips' was ensured by placing the assembly in side another glass tube of I.D. 1/4" and of appropriate length. Using clamps and 1/4" diameter rods on each side of the Al plugs, slight pressure was applied on the plugs and the uncured adhesive between them. The whole assembly was then placed in the vacuum oven at 175°C for about 1 hour. After the resin was fully cured the glass tube was broken away to yield the sample. Each sample was carefully checked for voids and other defects. In this way good bonding at the plugs as well as good sample shape was achieved. The plugs now served as the platens.

A.3 Results and Discussion

Creep and creep recovery measurements were made over a temperature range of 30 to 175°C, covering a wide range of time scale. Most of the runs lasted about 5000 seconds, but some were continued up to 100,000 seconds. Figure A.2 shows a typical set of measurements for sample I-D, a dry (D) sample; the logarithm of the creep compliance multiplied by factor $(T\rho/T_o\rho_o)$ is plotted against the logarithm of time. T and ρ being the temperature in degrees Kelvin and density in gm/cm^3 respectively. The subscript "o" refers to the reference temperature which is 30°C. The factor $(T\rho/T_o\rho_o)$ takes into account the rubber like temperature dependence of the sample behavior (60). Its value was found to be negligibly small and hence is ignored in the subsequent graphs. After installing the sample, the sample chamber was alternatively evacuated and flushed with dry nitrogen several times in order to minimize the possibility of the oxidative degradation of the sample at higher temperatures. All measurements on the dry samples were made under nitrogen atmosphere.

The creep curves are analyzed according to the classical equation of creep compliance for a crosslinked system (63):

$$J(t) = J_g + J_d\psi(t) \qquad A.2$$

where J_g is the instantaneous time independent glassy compliance and is the long time limiting value of secondary dispersion arising from the deformations from side group motions. It also includes the stretching of inter and intra-molecular bonds. J_d is the delayed elastic compliance and $\psi(t)$ is known as the retardation function. It is a monotonically increasing function of time, being equal to zero at time equal to zero and approaches unity as time approaches infinity, J(t) is the creep compliance in $cm^2/dyne$ and t is time in seconds.

Our initial measurements on the sample (not shown here) at temperatures above 100°C resulted in creep curves which changed their shape and position on the time scale. These changes were found to be the result of the morphological changes in the sample possibly occurring due to the aging of the sample, if it is held for a prolonged period of time at higher temperatures. Besides this, discoloration of the samples was observed at temperatures above 100°C suggesting the onset of degradation and thus limited the higher temperature measurements. All the measurements made up to 100°C were found to be reproducible within experimental error which in our case is about $\pm$ 3%. However, high temperature runs varied over a range of $\pm$ 20%. This will be discussed later in detail.

Before the start of the series of measurements shown in Figure A.2, the sample was heated as quickly as possible to the temperature of cure (175°C) and was kept at that temperature for about 40 minutes. During this period at about every ten minutes interval, short creep and creep recovery runs, each lasting for about 100 seconds were made. This was done to ascertain the stability of the sample and to make sure that the sample had achieved its final state of cure. All the runs were found to be within 1%, indicating that the sample was fully cured.

Series of creep runs were then made as shown in Figure A.2. Initially, the measurements were limited only to 73°C and frequently reproducibility was checked. As was expected and can be noted at room temperature, the sample was glassy and had a modulus of about 9.8×10^9 dyne/cm^2. The transition occurs around 45°C as indicated by the run made at 44.1°C where the modulus changes over ten fold. The transition is probably due to the nylon component of the system. Butt & Cotter (13) during their studies on a nylon epoxy adhesive have also noted a transition around 40°C. The individual isothermal creep curves up to 73°C are parallel to one another and can be shifted along the time axis to obtain a master curve. The shift factors used for this construction fit a WLF type equation (60). However, the high temperature measurements gave creep

curves which are quite flat, Figure A.2, and the data cannot be reduced. Increase in the temperature simply shifts the curve upward with a resulting decreasing in modulus. The top curve of the graph represents two measurements. The open circles represent the measurements at 154°C. The curve obtained at 163.3°C overlaps the 154°C data and in part is represented by circles with pips. To distinguish the two measurements, only a few circles at the end of the curve are marked.

Careful observation of these high temperature measurements, reveal a very interesting feature of the sample response. The curves are extremely flat and there is apparently no hint of a secondary viscoelastic transition around 120-140°C which in the past has been observed during dynamical mechanical studies by other investigators on cured nylon-epoxy adhesives (13,61,62) who attributed the secondary transition to the epoxy component of the system. In our work the measurements above 100°C were made at every few degrees intervals, each covering a time scale of more than a few thousand seconds. Obviously, no transition could have been missed if it were present, even if some minor changes had been taking place during these measurements in the morphology of the sample; which is probably the case as indicated by the poor reproducibility of the data at these high temperatures. Some morphological changes could possibly arise from the presence of temperature sensitive hydrogen bonding and nylon micro-crystallites* present in the nylon-epoxy network. As the temperature is increased, the hydrogen bonding slowly diminishes and the crystallites melt causing a loss in the rigidity of the sample and consequently the curves shift vertically upward.

*The nylon used in the formulation of NE-A is alcohol soluble, but spherulites could be seen in a thin solid film of the nylon component cooled from a melt and observed under the polarized light microscope.

Figure A.3 is a cross plot of Figure A.2. In the graph, the inverse of compliance is plotted against the temperature at three different frequencies 6.28, 6.28×10^{-2} and 1.99×10^{-3} radians/sec. corresponding to 1, 100 and 3165 seconds respectively. The graph is somewhat misleading in the sense that it indicates two transitions, one in the neighborhood of 45° and the other around $130^{\circ}C$. The Figure is presented here because more data is available in the literature for the temperature dependence of mechanical properties measured at constant frequency than for isothermal time dependence data. A point to note from the graph is that the low temperature transition shifts from about 45° to $50^{\circ}C$ as the frequency is increased from 2×10^{-3} to 6.3 radians/sec. This is in accordance with the well established phenomenon of the glass transition, T_g; an increase in time scale decreases T_g.

The measurements made on a moist sample II-W (wet) are shown in Figure A.4. This sample was molded at about the same time and cured under identical conditions as Sample I-D. While the sample I-D was placed in a dessicator immediately after molding, sample II-W was kept in the laboratory on top of a shelf for about three weeks. During this period, the laboratory temperature and relative humidity varied from 22 to $27^{\circ}C$ and 40 to 70% respectively. Prior to installation, the sample was weighed and found to have picked up about 3% moisture. Four creep runs made between 35 to $60^{\circ}C$ are shown in the Figure A.4. (Note the difference in the ordinate scale of this graph and Figure A.2.) The curves are parallel and they extend over a wide range in time scale providing a good overlap. An excellent superposition of the data is achieved and the resulting reduced curve is shown in Figure A.5. The reference temperature of reduction is $43.7^{\circ}C$.

The measurements on sample II-W were made under atmospheric air, and the sample temperature was not allowed to exceed $65^{\circ}C$. After these measurements,

the sample was removed from the instrument and placed in a vacuum dessicator for about 24 hours. After this initial drying, the sample was reinstalled in the instrument. The instrument chamber was heated to 50°C and the sample was degassed for the next 48 hours infrequently flushing the sample chamber with dry nitrogen. The creep measurements made on this dry sample are shown in Figure A.6. The sample is now identified as II-D (dry). A number of isothermal measurements were made, some of which are not shown in the graph for clarity. Qualitatively, the curves have the same features as that of Figure A.2. For all practical purposes, sample I-D and II-D can be presumed to be the same. Below 70°C the curves are parallel and can be shifted along the time scale to obtain a master curve.

The reduced curve for sample II-D is shown in Figure A.7, the reference temperature of reduction being 43.7°C. In Figure A.8, shift factors used in constructing Figures A.5 and A.7 are plotted against temperature. Open circles represent the wet sample and circles with a vertical line represents the dry sample. In the adjoining graph of Figure A.8, the Arrhenius plot is attempted where the logarithm of shift factors are plotted against reciprocal of absolute temperature. The dry sample has somewhat higher activation energy. Table A.I lists the sift factors used.

In Figure A.9, the reduced curves of samples II-D and II-W are compared; the reference temperature of reduction for both the curve is 43.7°C and not change as to the position on time scale of these curves is made. Several important features of the sample response can be noted from this graph. Clearly the moisture has more effect thatn that of a simple plasticizer. The curve of the dry sample is not only shifted to longer times but has distinctly different shape from its wet counterpart. The transition region of the dry sample is widely dispersed and extends from about 1000 seconds to more than 150 million seconds. For the wet sample, it is much narrower extending only from about 50 seconds

to 100,000 seconds. The apparent equilibrium compliance of the two also differ by a factor of more than 5. It is lower for the dry sample. In its dry state, the sample response is governed by its state of equilibrium crosslinked density. When exposed to moisture the latter is disturbed by the interactions of water molecules with the hydrogen bonding present in the network and possibly lowers its effective crosslink density. Qualitatively, this phenomenon is somewhat similar to those exhibited by early studies (63,64) on crosslinked styrenated polyesters and phenol-formaldehyde resins which showed that the transition region broadens as the crosslink density of the system increases. On the other hand, the mechanical studies (65) of highly crosslinked natural rubber have been found to result in curves which have the same shape, although T_g of the system increased with degree of cross linking. At present, we cannot shed much light on the deformation mechanisms responsible for the relaxation process occurring in the transition region of the two states of the sample studied here.

To quantitatively evaluate the steepness of the transition region Tobolsky (66) and his coworkers have proposed an alternative form of the master curve which can be represented in the form of a Gauss Error Integral equation. This equation in terms of compliance can be written as,

$$\log J(t) = 1/2 \{-\log J_1(t) \cdot J_2(t) + \log \left[J_2(t)/J_1(t) \right] \operatorname{erf} \left[h \log (t'/t) \right] \} \qquad A.3$$

or

$$\log (J_2/J)/\log (J_2/J_1) = 1/2 \{1 + \operatorname{erf} \left[h \log (t'/t) \right] \} \qquad A.4$$

where

$$\operatorname{erf} x = 2\pi^{1/2} \int_0^x e^{-u^2} du \qquad A.5$$

is error integral and h is the parameter of the Gauss error curve and represents the steepness of the compliance-time curve. J_1 and J_2 are the lower and upper asymptotic values of the creep compliance. Here t is the reduced time and t'

is the time where $J=(J_1 \cdot J_2)^{1/2}$.

A plot of left hand side equation A.4 when plotted against log (t'/t) on normal probability paper should yield a straight line. The value of "h" can then be determined from the slope of this line using one of the following relation.

$$h = 1.645/(I_1-I_{50}) = 0.946/(I_{50}-I_{91}) = 0.477/(I_{25}-I_{50}) \qquad A.6$$

where Iy is the intercept on the abscissa at y% ordinate etc. Figure A.10 shows such a plot for the wet and dry state of the sample. Within experimental error for each state the data in the intermediate region of the transition can be represented by a straight line. The value of h for the wet sample is large being equal to 0.70 than the dry sample which has h value of 0.5; this indicates that the wet sample has much steeper dispersion curve (see also Figure A.9). Theocaris (63) and Kwei (64) in their study of crosslinked epoxy resins found that their mechanical data when plotted according to equation A.4 results in two straight lines with different slopes for each sample. The data below and above transition were described in terms of two sets of parameters h_g (glassy) and h_r (rubbery). Strictly speaking, however, as Tobolsky pointed out, the equations A.3 and A.4 are applicable only in the transition region.

Finally, Figure A.11 depicts the retardation spectra for the wet and dry sample at 43.7°C. The function (L) was calculated using a computer program (65) based on Schwarzl and Staverman's (66) second order approximation. The shape of the curve presented in the graph is such that when it is used to back calculate the reduced creep compliance function J(t), it gives data which are within experimental error. Examination of the two curves show that the distribution of the retardation times of two samples is drastically different from each other. The dispersion region for the dry sample is much broader than the wet sample as noticed earlier in Figure A.9. The continued slow rise of the compliance curve for sample II-D of Figure A.9 shows up in its retardation function as a broad peak.

Its position on the time scale is around 10 million seconds. The wet sample has a clear sharp peak at about 100,000 seconds.

A.4 Conclusions

It is demonstrated that in nylon-epoxy adhesives at moderately low temperatures, the presence of moisture has significant effect on the creep rate and creep compliance. Hence, the retention of the cohesive properties of the system are severely hampered. The problem of predicting the physical state of the bulk adhesive at higher temperatures is found to be complicated by the presence of moderate amount of crystallinity due to the nylon component. The anomalous behavior at higher temperatures would be consistent with the "melting" of these microcrystallites although no conclusive evidence of this has yet been found.

Table A.1

Temperature Dependences - Shift Factors for Samples I-D, II-D and II-W

Temperature °C	log a_T		
	Sample I-D	Sample II-D	Sample II-W
30.4	+2.27	—	—
35.9	—	—	+2.20
38.3	+1.40	—	—
43.7	—	0.00	0.00
44.1	0.00	—	—
47.7	-1.85	—	—
51.2	—	-2.20	-1.90
52.9	-2.32	—	—
59.7	—	-3.40	-4.10
63.7	-4.60	—	—
69.9	—	-6.20	—
72.8	-6.20	—	—
Apparent equilibrium Compliance log $J_{e,a}$ (cm^2/dyne)		-8.30	-7.60

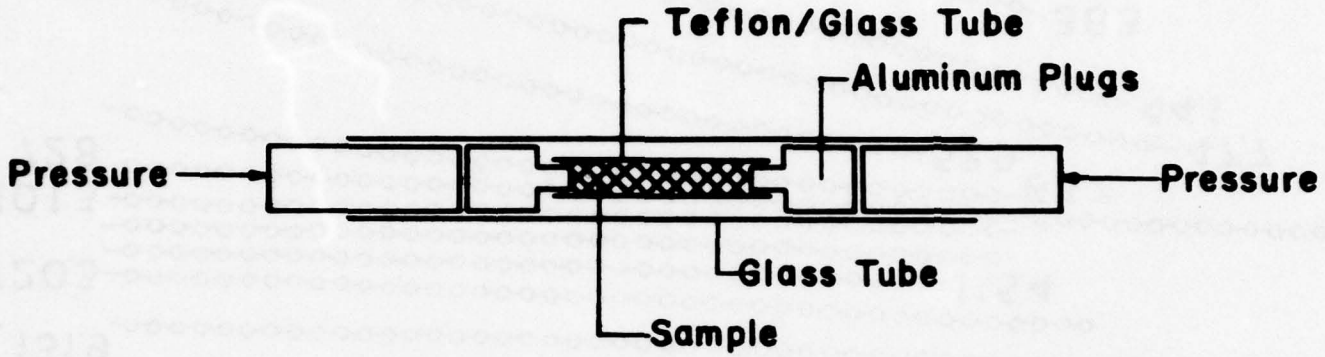

Figure A.1 Setup for the Sample Molding

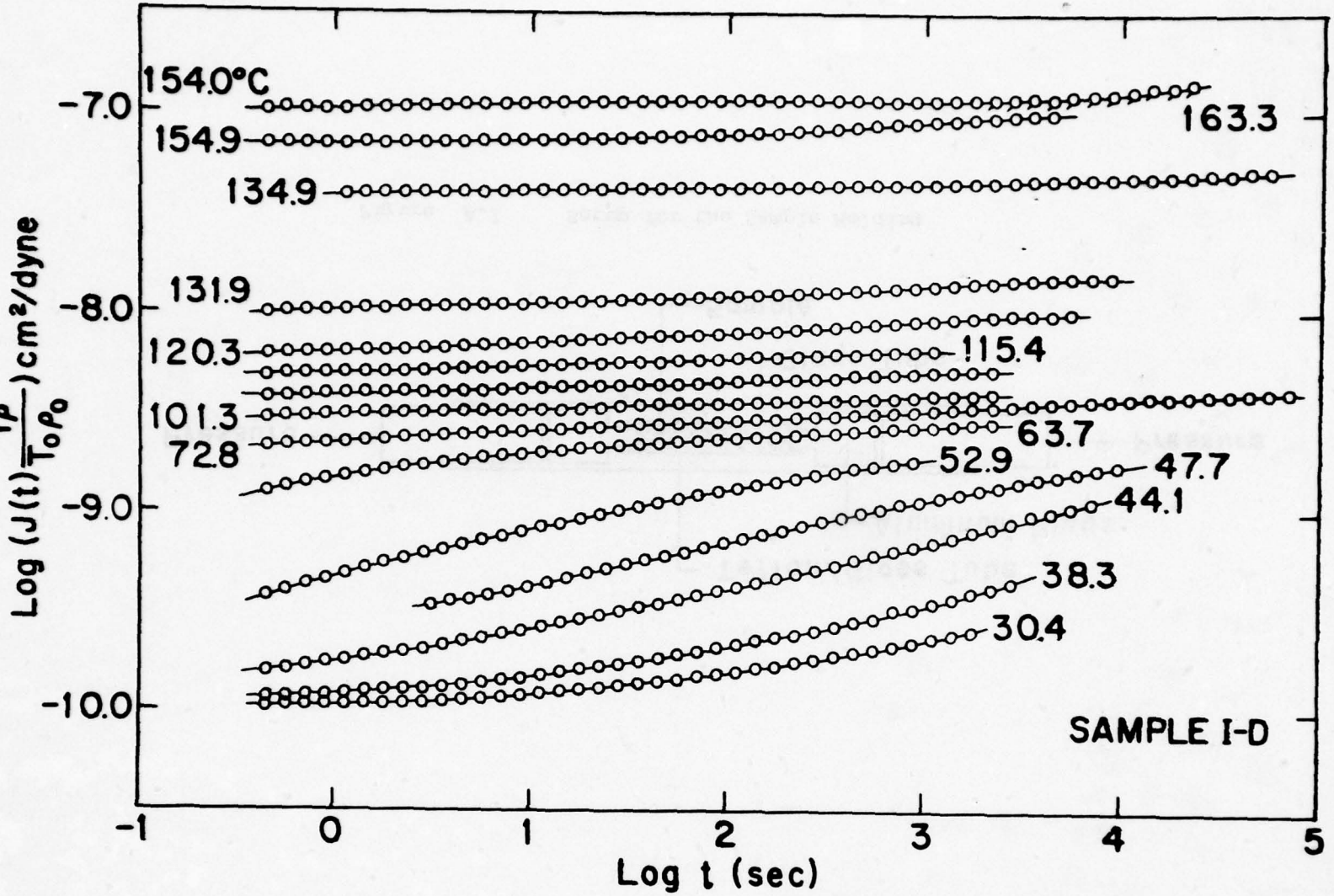

Figure A.2 Logarithmic Plot of the Measured Compliance $(J(t)\ \frac{T\cdot\rho}{T_o\rho_o})\ cm^2/dyne$ versus Time, t, sec, for Sample I-D at the Indicated Temperatures.

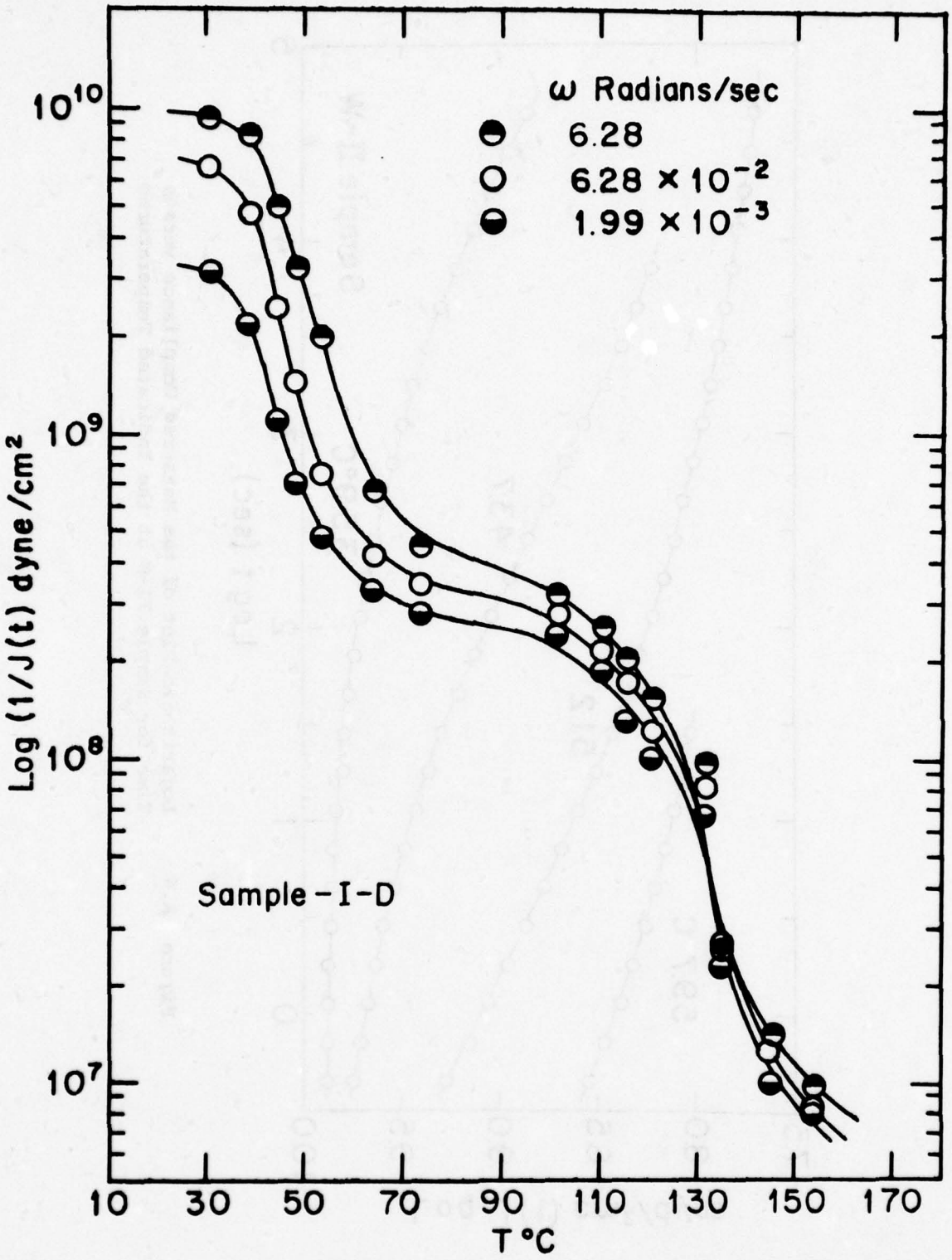

Figure A.3 Semilogarithmic Plot of the Inverse Compliance versus Temperature °C at Three Frequencies viz, 6.28, 6.28×10^{-2}, 1.99×10^{-3} radians/sec.

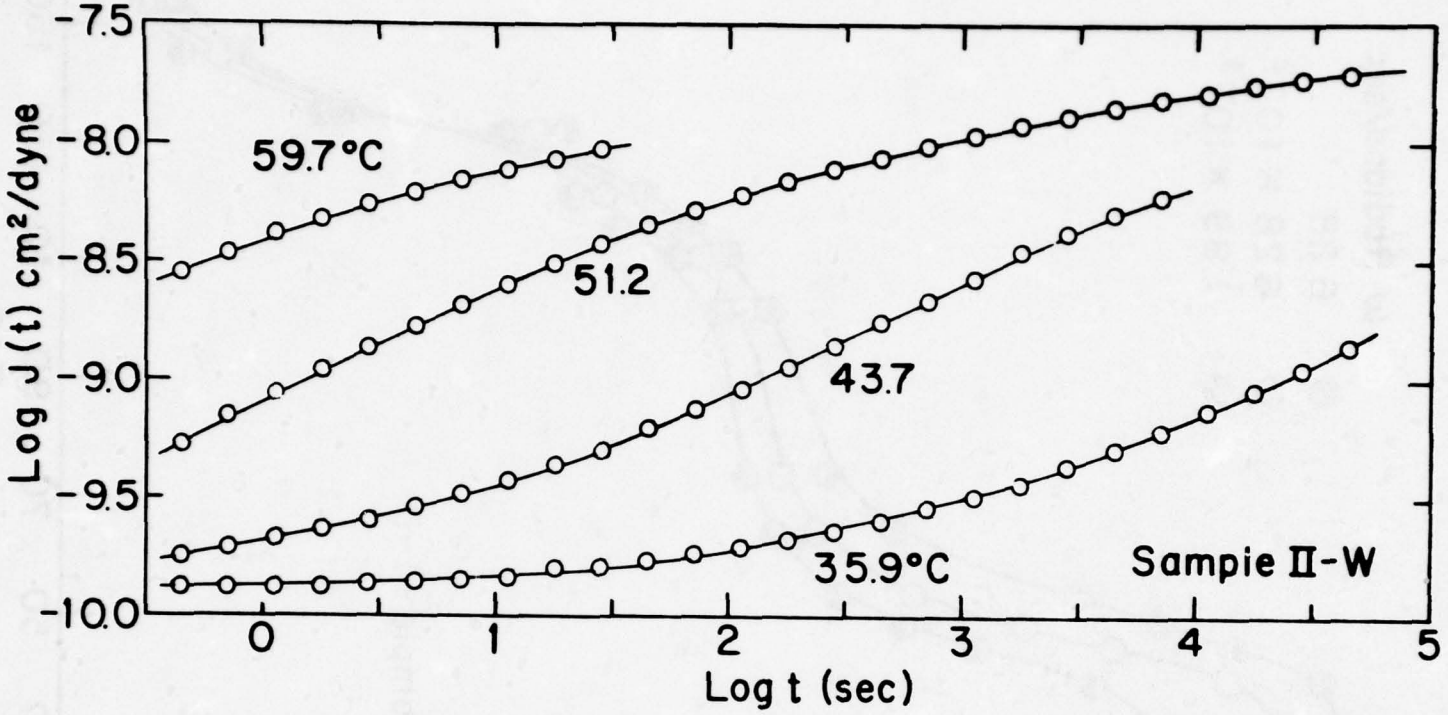

Figure A.4 Logarithmic Plot of the Measured Compliance versus Time for Sample II-W at the Indicated Temperatures

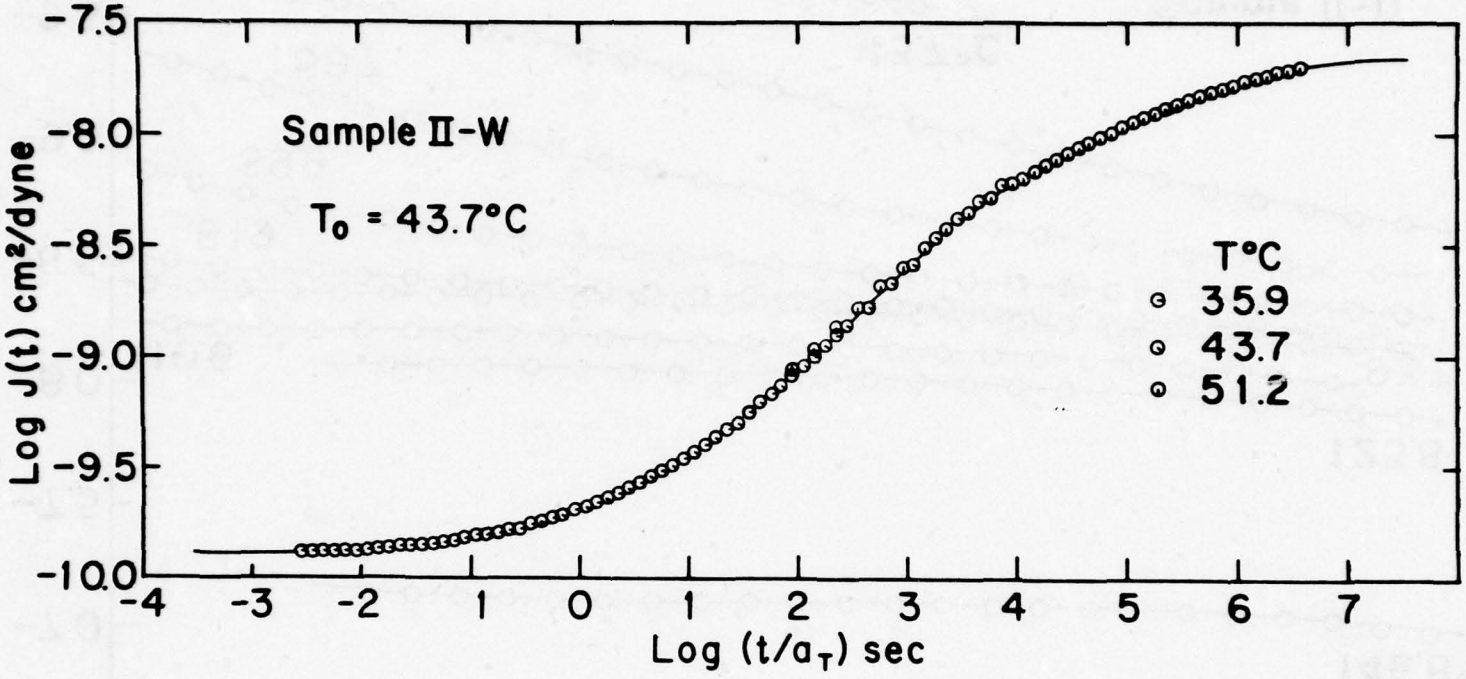

Figure A.5 Logarithmic Reduced Creep Curve for the Sample II-W, a_T is the Shift Factor for the Creep Compliance. Reference Temperature T_o = 43.7°C

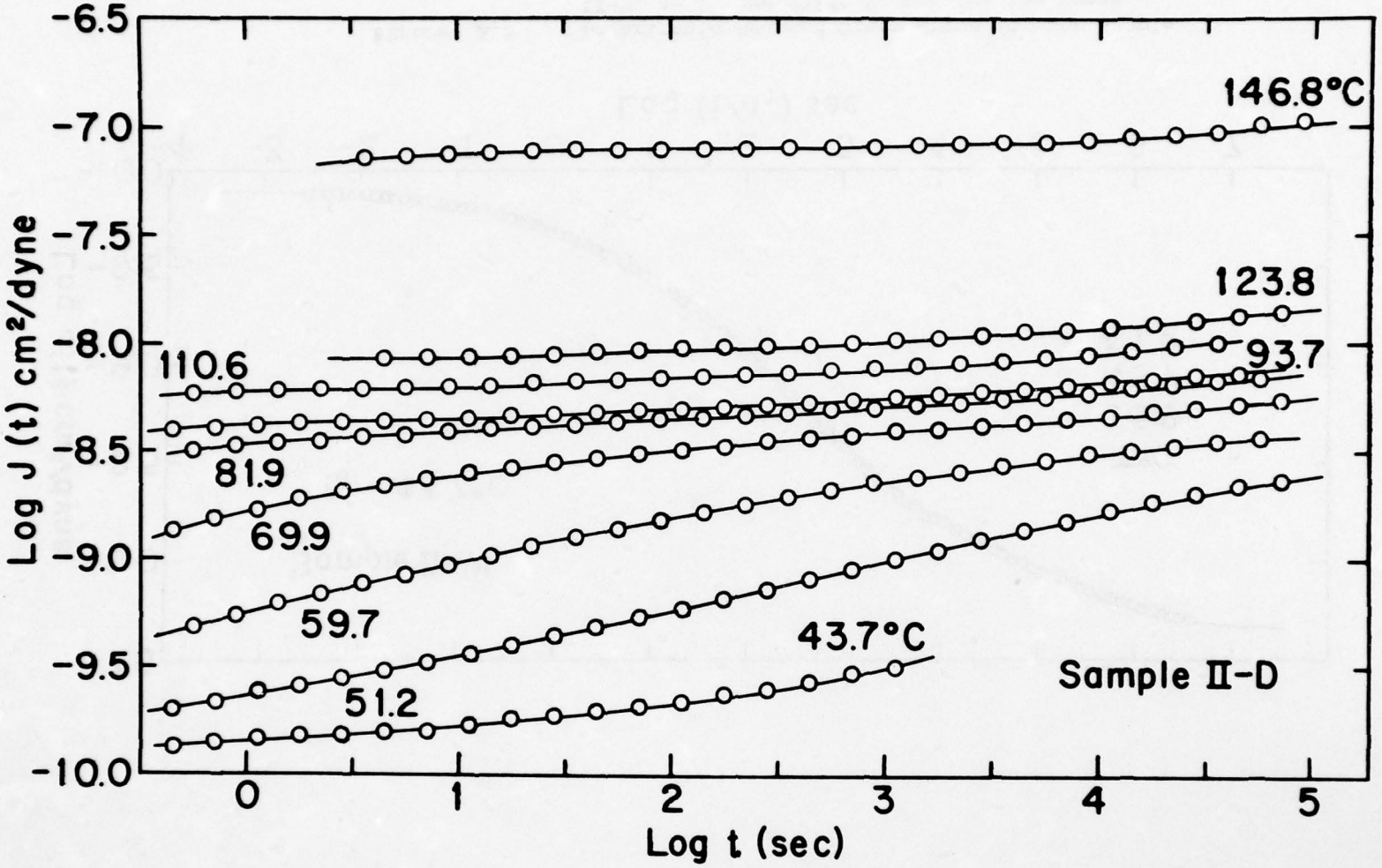

Figure A.6 Logarithmic Plot of the Measured Compliance versus Time for Sample II-D at the Indicated Temperatures

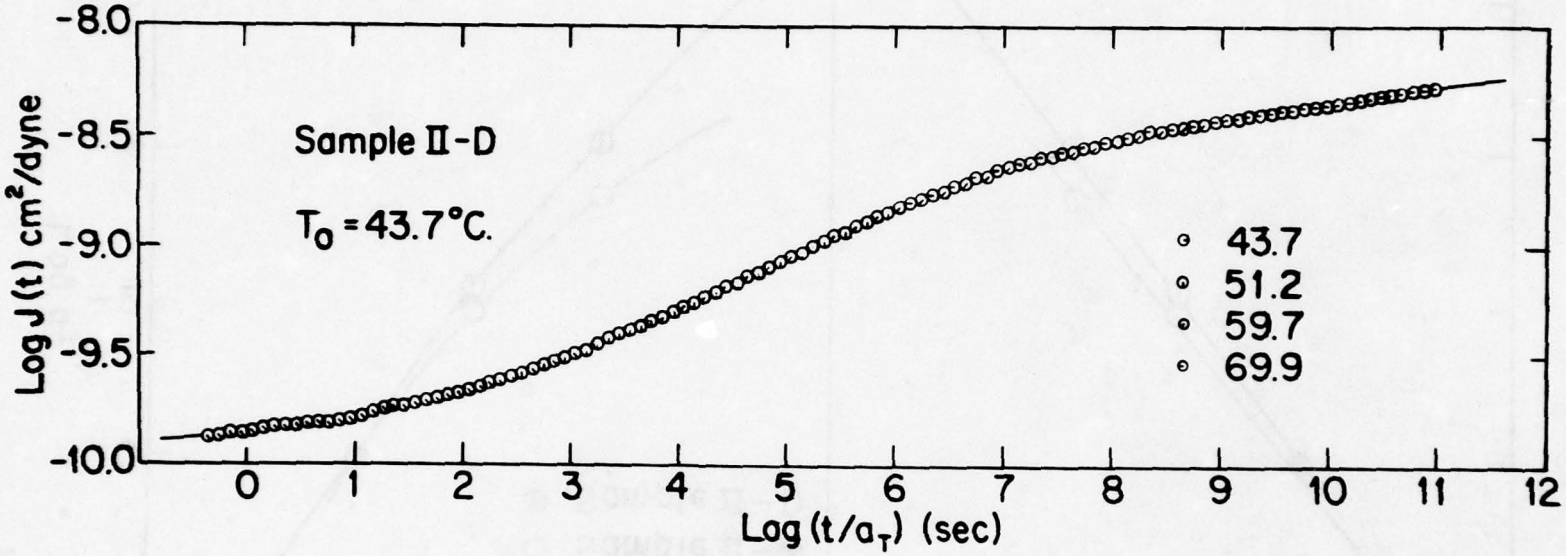

Figure A.7 Logarithmic Reduced Creep Curve for the Sample II-D, a_T is the Shift Factor for the Creep Compliance. Reference Temperature T_o = 43.7°C

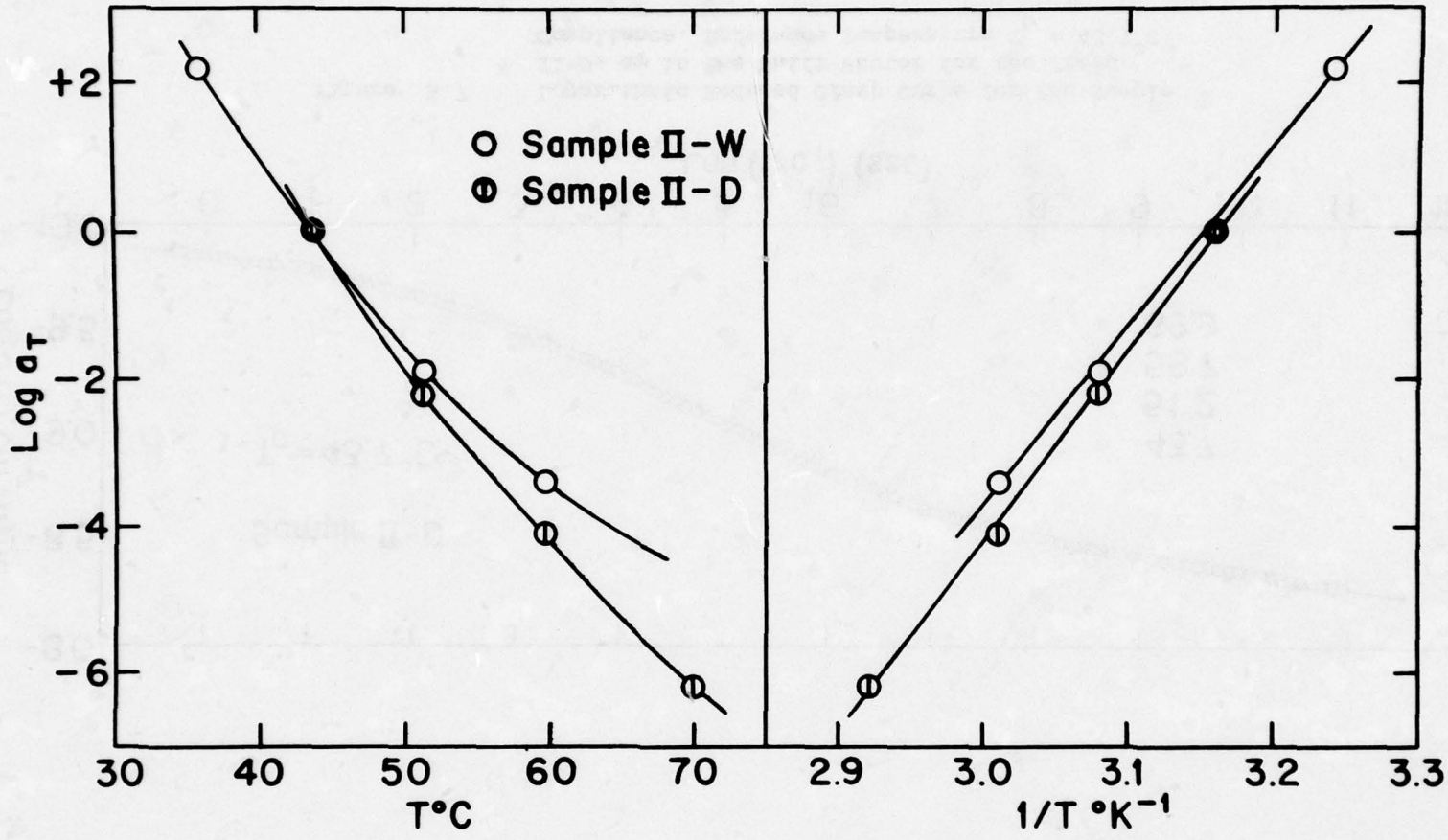

Figure A.8 Semilogarithmic Plot of Shift Factors versus Temperature ^{o}C and versus Inverse of Absolute Temperature $^{o}K^{-1}$

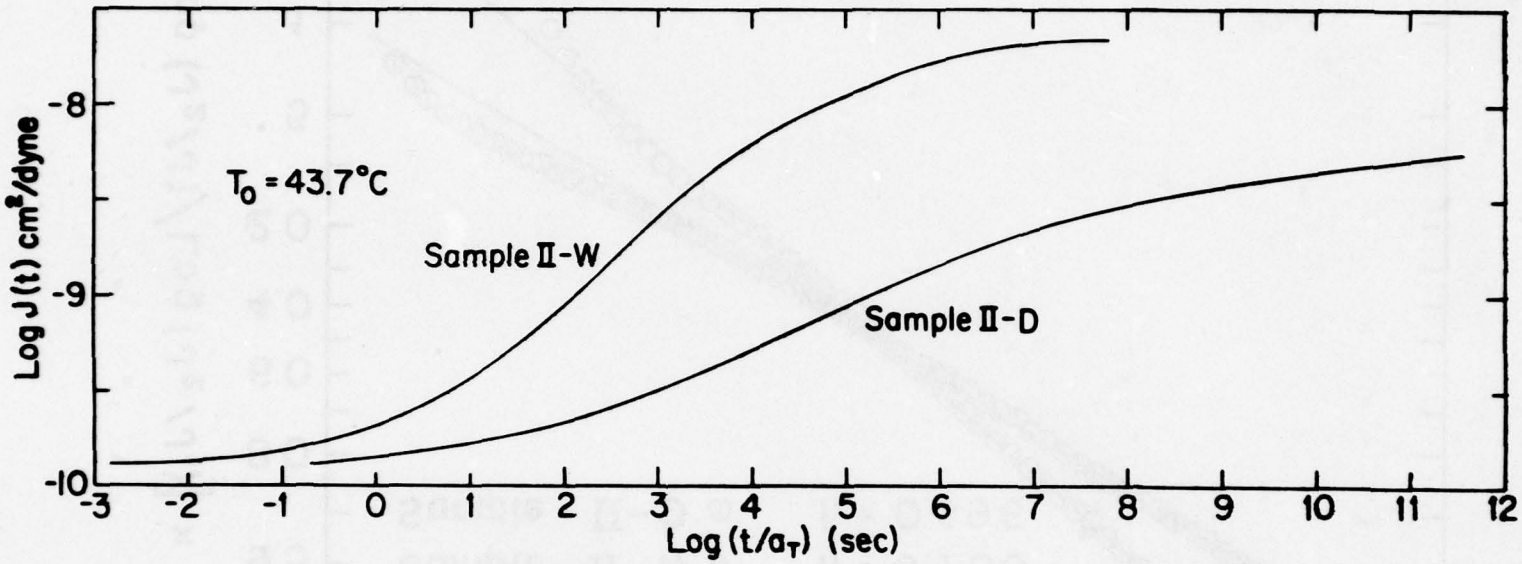

Figure A.9 Logarithmic Plot of the Reduced Curves of Samples II-W and II-D. Reference Temperature T_o = 43.7°C.

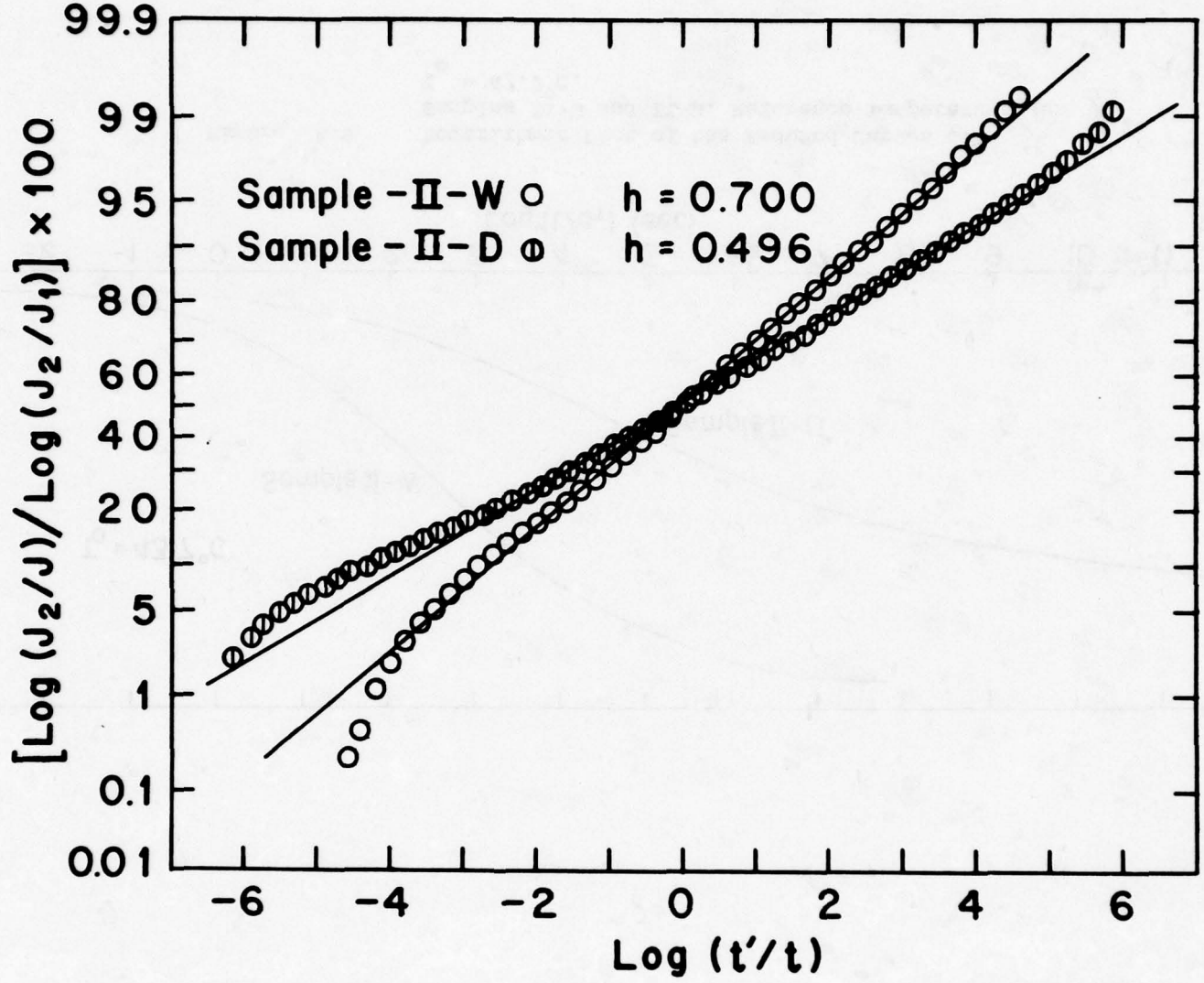

Figure A.10 Plot of Creep Compliance versus Time According to Equation A.4 on a Normal Probability Graph Paper.

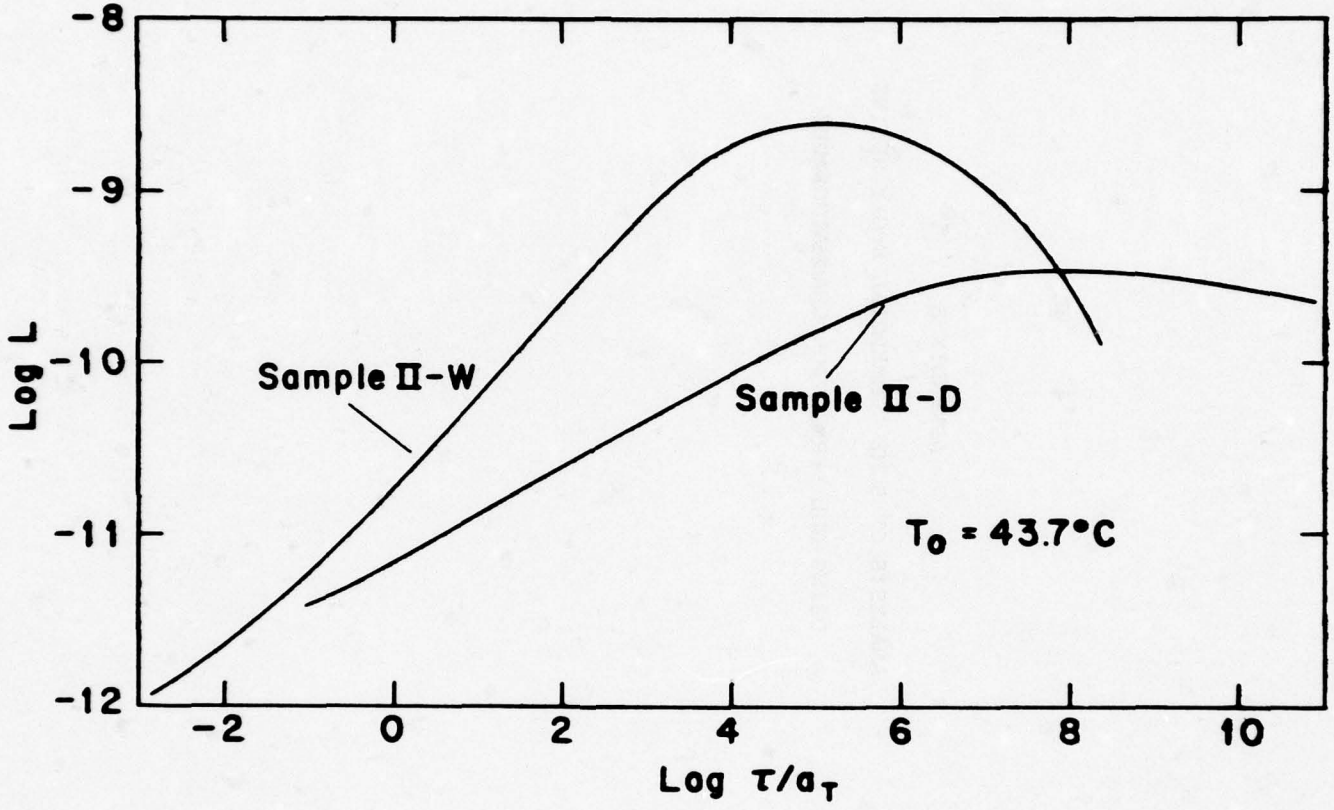

Figure A.11 Logarithmic Plot of the Retardation Function, L, versus Retardation Time, t, for Samples II-W and II-D. Reference Temperature $T_o = 43.7^{\circ}C$.

APPENDIX B

ANALYSIS OF SOME COMMERCIAL EPOXY RESINS

USING GEL PERMEATION CHROMATOGRAPHY

In the course of the investigation several other commercial epoxy resins were examined and their infra-red spectra and gel permeation chromatograms are shown in the Figures B.1-7 following this appendix. In analyzing our GPC results and comparing them with previously published analyses it was found useful to correlate the peak elution counts with the effective chain length (ECL) as a suitable molecular size parameter. From studies (71) on the GPC behaviour of model compounds it has been found that various chemical groups could be assigned values of the ECL such that the elution count of a complex molecule could be predicted by the ECL summation of its component groups. The method seems to work well for relatively low molecular weight materials and has been found useful in this work in assigning the various GPC peaks to particular oligomers and for recognizing impurities. The values of the ECL found by Hendrickson and Moore and used here for the analysis of DGEBA epoxy resins are given in Table B.1. The predicted ECL for the various DGEBA oligomers are tabulated in Table B.2; the second column contains the molecular size parameter calculated where the eluting compound hydrogen bonds to the solvent. Such is the case for epoxy molecules containing hydroxyl groups with THF as the solvent; the correction is 2.5 units per hydroxyl group.

Using the above method the GPC results of Batzer and Zahir (42) are shown in Figure B.8. The impurities have been identified by these authors as having molecular structures which are intermediates, shown schematically in Figure B.9, in the chemical reactions leading to formation of the diepoxide. In the final product these residual impurities appear as characteristic satellite peaks on the chromatogram. The elution count versus ECL plot is shown in Figure B.10.

Biesenberger, et al. (39) have analysed four commercial epoxy resins of similar epoxy equivalent weight; their chromatograms, reproduced in Fibure B.11, clearly show that the Shell Epon 1004 was manufactured by the "taffy" process whereas the others, in which the n=1 and n=3 oligomers are virtually absent, must have been made by the advancement process. Their data are plotted in Figure B.12.

The data of Larsen (3), reproduced in Figure 16 and 17 in the preceding report, for Epon 836 and Epon 1001 have been analysed as shown in Figure B.13 and B.14. It would appear that both resins were made by the "taffy" process. Our analysis of these same two resins shows, however, that our sample of Epon 836 was made by the "advancement" process. The ECL analysis of the RE-A chromatogram (as in Figure 18) is shown in Figure B.15; the minor peak at elution count 32.0 would correspond to the ECL of bisphenol A, the presence of which would be expected in a resin made by the advancement process. The curing agent has a calculated ECL (in toluene solvent) of 13.0 and would be predicted to elute at about count 31. No shoulder on the main peak at count 30.3 can be seen and it is presumed that the concentration is small enough and the refractive index (unknown) may not differ much from that of the solvent so that a curing agent peak is not detected.

Table B.1

Atomic group	Effective Chain Length
C	1.0
O e.g. ether**	0.67
e.g. carbonyl	0.8
N	0.91
phenyl, C_6H_5	2.85
phenylene, C_6H_4	2.4

*From J. G. Hendrickson and J. C. Moore, J. Poly. Sci., A-1, 4, 167, (1966).

**It has been observed that in small ring cyclic ethers, e.g. epoxides epoxides the oxygen has a very small effect on the ECL, e.g. propylene oxide ECL=3.0.

Table B.2

Effective chain lengths of DGEBA oligomers

Oligomer	E.C.L.	
		H bonding solvent
n=0	15.1	15.1
n=1	27.9	29.5
n=2	40.7	43.9
n=3	53.5	58.3
n=4	66.3	72.7

Table B.3

Specifications of carboxy terminated butadiene-acrylonitrile elastomers (B.F. Goodrich Data Sheets)

	2000x162 CTB	1300x15 CTBN	1300x8 CTBN	1300x13 CTBN	1300x9 CTBNX	1300x18 CTBNX[2]
Viscosity, Brookfield, cP at 27°C (81°F)	40,000	50,000	125,000	550,000	155,000	350,000
Percent carboxyl	1.9	2.47	2.37	2.40	2.93	3.0
Molecular weight	4,800	3,500	3,500	3,500	3,500	3,500
Functionality	2.01	1.9	1.85	1.85	2.3	2.3
Acrylonitrile content, %	0	10	18	27	18	21
Solubility parameter	8.04	8.45	8.77	9.14	---	---
Specific gravity at 25°C(77°F) 25%	0.907	0.924	0.948	0.960	0.955	0.958

Calculations based on molar attraction constants

Table B.4

Specifications of some commercial DGEBA epoxy resins

	Epoxy equiv. wt.	Viscosity
DOW DER 332	172-176	4,000-5,500
331	186-192	11,000-14,000
337	230-250	"semisolid"
661	475-575	low melting solid
667	1600-2000	solid
669	3500-5500	
Shell Epon 828	185-192	10,000-16,000
834	230-280	
836	290-335	
1001	450-550	solid
1004	875-1025	
1010	4000-6000	
CIBA 6004	185	5,000-6,000
6040	233-278	
6060	385-500	solid

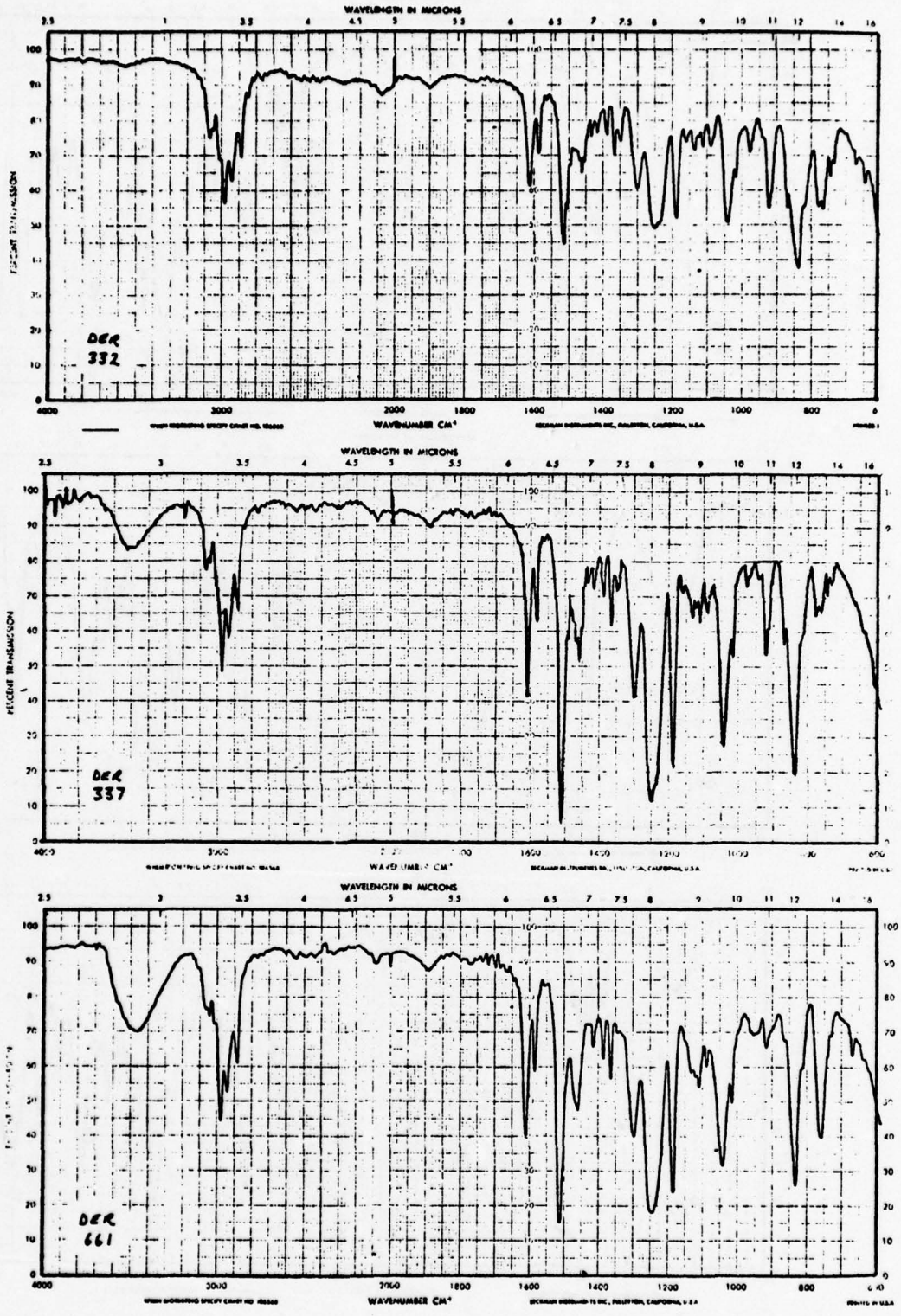

Figure B.1 **Infra-red Spectra of DGEBA Epoxy Resins; Dow Chem: DER 332,337,661**

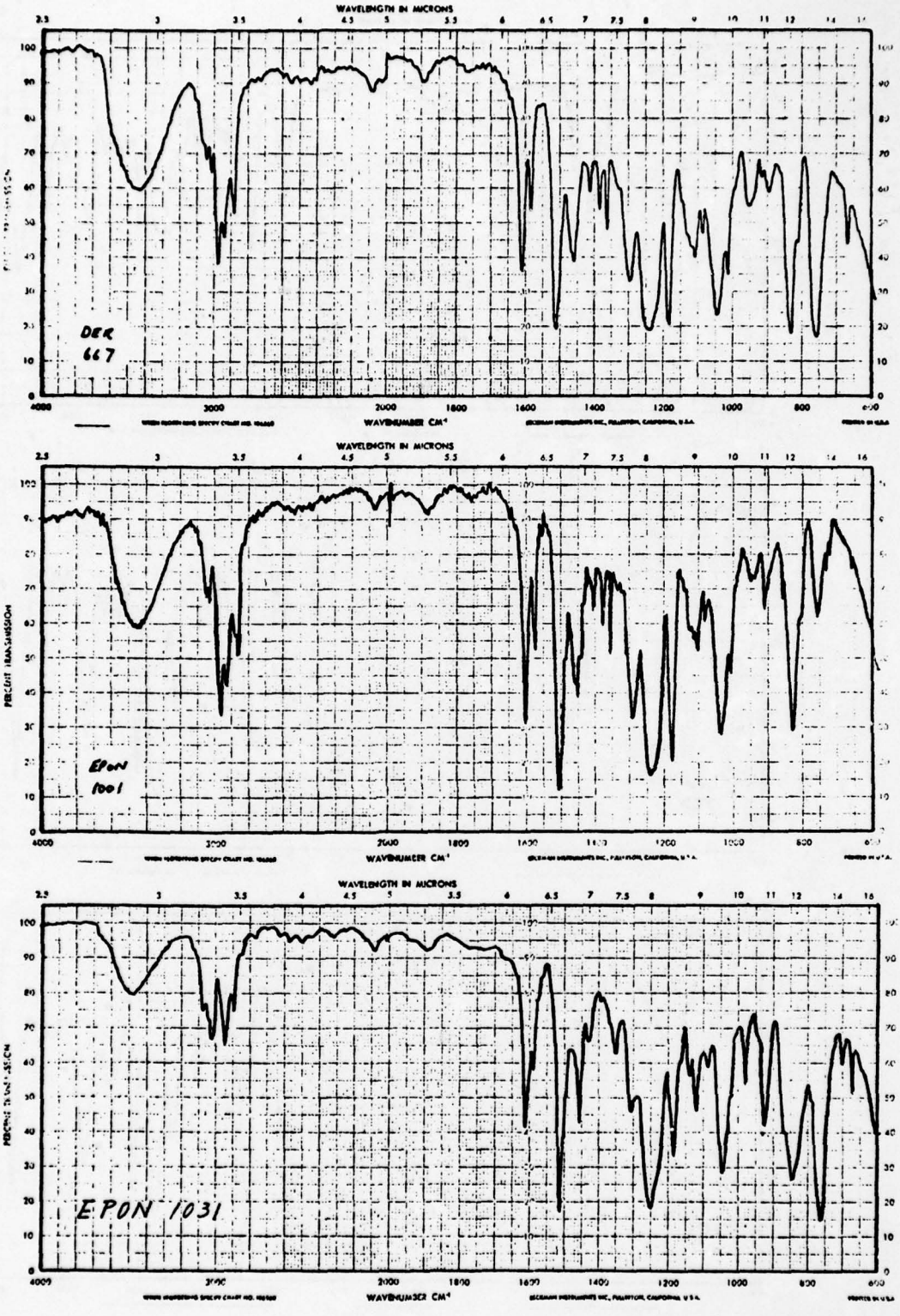

Figure B.2 **IR Spectra of DGEBA Epoxy Resins; Dow Chem. DER 667, Shell Chem. Epon 1001, Shell Chem. Epon 1031, tetra glycidyl ether of 1,1',2,2' tetrakis p-hydryxy phenyl ethane**

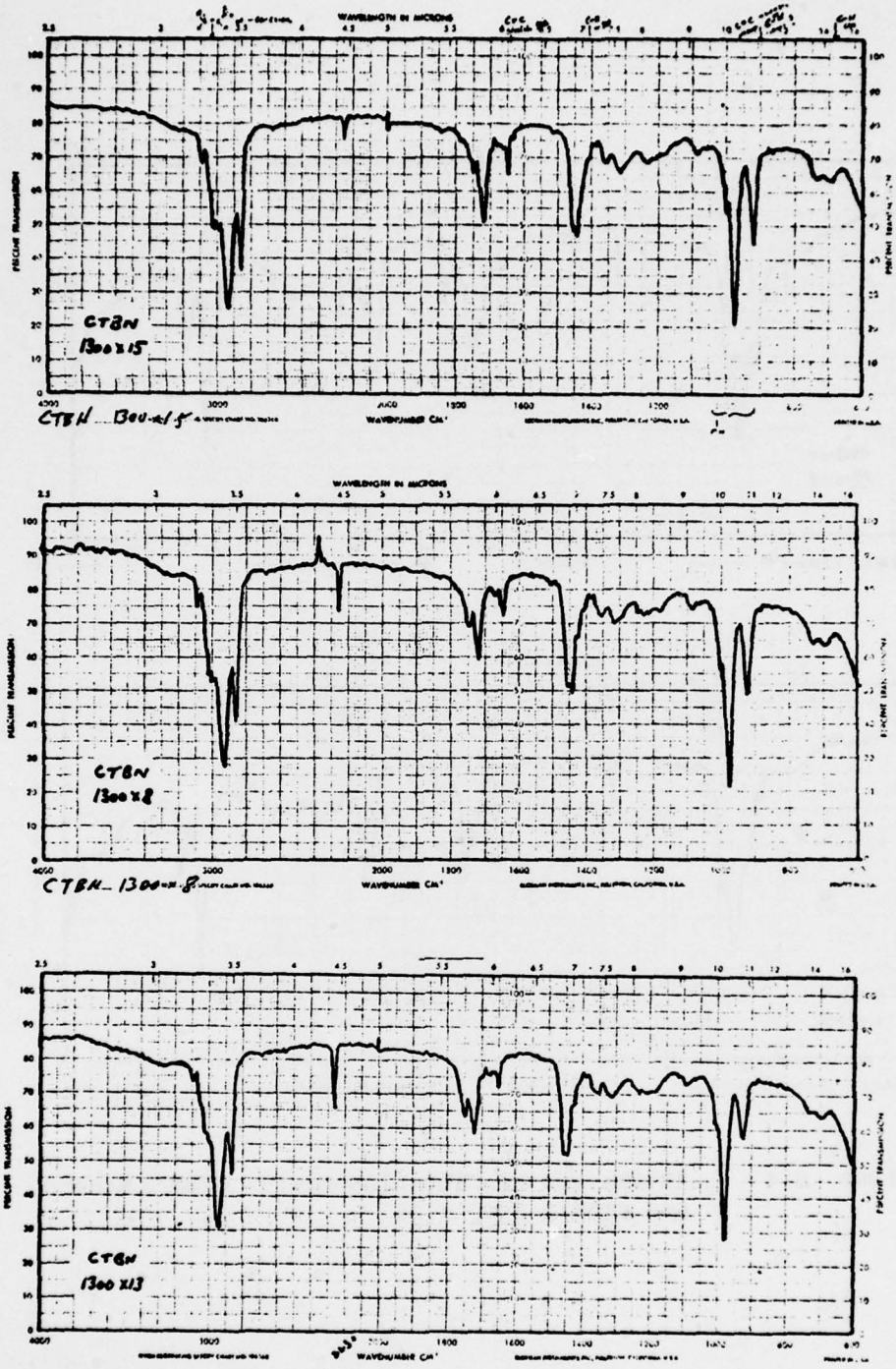

Figure B.3 **IR Spectra of Carboxy Terminated Butadiene-Acrylonitrile Elastomers: CTBN 1300 x 15, CTBN 1300 x 8, CTBN 1300 x 13 (B.F. Goodrich Co.)**

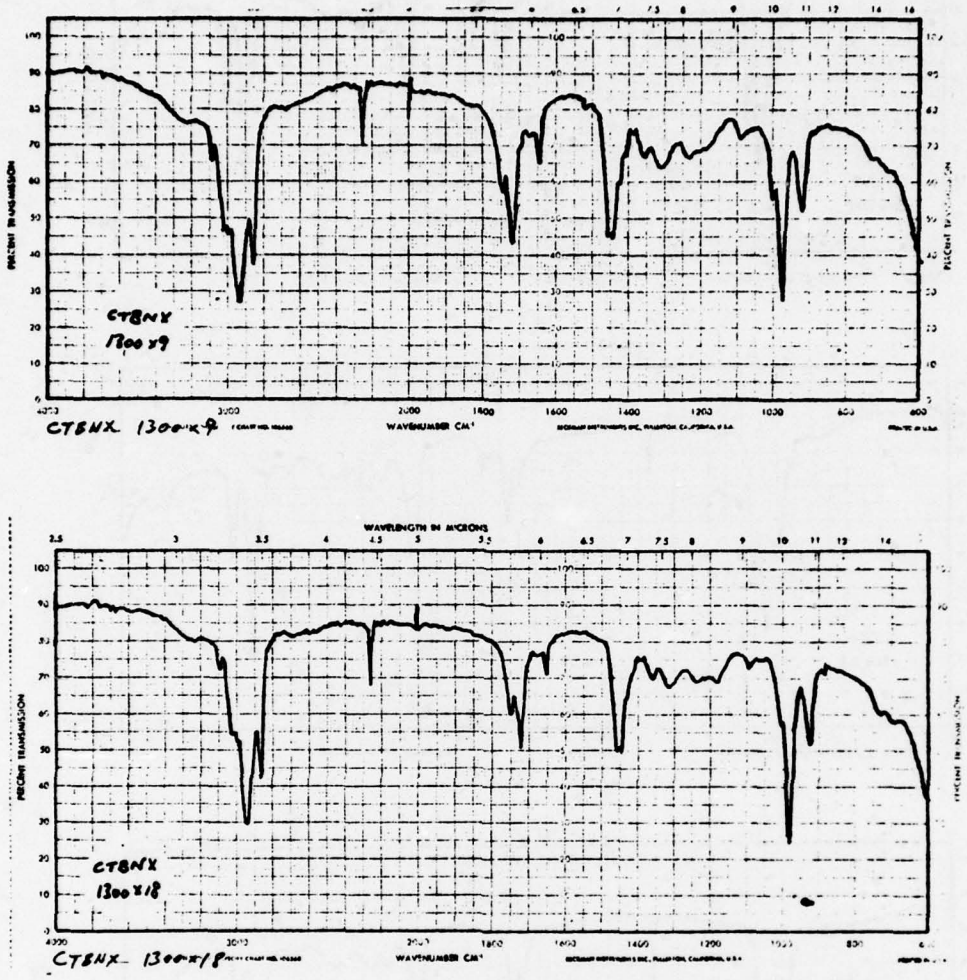

Figure B.4 IR Spectra of CTBN Elastomers: CTBN 1300 x 9 and CTBN x 1300 x 18

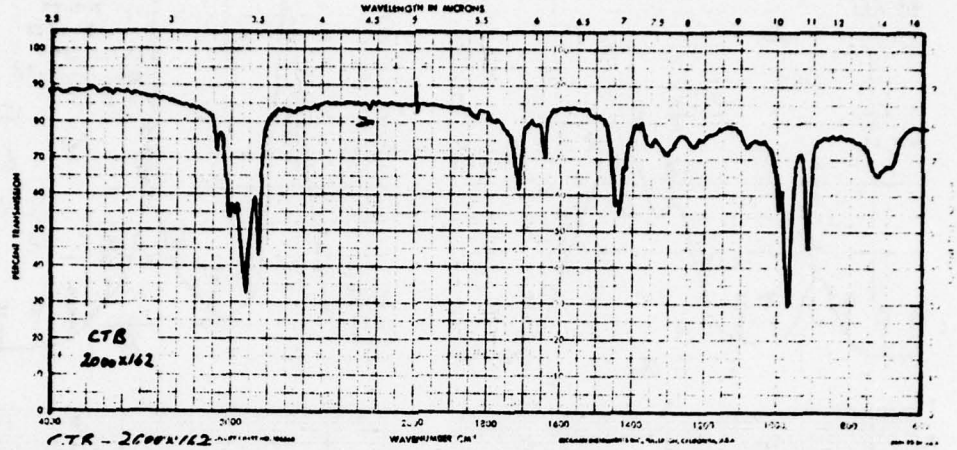

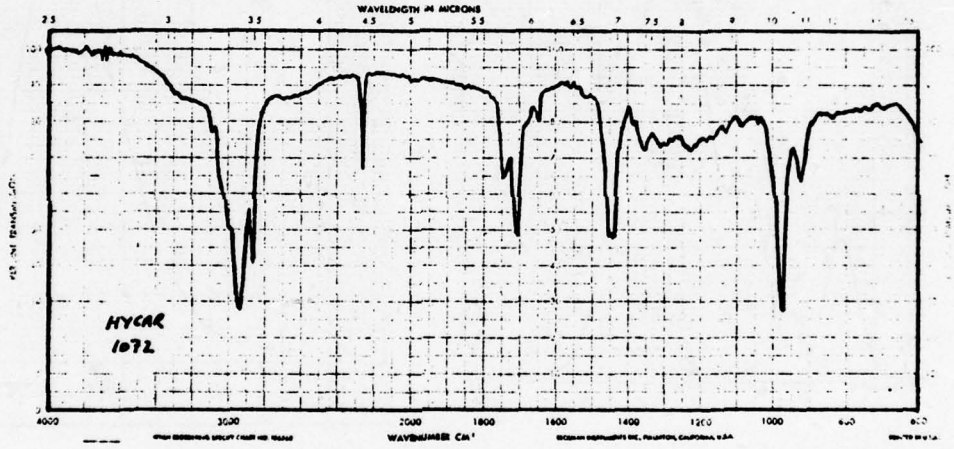

Figure B.5 **IR Spectra of Carboxy Terminated Butadiene Elastomer CTB 1200 x 162, and Butadiene-Acrylonitrile Elastomer Hycar 1072**

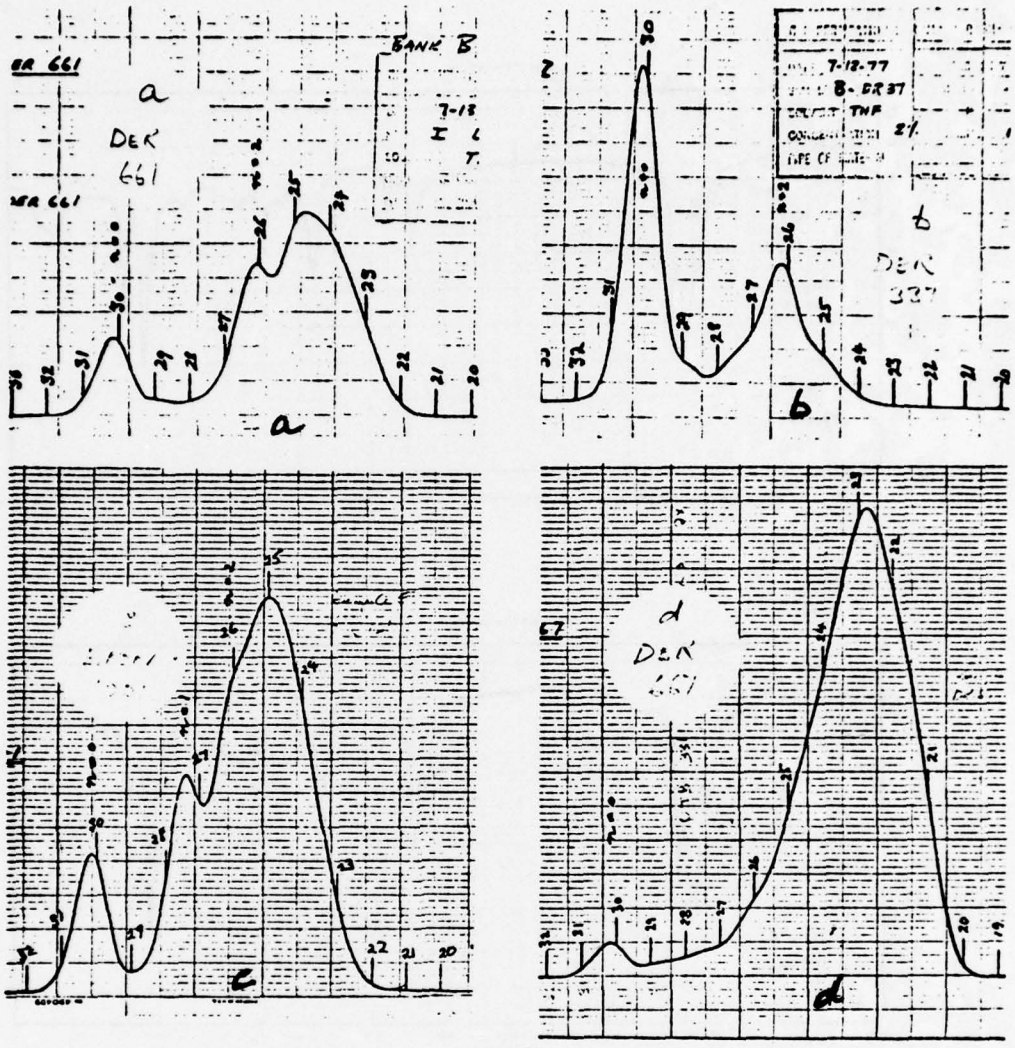

Figure B.6 **Gel Permeation Chromatograms (GPC); THF Solvent, Instrument B:**
(a) DER 661, (b) DER 337, (c) Epon 1001,
(d) DER 667

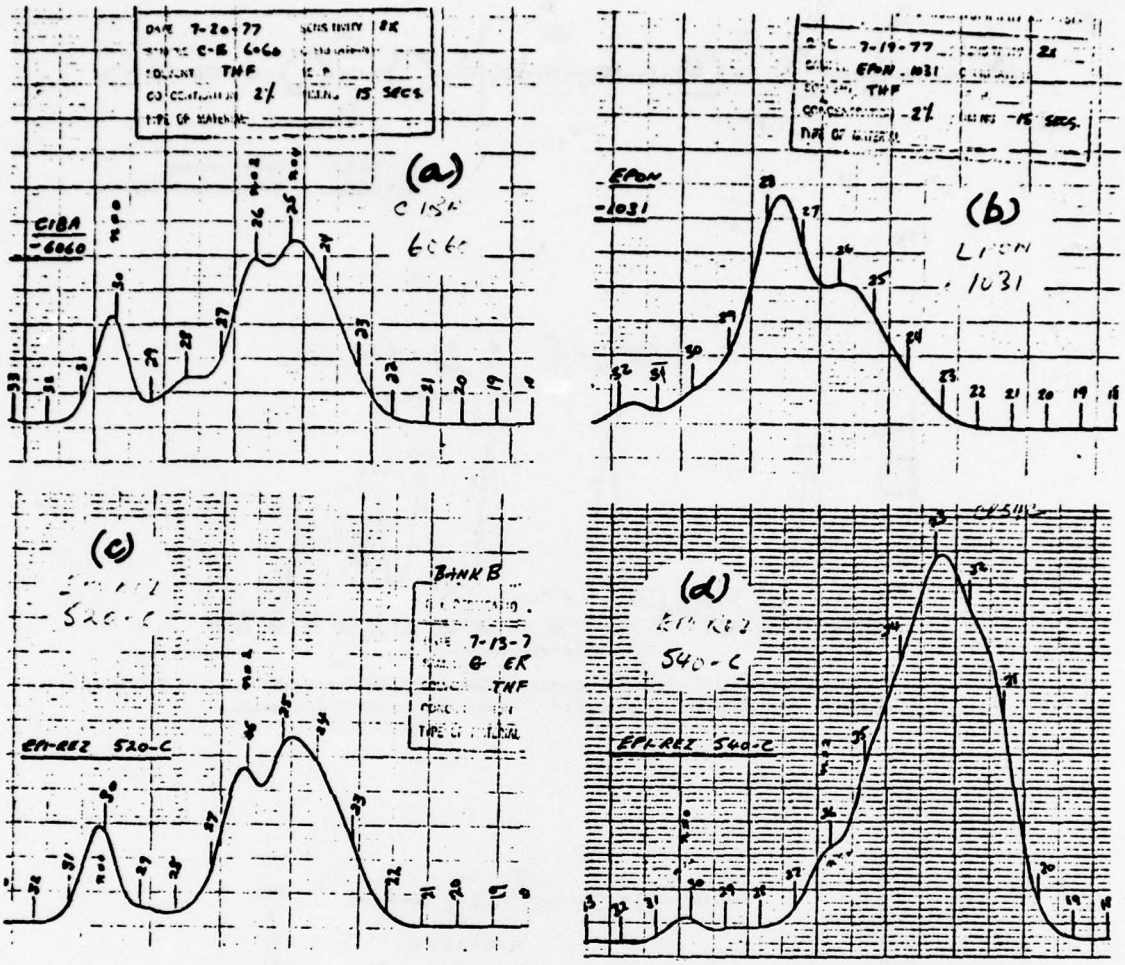

Figure B.7 GPC Chromatograms; THF Solvent, Instrument B: (a) CIBA 6060, (b) Epon 1031, (c) Epi-Rez 520-C, (d) Epi-Rez 540-C

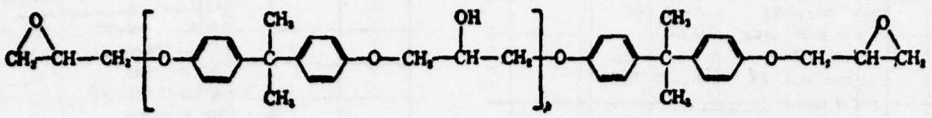

I

k = 0,1,2,3, . . . "taffy" process
k = 0,2,4,6, . . . "advancement" process

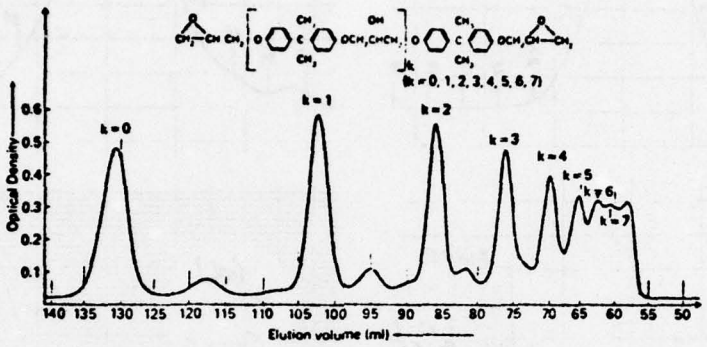

High-resolution GPC curve (polystyrene gel Biorad SX2, with tetrahydrofuran as solvent) of a low molecular weight solid epoxide resin made by the "taffy" process.

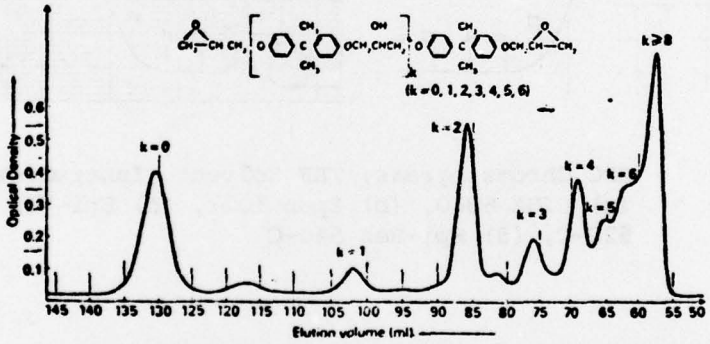

High-resolution GPC curve (polystyrene gel Biorad SX2, with tetrahydrofuran as solvent) of a low molecular weight solid epoxide resin made by the "advancement" process.

Figure B.8 **GPC Chromatograms of Epoxy Resins Prepared by the "Taffy" Process and by the "Advancement" Process. (Reproduced from Batzer and Zahir, Ref. 37, Figures 4 and 5)**

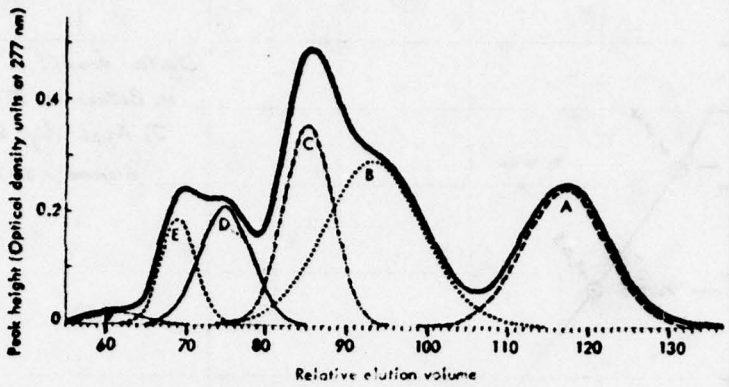

Fig. 4. Typical chromatographic curve of a sample taken from a kinetic run of the reaction of bisphenol A (0.2 m/l.) with epichlorohydrin (1.28 m/l.) and NaOH (0.4 m/l.) in methanol at 25°C. Gel = Sephadex LH 20; solvent = $CHCl_3/C_2H_5OH$, 2:1 (v/v). The various peaks shown in the curve are of reaction products having the general structural formula

$$R_1\text{—}\{\text{O—AR—O—CH}_2\text{—CHOHCH}_2\}_n\text{O—AR—O—}R_2$$

where

AR = 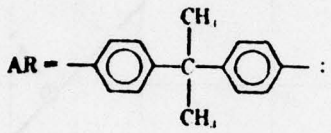 :

(A) $R_1 = R_2 = H$, $n = 0$

(B) $R_1 = H$, $R_2 = \text{—CH}_2\text{—CHOHCH}_2\text{Cl}$ or $\text{CH}_2\text{—CH(O)—CH}_2$, $n = 0$

(C) $R_1 = R_2 = \text{—CH}_2\text{—CHOHCH}_2\text{Cl}$, $n = 0$

(D) $R_1 = \text{—CH}_2\text{CHOHCH}_2\text{Cl}$, $R_2 = \text{CH}_2\text{—CH(O)—CH}_2$, $n = 0$

(E) $R_1 = R_2 = \text{—CH}_2\text{—CH(O)—CH}_2$, $n = 0$

(F) $R_1 = R_2 = \text{—CH}_2\text{CH(O)—CH}_2$, $n = 1$

The full-line curve is the actual GPC profile. The dotted and dashed line curves are the corrected computer-separated individual peaks.

Figure B.9 **GPC Chromatograms of Intermediates in Epoxy Resin Syntehsis. (Reproduced from Batzer and Zahir, Ref. 42, Figure 4)**

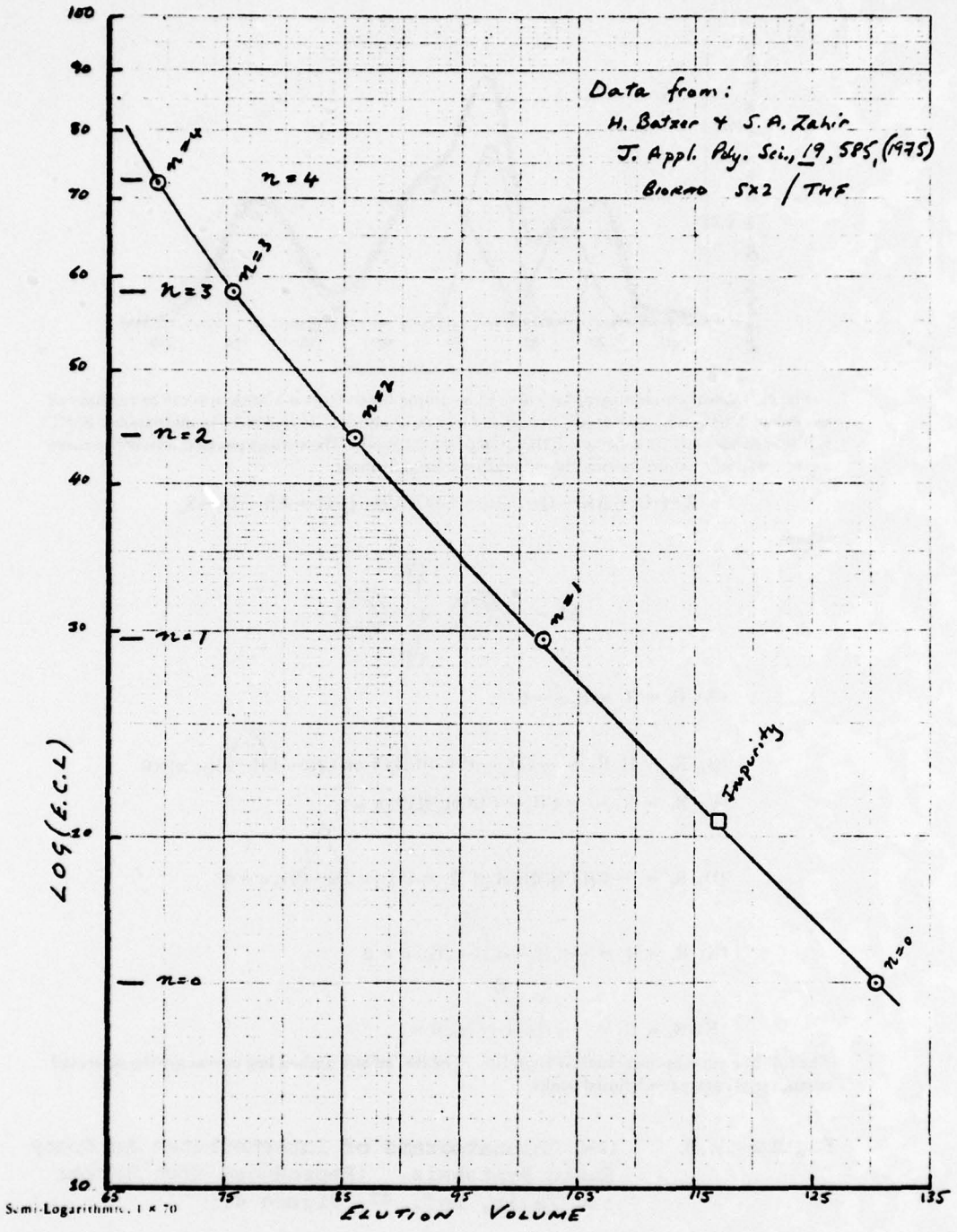

Figure B.10 Elution Volume versus Effective Chain Length (Data from Figure B.8)

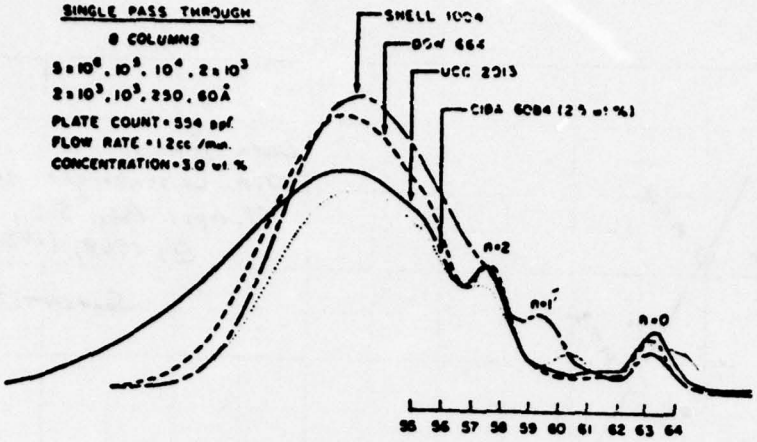

Epoxy resin GPC spectra resulting from one pass through eight columns.

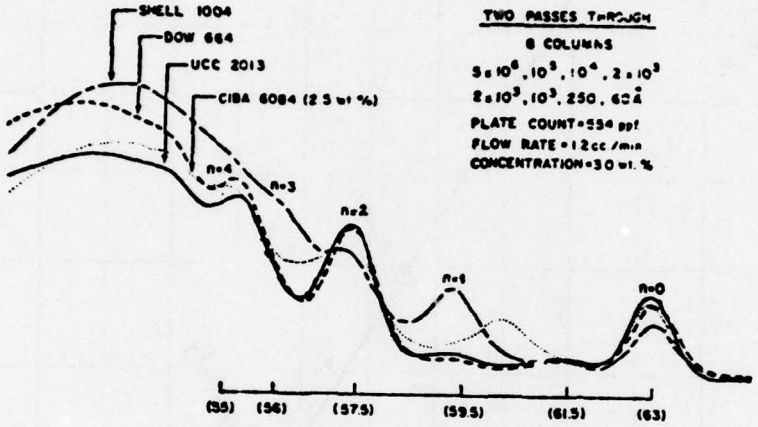

Epoxy resin GPC spectra resulting from two passes through eight columns.

Figure B.11 GPC Chromatograms of Commercial DGEBA Epoxy Resins: Epon 1004, DER 664, UCC 2013 (Union Carbide), CIBA 6084, (Reproduced from Beisenberger, et al., Ref. 139)

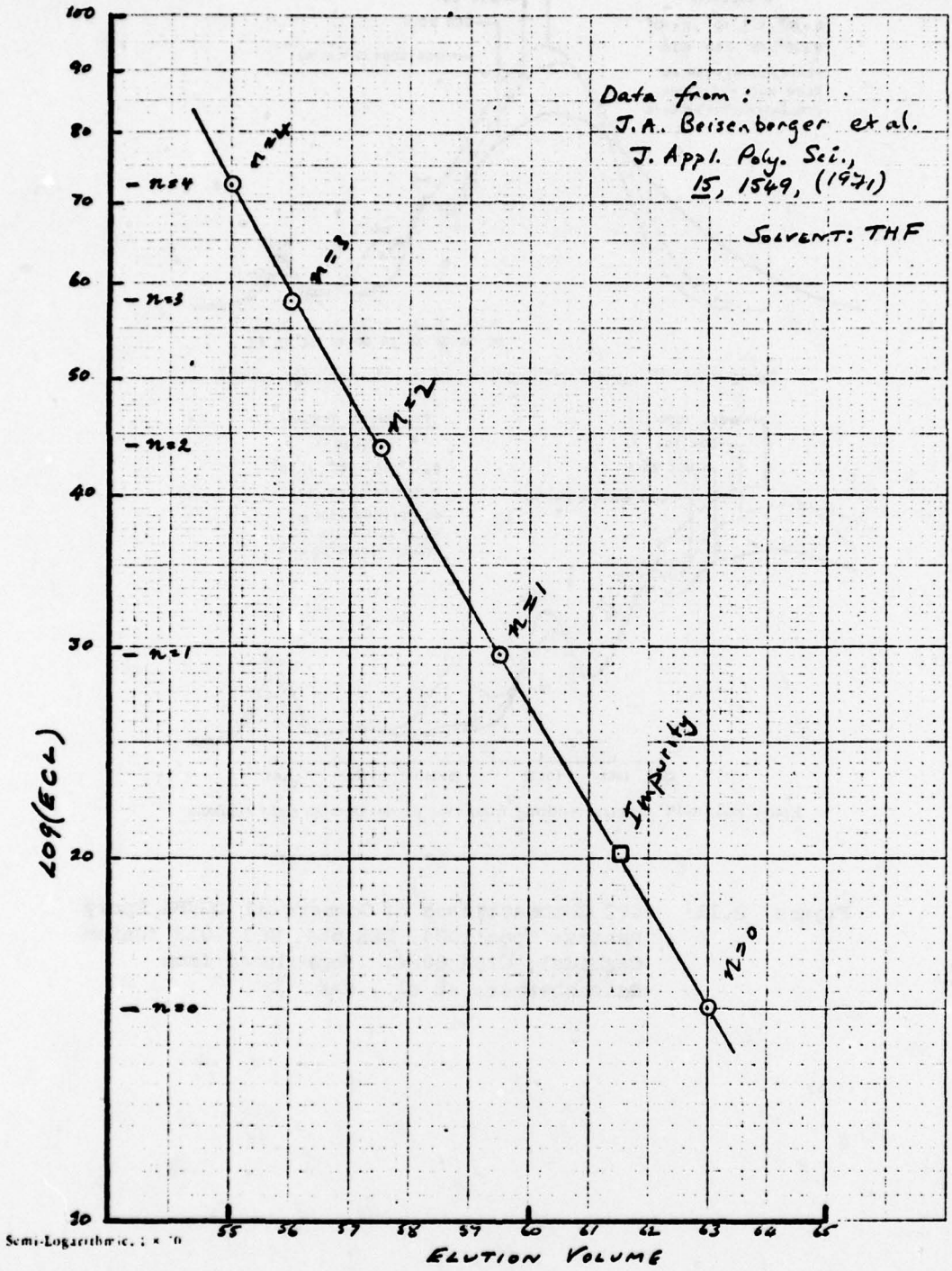

Figure B.12 Elution Volume versus Effective Chain Length (Data from Figure B.11)

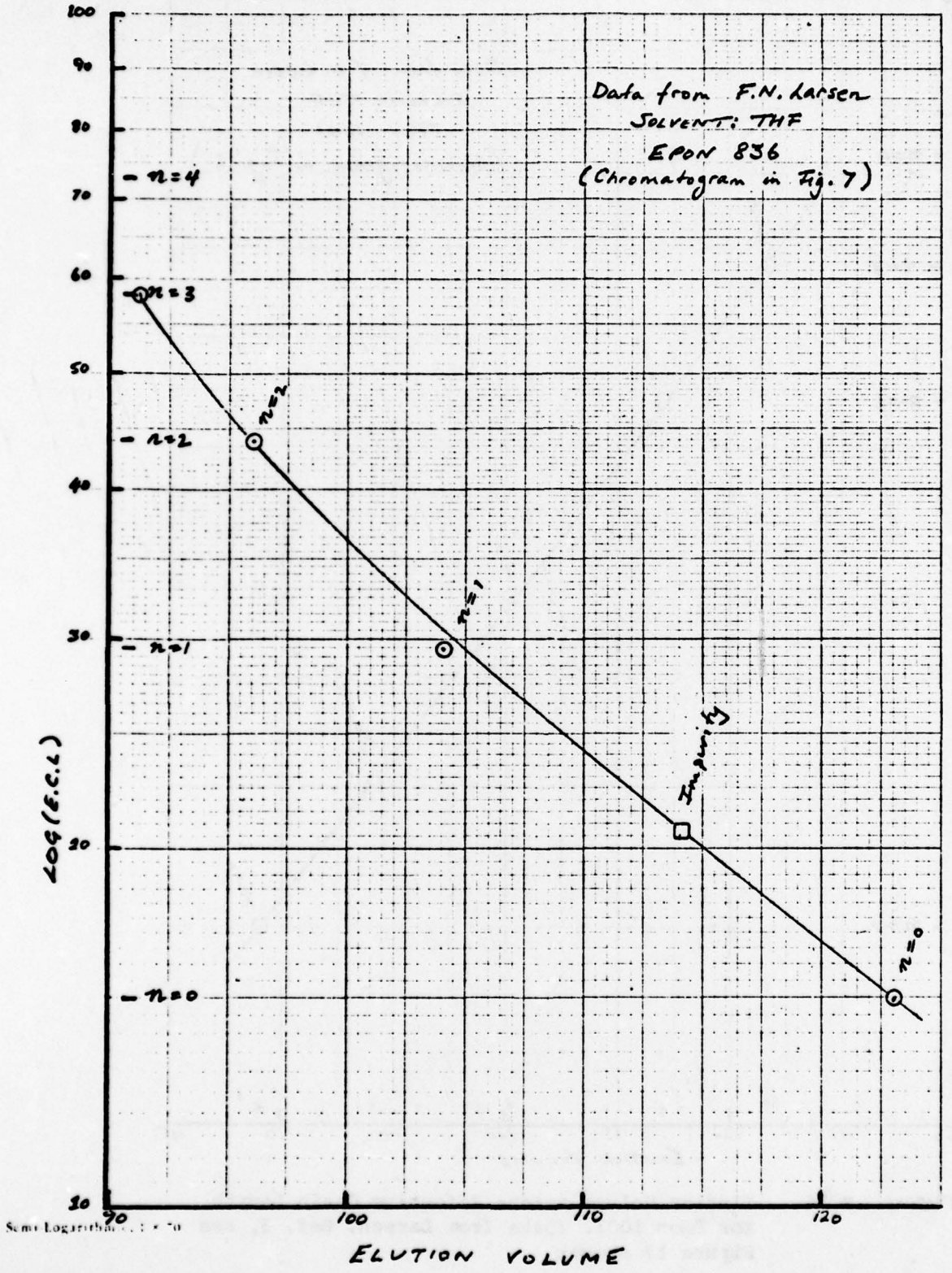

Figure B.13 Elution Volume versus Effective Chain Length for Epon 836. (Data from Larsen, Ref. 3, see Figure 17 above)

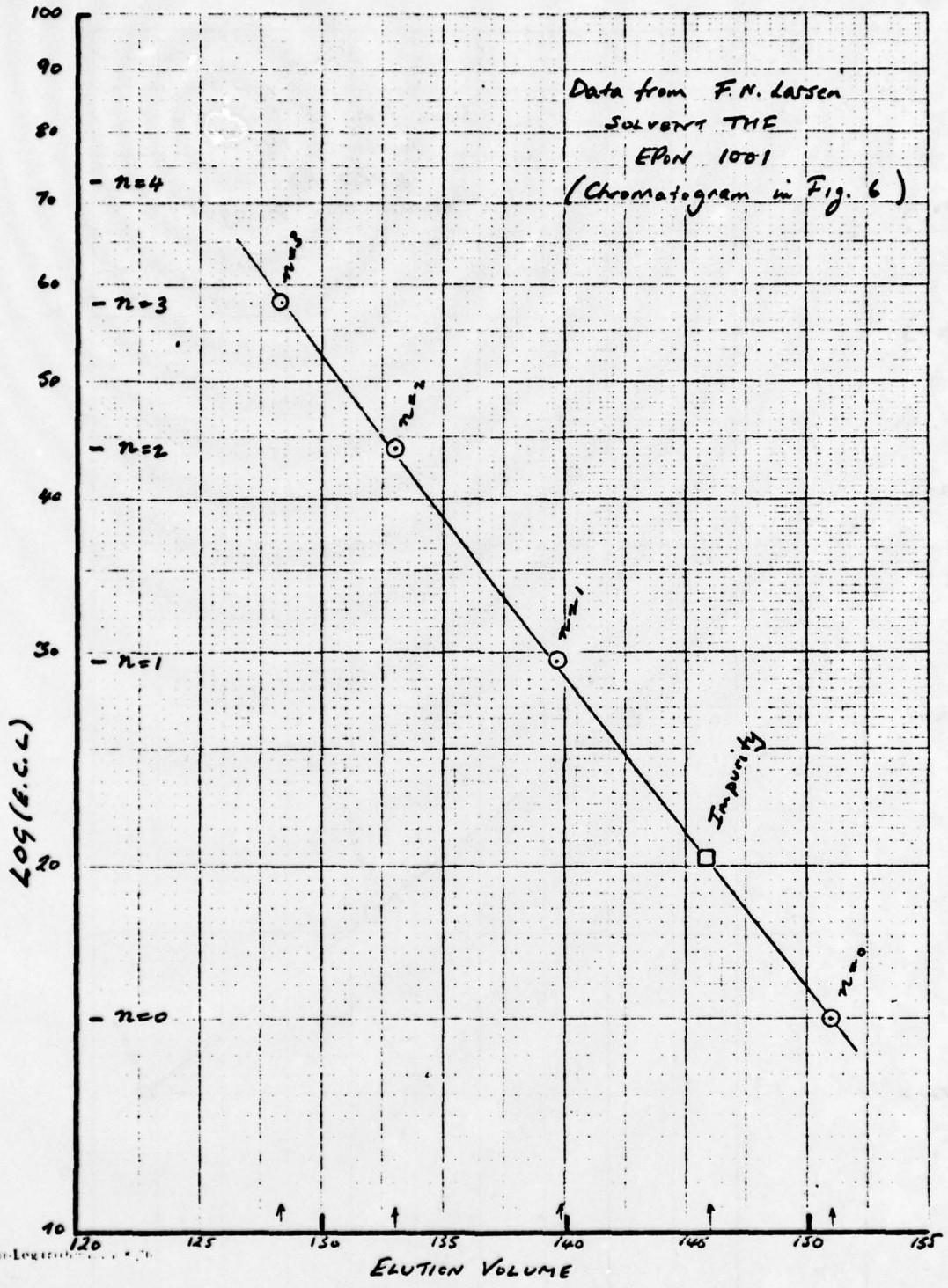

Figure B.14 **Elution Volume versus Effective Chain Length for Epon 1001. (Data from Larsen, Ref. 3, see Figure 17 above)**

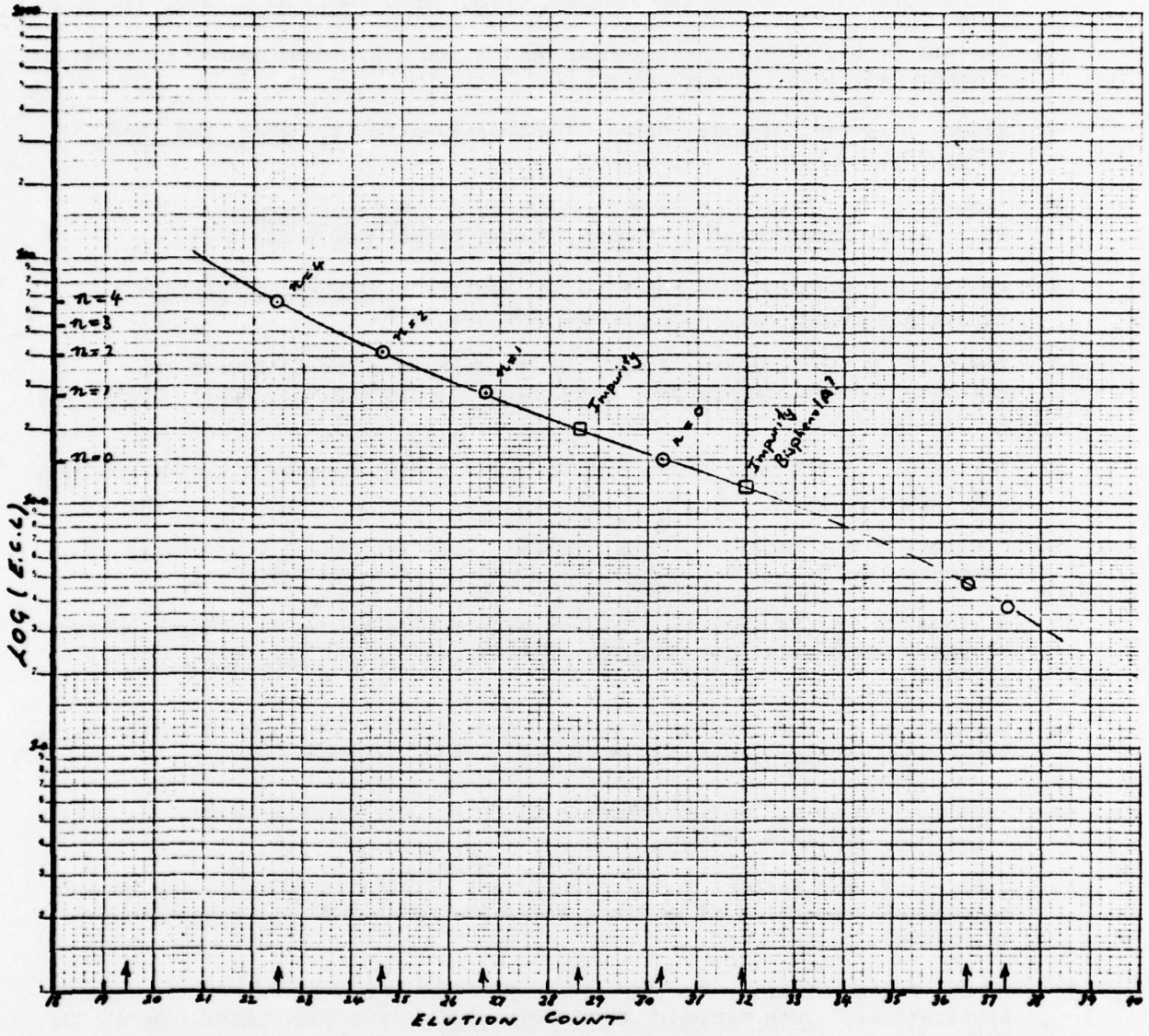

Figure B.15 Elution Volume versus Effective Chain Length for RE-A. Data from Figure 19a.

REFERENCES

1. Gee, G., et al., "A Discussion on Rubber Elasticity," Proc. Roy. Soc., A351, 295-406, (1976).

2. Edwards, S. F. and Stockmayer, W. H., "The Equation of State of Materials Intermediate to Rubbers and Glasses," Proc. Roy. Soc., A332, 439, (1973).

3. Larsen, F. N., Sixth International Seminar on GPC, Miami Beach, Florida, October 7-9, 1968. Preprints p. 111.

4. Allen, G., "The Molecular Basis of Rubber Elasticity," Proc. Roy. Soc., A351, 396, (1976).

5. Labana, S. S., Newman, S. and Chompff, A. J., Polymer Networks, p. 453, Edit. A. J. Chompff and S. Newman, Plenum Press, New York, 1971.

6. Haslam, J., Willis, M.A. and D. C. M. Squirrell, Identification and Analysis of Plastics, Iliffe Books, London, 1972.

7. Lewis, A. F. and Gillham, J. K., "Novel Technique for Following the Rigidity Changes Accompanying the Curing of Polymers," J. Applied Poly. Sci., 6, 422 (1962).

8. Lewis, A. F., "Dynamic Mechanical Behavior During Thermoset Curing Process," SPE Transactions 3, 201 (1963).

9. Gillham, J. K., Benci, J. A. and Noshay, A., "Isothermal Transitions of a Thermosetting System," J. Polymer Sci. Symp. #46, 279 (1974).

10. Gillham, J. K., "A Semimicro Thermomechanical Technique for Characterizing Polymeric Materials: Torsional Braid Analysis," AICHE Journal, 20 #6, 1066 (1974).

11. Marshal, A. S. and Petrie, S. E. B., "Rate Determining Factors for Enthalpy Relaxation of Glassy Polymers," J. Appl. Phys., 46, 4223 (1975).

12. Petrie, S. E. B., "Thermal Behavior of Annealed Organic Glasses," J. Poly. Sci., A-2, 10, 1255 (1974).

13. Butt, R. I. and Cotter, J. L., "The Effect of High Humidity on the Dynamic Mechanical Properties of an Epoxy-Polyamide Adhesive," J. of Adhesion, 8, 11, (1976).

14. Drake, R. and Siebert, A., "Elastomer Modified Epoxy Resins for Structural Applications," 20th National SAMPE Symposium, San Diego, Calif., April 29, 1975.

15. Riew, C. K., Rowe, E. H. and Siebert, A. R., "Rubber Toughened Thermosets," Advances in Chemistry, Vol. 154, 326, (1976).

16. Kambour, R. P., "A Review of Crazing and Fracture in Thermoplastics," Macromolecular Reviews, 7, 109, (1973).

17. Sultan, J. N., Ph.D. Thesis, Massachusetts Institute of Technology, Dept. of Civil Engineering (1969).

18. Bucknall, C. B. and Yoshii, T., S.C.I. Conference; Mechanical Performance of Polymers, Cranfield Institute of Technology, 5/6 Jan. 1977, preprint.

19. Scott, R. L., "The Thermodynamics of High Polymer Solutions," J. Chem. Phys., 17, 279 (1949).

20. Krause, S., "Polymer Compatibility," J. Macromol. Sci., Revs. Macromol. Chem., C7, 251, (1972).

21. McMaster, L. P., "Aspects of Polymer-Polymer Compatibility," Macromolecules, 6, 760, (1973).

22. Koningsveld, R., Kleintjens, L. A. and Schoffeleers, H. M., "Thermodynamic Aspects of Polymer Compatibility," Pure and Appl. Chem., 39, 1, (1974).

23. Siebert, A. R. and Riew, C. K., "Chemistry of Rubber Toughened Epoxy Resins," ACS 161st National Meeting, Org. Coatings and Plast. Div., March, (1971).

24. Sultan, J. N. and McGarry, F. J., Technical Report AFML-TR-69-86, Air Force Materials Lab, May 1969.

25. Laible, R. C. and McGarry, F. J., "Toughening of High Temperature Resistant Epoxy Resins," Polym.-Plast. Technol. Eng., 7 (1), 27 (1976).

26. McGarry, F. J., "Building Design with Reinforced Materials," Proc. Roy. Soc. London, A319, 58 (1970).

27. Sultan, J. N. and McGarry, F. J., "Effect of Rubber Particle Size on Deformation Mechanisms in Glassy Epoxy," Polym. Eng. and Sci., 13, 29 (1973).

28. Meeks, A. C., "Fracture and Mechanical Properties of Rubber-Modified Epoxy Resins," Polymer, 15, 675 (1974).

29. Bascom, W. D., Cottingham, R. L., Jones, R. L. and Peyser, P., "The Fracture of Epoxy and Elastomer-Modified Epoxy Polymers in Bulk and as Adhesives," J. Appl. Poly. Sci., 19, 2545, (1975).

30. Bascom, W. D., Timmons, C. D. and Jones, R. L., "Apparent Interfacial Failure in Mixed-Mode Adhesive Fracture," J. Mater. Sci., 10, 1037, (1975).

31. Mostovoy, S. and Ripling, E. J., Final Report: N00019-73-C-0163 Naval Air Systems Command, Jan. 31, 1974 and Mostovoy, S., Brusset, T. R. and Chin, S. T., Reports: F33615-75-C-5224, Air Force Materials Lab.

32. Gillham, J. K., Glandt, C. A. and McPherson, C. A., in Chemistry and Properties of Crosslinking Systems, edit S. Labana, Academic Press, p. 491, 1977.

33. Wang, S. S., Mandell, J. F. and McGarry, F. J., "Effects of Crack Elevation in TCDB Adhesive Fracture Test," Report R76-3, Dept. Materials Science and Engineering, MIT, April 1976.

34. Goodman, I. and Nesbitt, B. F., "The Structures and Reversible Polymerization Cyclic Oligomers from Poly(ethyleneterephthalate)," Polymer, 1, 384 (1960).

35. Lee, H. and Neville, K., Handbook of Epoxy Resins, McGraw Hill, Inc., p. 4-3, New York 1967.

36. Bomstein, J., "Infra Red Spectra of Oxirane Compounds," Anal. Chem., 30, 544 (1958).

37. Batzer, H. and Zahir, S. A., "Studies in Molecular Weight Distribution of Epoxide Resins. I. Gel Permeation Chromotography of Epoxide Resins," J. Appl. Polym. Sci., 19, 585, (1975).

38. Dark, W. A., Conrad, E. C. and Crossman, L. W., Jr., "Liquid Chromatographic Analysis of Epoxy Resins," J. Chromatography, 91, 247, (1974).

39. Biesenberger, J. A., Tan, M. and Buvdevani, I., "Recycle Gel Permeation Chromatography. II. Analysis of Epoxy Resins," J. Appl. Poly. Sci., 15, 1549, (1971).

40. Eggers, E. A. and Humphrey, J. S., Jr., "Applications of Gel Permeation Chromatography in the Manufacture of Epoxy-Glass Printed Circuit Laminates," J. Chromatography, 55, 33, (1971).

41. Dark, W. A., private communication, June 1977.

42. Batzer, H. and Zahir, S. A., "Studies in the Molecular Weight Distribution of Epoxide Resins," J. Appl. Poly. Sci., 21, 1843, (1977).

43. Slonimskii, G. L. and Struminskii, G. V., "The Mutual Solubility of Polymers. IV The Effect of Packing Density of Polymer Molecules on Their Mutual Solubility," Rubber Chem. and Tech., 31, 257, (1958).

44. Flory, P. J., Principles of Polymer Chemistry, Cornell University Press, Ithaca, N.Y., 1953.

45. Huggins, M. L., Physical Chemistry of High Polymers, Wiley, New York, (1958).

46. Prigogine, I., The Molecular Theory of Solutions, North American Publishing Co., Amsterdam, Chap. 16, 1957.

48. Flory, P. J., "Statistical Thermodynamics of Liquid Mixtures," J. Amer. Chem. Soc., 87, 1833, (1965).

49. Mazony, Y., Stadnicki, S. J. and Gillham, J., "Low Frequency Thermomechanical Spectrometry of Polymeric Materials: Computerized Torsional Braid Experiments," Amer. Chem. Soc., Polymer Preprints 15 (1), 562 (1974).

50. Babayevsky, P. G. and Gillham, J. K., "Epoxy Thermosetting Systems: Dynamic Mechanical Analysis of the Reactions of Aromatic Diamines with Diglycidyl Ether of Bisphenol A," J. Appl. Polym. Sci., 17, 2067 (1973).

51. Hata, N. and Kumanotani, J., "Viscoelastic Properties of Epoxy Resins. III. Effect of Molecular Weight of Antiplasticizers in Highly Crosslinked Antiplasticization System," J. Appl. Polym. Sci., 21, 1257, (1977).

52. Young, R. J. and Beaumont, P. W. R., "Failure of Brittle Polymers by Slow Crack Growth," J. Mater. Sci., 10, 1261, (1975).

53. Gledhill, R. A. and Kinlock, A. J., "Crack Growth in Epoxide Resin Adhesives," J. Mater. Sci., 10, 1261, (1975).

54. Yamini, S. and Young, R. J., "Stability of Crack Propagation in Epoxide Resins," Polymer, 18, 1075, (1977).

55. Redhill, R. A., Kinloch, A. J., Yamini, S. and Young, R. J., "Relationship between Mechanical Properties of and Crack Propagation in Epoxy Adhesives," Polymer, 19, 574, (1978).

56. Smith, M. B. and Sussman, S. E., Summary Report, Narmco Research and Development (NASA contact NAS-8-1565) May (1963).

57. Bolger, J. C., in Treatise on Adhesion and Adhesives, R. L. Patrick, Ed., Dekker, New York (1973).

58. Bell, J. P., "Structure of a Typical Amine-Cured Epoxy Resin," J. Polym. Sci., Part A-2, 6 417 (1970).

59. Plazek, D. J., "Magnetic Bearing Torsional Creep Apparatus," J. Polym. Sci., Part A-2, 6 621 (1968).

60. Ferry, J. D., Viscoelastic Properties of Polymers, 2nd Ed., John Wiley, New York (1970).

61. Kaelble, D. H., Cirlin, E. H. and Dynes, P. S., "Dynamic Mechanical Characterization of Epoxy Structural Adhesives," Proc. 19th Nat. Sym., Buena Park, California, April, 469 (1974).

62. Kline, D. E., "Dynamic Mechanical Properties of Polymerized Epoxy Resin," J. Polym. Sci., 47, 237 (1960).

63. Shibayama, K. and Suzuki, Y., "Effect of Crosslink Density on the Viscoelastic Properties of Unsaturated Polyesters," J. Polym. Sci., A3 2637 (1965).

64. Drumm, M. F., Dodge, C. W. H. and Nielson, L. E., "Crosslinking of a Phenol-Formaldehyde Novolac," Ind. Eng. Chem., 48, 76 (1956).

65. Heinz, H. D., Schmeider, K., Schnell, G. and Wolf, K. A., "Temperature Shift of the Second Order Transition of Natural Rubber by Crosslinking," Rubber Chem. Tech. 35 776 (1960).

66. Tobolsky, A. V., Properties and Structure of Polymers, John Wiley, NY, (1960).

67. Theocaris, P. S., "Rheological Behavior of Epoxy Resins in the Transition Region," J. Appl. Polym. Sci., 8, 399 (1964).

68. Kwei, T. K., "Viscoelasticity of Crosslinked Epoxy Polymer in the Transition Region," J. Polym. Sci., Part A-2, 4, 943 (1966).

69. Orbon, S., Ph.D. Thesis, University of Pittsburgh, Pittsburgh, Pennsylvania, 1978.

70. Schwarzl, F. and Staverman, "Higher Approximation Methods for the Relaxation Spectrum from Static and Dynamic Measurements of Viscoelastic Materials," Appl. Sci. Res. A, 4, 127 (1954).

71. Hendrickson, J. G. and Moore, J. C., "Gel Permeation Chromatography III. Molecular Shape versus Elution," J. Poly. Sci., A-1, 4, 167 (1966).

*U.S.Government Printing Office: 1979 — 657-002/560